9-14-77
230

Lib. 1408

ICP-1123

TECHNICAL DIVISION QUARTERLY PROGRESS REPORT
APRIL 1 - JUNE 30, 1977

CYRIL M. SLANSKY B. C. MUSGRAVE
B. R. DICKEY K. L. ROHDE

July 1977

Allied Chemical

IDAHO NATIONAL ENGINEERING LABORATORY

ENERGY RESEARCH AND DEVELOPMENT

IDAHO OPERATIONS OFFICE UNDER CONTRACT EY-76-C-07-1540

DISTRIBUTION OF THIS DOCUMENT IS UNLIMITED

Printed in the United States of America
Available from
National Technical Information Service
U S Department of Commerce
5285 Port Royal Road
Springfield, Virginia 22161
Price Printed Copy ~~$6 00~~, Microfiche $3 00
$7.25

NOTICE

This report was prepared as an account of work sponsored by the United States Government Neither the United States nor the Energy Research and Development Administration, nor the Nuclear Regulatory Commission, nor any of their employees, nor any of their contractors, subcontractors, or their employees, makes any warranty, express or implied, or assumes any legal liability or responsibility for the accuracy, completeness or usefulness of any information, apparatus, product or process disclosed, or represents that its use would not infringe privately owned rights

DISCLAIMER

This report was prepared as an account of work sponsored by an agency of the United States Government. Neither the United States Government nor any agency Thereof, nor any of their employees, makes any warranty, express or implied, or assumes any legal liability or responsibility for the accuracy, completeness, or usefulness of any information, apparatus, product, or process disclosed, or represents that its use would not infringe privately owned rights. Reference herein to any specific commercial product, process, or service by trade name, trademark, manufacturer, or otherwise does not necessarily constitute or imply its endorsement, recommendation, or favoring by the United States Government or any agency thereof. The views and opinions of authors expressed herein do not necessarily state or reflect those of the United States Government or any agency thereof.

DISCLAIMER

Portions of this document may be illegible in electronic image products. Images are produced from the best available original document.

ICP-1123

Distributed Under Category:
UC-2
General, Misc., Progress . . .
UC-10
Chemical Separations Proc., Pu. . .

TECHNICAL DIVISION QUARTERLY PROGRESS REPORT

APRIL 1 - JUNE 30, 1977

Cyril M. Slansky, Editor

Work performed under the direction of:

B. C. Musgrave, Manager
Technical Division

B. R. Dickey, Assistant Manager
Technical Division

K. L. Rohde, Assistant Manager
Technical Division

Date Published - July 1977

NOTICE
This report was prepared as an account of work sponsored by the United States Government. Neither the United States nor the United States Energy Research and Development Administration, nor any of their employees, nor any of their contractors, subcontractors, or their employees, makes any warranty, express or implied, or assumes any legal liability or responsibility for the accuracy, completeness or usefulness of any information, apparatus, product or process disclosed, or represents that its use would not infringe privately owned rights.

ALLIED CHEMICAL CORPORATION
IDAHO CHEMICAL PROGRAMS - OPERATIONS OFFICE

Prepared for
ENERGY RESEARCH AND DEVELOPMENT ADMINISTRATION
IDAHO OPERATIONS OFFICE
UNDER CONTRACT EY-76-C-07-1540

MASTER

DISTRIBUTION OF THIS DOCUMENT IS UNLIMITED

ABSTRACT

Progress for the second quarter of 1977 is reported on ERDA-budgeted activities contracted to Allied Chemical Corporation at the Idaho National Engineering Laboratory. The work is divided into three categories.

Fuel Cycle Research and Development

Results are presented on the fluidized-bed calcination of high-level radioactive waste from the reprocessing of spent commercial nuclear fuel, on the post treatment of the calcine, and on the removal of actinide elements from the waste prior to calcination. Other projects include the development of storage technology for ^{85}Kr waste; a study of the hydrogen mordenite catalyzed reaction between NO_x and NH_3; the adsorption and storage of ^{129}I on silver exchanged mordenite; physical properties, materials of construction, and unit operations studies on the evaporation of high-level waste; the behavior of volatile radionuclides during the combustion of HTGR graphite-based fuel; and the use of the uranium-ruthenium system in age-dating uranium ore bodies.

Special Materials Production

The long-term management of defense waste from the ICPP covers post-calcination treatment of ICPP calcined waste; the removal of actinide elements from first-cycle raffinate; the retrieval and handling of calcined waste from ICPP storage vaults; and the preparation of the "Defense Waste Document". Process improvements are reported on the Fluorinel headend process for Zircaloy-clad fuels and on uranium accountability measurements. Other development results cover the process for recovering spent Rover fuel, buried pipeline transfer systems, support to the Waste Management Program, and effluent monitoring methods evaluation and development.

Other Projects Supporting Energy Development

In this category are studies on nuclear materials security; application of a liquid-solid fluidized-bed heat exchanger to the recovery of geothermal heat; inplant reactor source term measurements; burnup methods for fast breeder reactor fuels; absolute thermal fission yield measurements; analytical support to light water breeder reactor development; research on analytical methods; and the behavior of environmental species of iodine.

SUMMARY

FUEL CYCLE RESEARCH AND DEVELOPMENT

I. FLUIDIZED-BED CALCINATION AND POST-TREATMENT OF COMMERCIAL WASTE

1. Fluidized-Bed Calcination of Commercial Waste

About 0.3 m^3 of simulated Allied General Nuclear Services high-level liquid waste-intermediate-level liquid waste (AGNS HLLW-ILLW) with rare earths substituted for uranium was calcined during the first test in the enclosed 10-centimetre-diameter (4-inch) calciner. A long-term test calcining denitrated AGNS HLLW-ILLW in the 7.5-centimetre-diameter (3-inch) calciner at 725 K with indirect heating confirmed earlier observations at 675 K that the steady-state (denitrated) bed agglomerates.

The structural design of the new 30-centimetre-diameter (12-inch) calciner modules has been completed.

2. Post-Calcination Treatment of Commercial Waste

Simulated commercial waste pellets were made using boric acid and metakaolin as solid binders. The viscosities of the liquid sprays (mixture of H_3PO_4 and HNO_3) used were higher than desired to produce consistently uniform pellets. A new type of flanged O-ring canister connection for casting a metal matrix was tested.

Application of microwave heating to evaporate or concentrate liquid waste for calcining or for glass melting is being examined.

3. Study of Bidentate Compounds for Separation of Actinides From Commercial LWR Reprocessing Waste

Extraction, scrub, and strip distribution coefficients for actinides and other key elements between synthetic LWR waste solution, made 0.1 M in nitrite, and 30% dihexyl-N,N-diethylcarbamylmethylenephosphonate (DHDECMP) in diisopropylbenzene (DIPB) have been measured. Additional distribution studies have been made from reduced synthetic LWR waste solution. Distribution coefficients for Pu(IV) between 30% DHDECMP in DIPB and various concentrations of nitric acid have been determined. Measurement was made of the capacity of DHDECMP to load with rare earth elements. Further investigations into the extraction capabilities of DHDECMP are being pursued, such as nitrate ion dependency and structure of the extracted complex.

II. KRYPTON-85 STORAGE DEVELOPMENT

A contract was awarded to Fluor Corporation for preparation of the conceptual design of a hydrogen recombiner installation at ICPP. Measurements of Zr off-gas composition were made. Promising methods of immobilizing ^{85}Kr were evaluated for volume and weight requirements.

Pressurized cylinder material test specimens in rubidium and samples of zeolites containing encapsulated argon or krypton are being tested in a gamma-radiation field. A capital cost estimate (±30%) for a ^{85}Kr storage facility using pressurized cylinders was completed as part of the Generic Environmental Statement for Commercial Wastes. Storage facility costs for 40-years' ^{85}Kr production at a 2,000 Mg/yr commercial reprocessing plant are $208,500,000 in mid-year 1976 dollars. Storage characteristics of pressurized cylinders were recalculated using the Redlich-Kwong equation of state (instead of the Ideal Gas law, used earlier).

Krypton encapsulation experiments were run with zeolites, glass, quartz, and aluminum powders; only the zeolites gave good loadings at the test conditions. The pilot-scale development was delayed and the program adjusted to fit with anticipated commercial reprocessing needs. Using the calculated thermal conductivity of a packed zeolite bed and krypton gas at high pressure, the fractional extent of cooling (from the encapsulation temperature) of a 10- to 15-cm internal diameter pressure vessel was calculated at one and two hours. The results show that cooling a pilot- or production-scale high pressure encapsulation vessel could be a significant problem, i.e., affect the loading of krypton. Pilot-scale development was delayed and the program adjusted to fit with anticipated commercial reprocessing needs.

III. LWR OFF-GAS TREATMENT

Work is continuing on a topical report of the NO_x-NH_3 reaction catalyzed by hydrogen mordenite.

IV. IODINE-129 ADSORBENT AND STORAGE DEVELOPMENT

Recycle tests on a bed of silver-exchanged mordenite, in which airborne-elemental iodine is repeatedly loaded and stripped, are being conducted with simulated dissolver off-gas streams. Loadings of 187 mg I_2/g substrate are being obtained. About 79% of the Ag is being used. No decline in iodine loading in the first 5 recycles is apparent.

Iodine loadings of 400 mg iodine per gram lead-exchanged faujasite have been obtained downstream of the silver bed during regeneration. About 90% of the lead is being used. Iodine-loaded lead-exchanged faujasite has a low iodine-vapor pressure and iodine-water solubility which may be suitable for storage.

The final draft of a report entitled, "Airborne Elemental Iodine Capacities of Metal Zeolites and a Method for Recycling Silver Zeolite", has

been prepared. A process-flow diagram for full-scale application of silver-exchanged mordenite recycle technology to iodine recovery from dissolver off-gas streams is presented.

V. WASTE MANAGEMENT

The small-scale thermosiphon evaporator was operated successfully both with nitric acid and simulated high-level liquid waste (HLLW) during this quarter. The heat transfer coefficient varied from 760 to 2080 $W/m^2 \cdot K$(134 to 367 $BTU/hr \cdot ft^2 \cdot °F$) depending on the vapor velocities which varied from 0.3 to 1.22 m/s (1 to 4 ft/s). Scale, which formed on the reboiler tube during evaporation of the HLLW solution, is being investigated. The Type 304L stainless steel reboiler tube specimen had a corrosion rate of 517 μm/yr on a weight loss basis and 536 μm/yr based on the measured change of the inside diameter of the tube.

The laboratory storage tank and auxilary equipment have been completed and tested with water. The cooling coil water flow is entirely in the laminar flow range. A Reynolds number of 1000 was obtained at a nominal flowrate of 2.8 g/s. Improvements are continuing to reduce the 20 percent heat loss from the tank; this loss is at least partly due to the loss of nitric acid and heat in the condenser.

VI. HTGR FUEL REPROCESSING

Tube furnace experiments to determine semivolatile fission product vaporization and condensation characteristics have been completed. Antimony, cadmium, cesium, molybdenum, rubidium, ruthenium, selenium, and tellurium were all found to be volatile both in the elemental and oxide forms. Several chlorides were tested to determine if they could be substituted for the elemental or oxide form in future laboratory studies on vaporized fission product removal. Although the chloride forms are more available, they are much more volatile and cannot be used as substitutes.

The laboratory semivolatile removal device has been constructed. The apparatus consists of a fluidized bed mounted above the burner. This bed is cooled with internal cooling coils to lower the temperature of the gases from the 500-900°C range to approximately 25°C. During cooling, the semi-volatile fission products should condense out on the bed material.

VII. NATURAL FISSION REACTOR STUDIES

In 1972, the first known example of a sustained nuclear chain reaction in nature was discovered at the Oklo mine site in the Republic of Gabon. A synopsis of our recent work relative to ^{238}U spontaneous fission yield for ruthenium and the development of the uranium-ruthenium system for a new age-dating technique prepared for the Second IAEA Experts Conference on Natural Fission Reactors is given. Indirect evidence indicates that a new natural fission reactor has been discovered at the Oklobonda mine approximately one mile from the Oklo pit.

SPECIAL MATERIALS PRODUCTION

I. LONG-TERM MANAGEMENT OF ICPP HIGH-LEVEL WASTES

1. Post Calcination Treatment of High-Level ICPP Wastes

Experimental results show that H_3PO_4 concentrations in liquid spray binders for pellet formation have to be under 30% to spray properly.

Precalcination addition of boric acid and zinc oxide is being studied to simplify pelletization and improve pellet quality.

Waste characteristics such as compression strength; leachability of cesium, cerium, and strontium from the pellets; and loss of volatiles and nitrates from dried pellets stored at 450°C were determined. Compression strength tests show that dried pellets are stronger than heat-treated pellets, but both should be amply strong for transport and storage. Bulk leach resistance (weight change with time) of pellets in H_2O, acid, caustic, and brines is comparable to that of waste glasses, but cesium leach resistance, although improved over calcine, is still relatively high. Nitrates and moisture are released (mostly in the first 24 hours) when dried (200°C) pellets are stored at elevated (450°C) temperatures, but residual nitrate content is still 10 to 40% of the original.

Fifteen waste glass formulations were prepared; leach tests are under way. Tests on some glass samples stored 48 hours at 650°C indicate that slight devitrification has occurred.

A conceptual design for the ICPP post-treatment pilot plant was completed showing space requirements and indicating process development needs.

2. Actinide Removal

Actinide distribution measurements were continued. Measurement was made of the capacity of DHDECMP to load with rare earth elements. The D_{HNO_3} was determined over the aqueous acidity range of 0.15 - 10.0 M HNO_3. Purification of DHDECMP was begun using a centrifugal molecular still and an order for 120 L of DHDECMP, to be used in pilot plant experiments, was placed with Eastman Organic Chemicals, Rochester, N. Y.

3. Calcined Solids Retrievability and Handling

Major emphasis has been placed on project redirection and planning. Design and procurement have been initiated on equipment for sampling stored calcine in Bin Set No. 2. Cold zirconia calcine stored at 450°C and 90 kPa, and alumina calcine stored at 600°C and 90 kPa for 1500 hours showed essentially no tendency to agglomerate.

4. ICPP Defense Waste Document

A draft Defense Waste Document (DWD) describing alternatives for long-term management of ICPP high-level solid wastes was completed and transmitted to ERDA for comments. The document describes the existing technology for treating the calcine now stored at the ICPP and identifies further research and development efforts required for waste disposal. The costs and risks associated with converting the calcine to another waste form and storing it at either a Federal Repository or the INEL are presented in the document.

II. ICPP PLANT PROCESS IMPROVEMENT

1. Uranium Accountability Measurements

Development efforts have resulted in several areas of improvement. A better method for chemically separating the uranium for isotope dilution mass spectrometry (IDMS) has been developed, and its use has resulted in better mass spectrometer operation and in improved QC data. Two alternative procedures for the chemical separation have been found, and future work should identify which of the three available is the best. Several improvements have been made in the Mass Spectrometer Laboratory which provide more objective data handling and smoother operation of the Lab. The overall system has been better defined and work is proceeding on a single document which thoroughly describes the total measurements system.

2. Zirconium Fuel Recovery Process

An engineering evaluation of the operating characteristics of the proposed dissolver design for the Fluorinel process was completed. The evaluation included both the thermodynamic and hydraulic performance of the proposed dissolver.

III. ADVANCED GRAPHITE FUELS REPROCESSING

Tests were conducted to determine the transfer rates of Rover simulated burner ash and alumina bed material. Solids transfer rates were determined as a function of back-pressure in the receiving vessel, and the back-pressures that will stop flow were estimated.

Attrition of alumina bed material due to transport was studied. Alumina particles were pneumatically transferred through a solids transfer line. Measurements of the mass mean particle diameter after several transfers showed that the expected attrition is not excessive.

An ultrasonic flowmeter and differential pressure measurements were evaluated as a means of determining solids flow rate in the transfer lines. The pressure differential method was found superior to the ultrasonic meter and should provide an adequate means for determining solids flow.

Erosion of elbows and jets in the transport lines was found to be excessive during transport of alumina. A 90° elbow failed after 4 hours of alumina transport. The jet used for the transport tests was also eroded, causing a 50% reduction in performance. The erosion observed during transport of simulated burner ash was much less; a maximum of 12% wall loss in 8 hours was observed.

Erosion tests to compare the Tribaloy 700 hardfacing of the Rover pilot plant centrifuge with the ceramic coating previously tested are being conducted.

The cost estimate and expenditure authorization for the Rover plant support dissolver have been completed and material procurement begun.

IV. WASTE TRANSFER SYSTEMS

Field corrosion tests have been initiated on coated stainless steel pipe specimens and on bare stainless steel pipe specimens placed in ICPP soil. Samples will be monitored by measuring pipe-to-soil potentials. Periodically, samples will be removed from the test site for weight loss determination and visual inspection.

Laboratory analysis of stainless steel corrosion in soil has been initiated using the electronic corrosometer probe. This data will supplement the field test data.

Seismic analyses of four common secondary encasement designs has been completed. Metal and fiber reinforced polyethylene (FRP) pipe encasements and concrete encasements were evaluated and designs were formulated, where possible, to withstand an earthquake acceleration of 0.5 g.

V. ICPP WASTE MANAGEMENT DEVELOPMENT

1. Rover Flowsheet Development

Pilot plant testing of Rover waste calcination flowsheets has been completed. Based on the results of two 30-centimetre-diameter (12-inch) calciner runs, either of two blended flowsheets [1 vol Rover and 1 vol zirconium flowsheet waste (ZFW) or 1 vol Rover and 2 vol ZFW] are acceptable for demonstration in the WCF.

2. Tank WM-183 Flowsheet Development

Iron addition to WM-183 waste (a mixture of electrolytic, aluminum, and sodium-bearing wastes) was not successful in completely controlling particle agglomeration due to sodium. Pilot plant testing has begun on blending WM-183 waste with zirconium fluoride waste. One run using the 10-centimetre-diameter (4-inch) calciner has been completed; no agglomeration was experienced.

3. Sodium-Bearing Waste Flowsheet Development

The proposed flowsheet for calcining sodium-bearing waste (3 vol zirconium - 1 vol sodium-bearing wastes blend using a calcium-to-fluoride mole ratio of 0.7) produced excessive chloride volatility and rough calcine when tested in the WCF. Scoping tests are being made using a 10-centimetre-diameter (4-inch) calciner to find alternate flowsheets. None of the flowsheets tested produced fluidized-bed particle agglomeration within 14 hours, but all had other serious disadvantages.

4. Feed Control Valve Testing

A ball valve has been tested for controlling calciner feed. The full-port capability of the valve should eliminate plugging, valve cycling, and bellows failure now experienced with the WCF angle valves. The pilot-plant tests demonstrated that the reliability and controllability of the ball valve are excellent. The ball valve is recommended as a feed control device for either the NWCF or WCF.

5. Transport System Moisture Monitor

A moisture monitor has been ordered for the WCF transport air return line. If pilot-plant testing of the monitor is successful, it should be installed before the scheduled September 2 calciner startup. This monitor will provide information which will be used in controlling the moisture content in the solids transport system, thereby reducing the possibility of condensation and subsequent plugging in the transport air return line.

6. Calciner Nozzle Cap Material

Testing of eight materials for use as calciner nozzle caps has been completed. Haynes 25 and 188 were shown to be superior to 440-C, 304L, Hastelloy-X, and three ceramic coatings on 304L (Tribaloy-700, chrome oxide, tungsten carbide). Haynes 25 and 188 materials have been ordered for cap fabrication and installation in the WCF.

7. Waste Feed Chemistry Studies

The use of magnesium nitrate to suppress fluoride and chloride volatility during calcination of a blend of 3 vol zirconium and 1 vol sodium-bearing wastes with minimum production of gelatinous solids in calciner feed was evaluated in a 10-centimetre-diameter (4-inch) calciner. A magnesium-to-fluoride mole ratio greater than 0.5 is needed to effectively suppress chloride volatility.

8. Alternate Calciner Startup-Bed Material

Work has begun in an attempt to find a suitable alternative to Dolomite as a calciner startup-bed material. Several materials have been tested or are due to be tested with the preliminary results showing Fluorapatite to be a very promising candidate due to its low erosion potential.

9. Calcine Erosion During Transport

Preliminary tests have shown that simulated second-cycle waste calcine is 5 to 7 times more erosive than zirconium calcine.

VI. EFFLUENT MONITORING METHODS EVALUATION AND DEVELOPMENT

The program is to define specific problems and needs in off-gas monitoring technology from nuclear fuel reprocessing and waste solidification facilities, and to ensure that technology is available for existing and future commercial and ERDA plants. Funding started in FY-1977 with major emphasis scheduled for the second half of the fiscal year.

OTHER PROJECTS SUPPORTING ENERGY DEVELOPMENT

I. LIQUID FLUIDIZED-BED HEAT EXCHANGER FOR GEOTHERMAL APPLICATIONS

Scaling of heat-transfer surfaces is a barrier to rapid development of binary systems using moderate temperature geothermal resources with high scaling potential. Liquid fluidized beds scrub the tube surfaces and control the build-up of scale. The objective of this program is to develop liquid fluidized-bed technology to the point of a demonstration-scale plant. During the past quarter, work proceeded in three areas: a) a scale-control experiment on the Geothermal Component Test Facility (GCTF), b) flow distribution experiments at Raft River, and c) an updated size-cost analysis of vertical and horizontal preheaters.

II. IN-PLANT SOURCE TERM MEASUREMENTS

The inplant source term measurement program has continued at the Zion Nuclear Generating Station. Selection of the third and fourth sites for the program is under way by NRC and measurements should begin early in the next quarter.

III. BURNUP METHODS FOR FAST BREEDER REACTOR FUELS

Analysis of two dissolved irraidated samples of ^{241}Am has started. A rigorous error analysis of the data from the analysis of four capsules of ^{239}Pu fast reactor fission yields has been completed. The first draft of a paper giving ^{239}Pu and ^{241}Pu fast reactor fission yields has been completed. Approximately 30 contributions have been received for the preparation of a review paper for the IAEA Second Advisory Group Meeting on Fission Product Nuclear Data.

IV. ABSOLUTE THERMAL FISSION YIELD MEASUREMENTS

A new program to remeasure ^{235}U and ^{239}Pu absolute thermal fission yields is under way. The bulk of the fission product analyses on six irradiated capsules of ^{235}U has been completed. Because of the development of an improved mass spectrometric measurement technique, La and Ce analyses are being repeated. A series of 14 ATR fuel plate punchings will be analyzed for U, Cs, and Nd to better define the problems of the accurate measurement of burnup in high flux reactor fuels.

V. LIGHT WATER BREEDER REACTOR (LWBR) - ANALYTICAL SUPPORT

Bettis Atomic Power Laboratory has requested that three irradiated duplex fuel pellets be analyzed for fuel depletion analysis on an urgent basis. Present commitments would be postponed for this work. Fuel dissolution has been completed for 9 of the first 15 high priority fuel rod sections. A total of 28 irradiated fuel rod sections and 9 unirradiated duplex pellets have been received.

VI. RESEARCH ON ANALYTICAL METHODS

1. A Rapid Determination of ^{241}Am in Soil Samples at the Radioactive Waste Management Complex

One gram of finely ground soil is analyzed for ^{241}Am by measuring its 59.4 KeV gamma against a standard using the KeVex silicon detector.

2. Determination of ^{241}Am in ICPP Stack Filters

Leaches of stack filter samples using 12 M or greater HNO_3 are extracted into a bidentate solvent and the Am determined by gamma scanning.

3. Revision of the Chemical Analysis Work Sheet for Direct Computer Output

Counting data is recorded in longhand on a revised work sheet with the calculations performed and the results printed by computer on the same work sheet.

4. Potentiometric Determination of Mercury in Fuel Dissolvent Solutions

A method was developed for the determination of Hg(II) in nitric acid fuel dissolvent solutions including those containing gadolinium. The procedure involves the potentiometric titration of Hg(II) with sodium iodide using an iodide selective indicator electrode to mark the equivalence point.

5. Application of Ion Chromatography to Anion Analysis

An analytical ion chromatograph was acquired to study the determination of anions in a variety of matrices. Preliminary results appear promising for the determination of sulfate and organic phosphate anions.

6. Determination of Ruthenium in Solid Samples

In support of studies on the solidification of nuclear wastes, a rapid method for the determination of as little as 100 ppb of natural ruthenium in solid samples was developed. The method employs a fusion step followed by extraction of ruthenium as an ammonium pyrrolidinedithiocarbamate complex. The ruthenium concentration is determined directly in the organic phase by atomic absorption spectroscopy with a flame or flameless atomizer as the absorption cell.

7. Accurate Determination of 5-25 mg U

A precise and selective potentiometric method for determining 5-25 mg of uranium was developed. The method, which is essentially a scaled-down version of the modified Davies-Gray titrimetric method, has been automated by interfacing a 10-mL Mettler buret with a programmed HP 9830 calculator. The calculator controls the delivery of titrant so that the end-point is approached as rapidly as possible, but still delivers only small increments of titrant near the equivalence point. A precision and accuracy of 0.05% or better is obtainable with this method. It will be used to verify various standards prepared by the Quality Control and Accountability Group.

8. Chemical Separation of Uranium for Mass Analysis

Two "clean-up" procedures were developed for separating uranium from impurities in samples resulting from the dissolution of zirconium fuel. These impurities, which are not completely removed by Method U-Sep-1, cause difficulties in the determination of uranium by isotope dilution mass spectrometry. The two procedures developed involve desorption on an ion exchange resin of uranium as an anionic complex from strong HCl media or extraction of uranium with triisooctylamine into xylene. Both methods are effective in eliminating the impurities which previously affected the mass analysis.

9. Rapid Spectrophotometric Determination of Uranium

Two methods were evaluated for the rapid determination of uranium in fuel reprocessing solutions. Both methods are based upon the colorimetric determination of U as the yellow thiocyanate complex and require a prior separation of U from fission products and other interferences. In one method the thiocyanate complex is developed in a butyl cellosolve-water solvent while the other method involves extraction of the uranyl cyclamine-thiocyanate-triisocylamine anion complex into xylene or hexone.

10. Unirradiated Rover Fuel Assay Program

The unirradiated uranium-graphite fuel from the Rover project is to be nondestructively assayed prior to processing for recovery of the uranium. The analysis of the fuel will be accomplished using an isotopic source assay system (ISAS) which uses a ^{252}Cf neutron source and plastic scintillation detectors. The ISAS will be interfaced to an HP 9825 for ease of operation and data handling. Progress of system calibration is discussed.

VII. ENVIRONMENTAL IODINE SPECIES BEHAVIOR

Cryogenic air samplers for xenon measurements have been evaluated and field tested. Laboratory studies involving basic aqueous iodine chemistry and gaseous wet deposition of iodine species continued. The field measurement program has been initiated.

CONTENTS

FIGURES AND TABLES (by Section)

FUEL CYCLE RESEARCH AND DEVELOPMENT

Figures

Tables

SPECIAL MATERIALS PRODUCTION

Figures

Tables

OTHER PROJECTS SUPPORTING ENERGY DEVELOPMENT

Figures

Tables

RESULTS

FUEL CYCLE RESEARCH AND DEVELOPMENT

I. FLUIDIZED-BED CALCINATION AND POST-TREATMENT OF COMMERCIAL WASTES

1.0 AGNS Waste Calcination Studies

1.1 Flowsheet Development Studies (J. H. Valentine, G. G. Simpson, R. E. Schindler)

An enclosed, 10-centimetre-diameter (4-inch) calciner was built to allow experimental calcination of wastes containing uranium. In the reporting quarter, the calciner was checked out and procedures (SOPs) were approved for operating the calciner both with and without uranium.

The first run in the enclosed 10-centimetre-diameter (4-inch) calciner (EM-1) was made in which simulated AGNS HLLW-ILLW (1974 flowsheet) waste with rare earths substituted for uranium was calcined. The purposes of the run were to test the entire calciner system and acquire base-line data on calcine properties, ruthenium volatility, and calciner operation. About 0.3 m^3 of simulated waste was calcined at 775 K during 100 h of operation with in-bed combustion. The product to fines ratio was 6; the attrition index of the product (bed) was about 50. The ruthenium volatility data are pending sample analysis.

1.2 Feed Denitration Studies (M. S. Walker, R. E. Schindler)

A previous long-term test in which denitrated (with formic acid) AGNS HLLW-ILLW was calcined at 675 K with indirect heating in the 7.5-centimetre-diameter (3-inch) calciner was terminated by bed agglomeration when the steady-state bed was formed. A second long-term test (this quarter) in which denitrated AGNS HLLW-ILLW (with uranium) was calcined in the 7.5-centimetre-diameter (3-inch) calciner at 725 K with indirect heating was also unsuccessful. Bed agglomeration occurred after about 60% turnover of the (nitrated) initial bed. The bed particles were cemented together by a white material believed to be sodium hydroxide. The tentative conclusion reached, based on the poor results of the long-term tests with denitrated and basic HLLW-ILLW, is that dissolved iron does not complex sodium hydroxide when calcining a basic solution. Hence, feed denitration cannot be used (in the temperature range of 675 to 725 K) for sodium-containing wastes when the denitration process also turns the feed basic.

1.3 Upgrade of 30-Centimetre-Diameter (12-inch) Calciner (J. A. Hendricks, R. E. Schindler)

The existing 30-centimetre-diameter (12-inch) calciner is being replaced with a new calciner system. The primary design objectives are to: (1) provide better access to equipment, (2) provide an off-gas system more representative of a production calciner, and (3) replace corroded

or worn equipment. The module structural design consisting of module design, placement and mounting of major vessels, and major piping has been completed.

Plans for Next Quarter

Simulated AGNS HLLW-ILLW containing uranium will be solidified in the 10-centimetre-diameter (4-inch) calciner. Ruthenium volatility will be measured in both low-acid (2-4 M) and high-acid (8-10 M) solutions.

2. Post Calcination of Commercial Waste (K. M. Lamb, S. J. Priebe)

A pelleted waste form was prepared from simulated commercial waste using 10% metakaolin and 5% boric acid as solid binders. Three different liquid binders were used: 11 M H_3PO_4 and 4 M HNO_3, 7.4 M H_3PO_4 and 4 M HNO_3, and 4 M H_3PO_4 and 3 M HNO_3. All the binders formed pellets which were physically hard, but were somewhat irregular in shape. The liquid binders used were too viscous to develop a proper spray pattern and caused material buildup on the plows due to locally high liquid concentrations. This buildup contributed to the formation of the irregular shaped pellets. Heat treatment and leach-resistant properties of the pellets have not been determined.

Metal-matrix casting of pellets in a canister fitted with a new type of flange and metal O-ring seals was tested. The seal was not good enough to hold the 1 to 5 torr vacuum needed to pull molten aluminum alloy into the casting canister, probably because of an improper seal.

Studies to determine the feasibility of using microwave heat to evaporate or dry high-level liquid wastes were initiated. Energy requirements and microwave efficiencies to heat slurries and solidified waste will be evaluated. Small-scale experiments to measure waste concentration properties are being formulated.

Plans for Next Quarter

Commercial pellet and metal-matrix development work has been terminated. Feasibility studies of microwave application to evaporation and concentration of liquid commercial waste will continue.

3. Study of Bidentate Compounds for Separation of Actinides From Commercial LWR Reprocessing Waste (L. D. McIsaac, J. D. Baker, R. E. LaPoint, N. C. Schroeder)

3.1 Synthetic LWR Waste

Additional distribution coefficients for actinides and other key elements between synthetic commercial LWR waste solution and 30% dihexyl-N,N-diethyl-carbamylmethylenephosphonate (DHDECMP) in diisopropylbenzene (DIPB) were measured. Extraction, scrub, and strip data reported in Table 1 were obtained using the same procedures described in the previous quarterly report. Table 1 is a composite of newly obtained data and values reported in the previous quarterly.

TABLE 1

DHDECMP Extraction-Scrub-Strip Studies With Synthetic Purex First-Cycle Waste (HAW) Solution Made 0.1 M in Nitrite

Feed Component	Extraction Contact	Distribution Coefficients: Scrub Contacts 1	Scrub Contacts 2	Strip Contacts 1	Strip Contacts 2	Strip Contacts 3
Cm(III)	3.0	2.9	3.7	0.50	0.11	0.10
Am(III)	4.3	4.1	5.7	0.70	0.13	0.18
Pu(IV)	304.0	122.0	25.0	0.70	0.068	0.16
Np(V,VI)	2.2	2.0	3.6	0.060	0.84	
U(VI)	51.0	62.0	52.0	13.9	2.74	2.40
Gd(III)	2.1	2.4	2.6	0.33	0.061	
Eu(III)	2.9	3.2	3.3	0.46	0.086	0.048
Sm(III)	3.4					
Pm(III)	4.2					
Nd(III)	4.3					
Pr(III)	5.3					
Ce(III)	5.8	5.2	7.1	1.02	0.18	0.1
La(III)	6.5	6.1	7.8	1.01	0.16	0.085
Ba(II)	0.013	0.012				
Cs(I)	0.00050					
Te(IV)	0.020	0.0084				
Sb(V)	0.036					
Sn(IV)	0.002					
Cd(II)	0.0067					
Ag(I)	0.028	0.026				
Pd(II)	0.53	0.47	0.41	1.10	1.20	2.8
Rh(III)	0.018					
Ru(III,IV)	0.27	0.96		15.0	15.0	
Tc(VII)	2.3	1.40		8.3	5.1	
Mo(VI)	0.39	0.10	0.041			
Nb(V)	0.51	0.017	0.75			
Zr(IV)	1.8	0.022	0.0028			
Y(III)	0.60	0.66	0.70	0.076	0.1	
Sr(II)	0.017	0.019				
Rb(I)	0.00064					
Fe(III)	0.0015					
Cr(III)	0.0033					
H^+	0.23					

Under the conditions used for the extraction contact (0.1 M nitrite), favorable distribution coefficients were obtained for actinides and lanthanides. Of the non-actinide and lanthanide elements present in synthetic LWR solution, only Zr, Y, Tc, Pd, Nb, Mo, and Ru are extracted to any large extent. Of these, Zr, Nb, and Mo are removed from the organic phase by contacting it with 3 M HNO_3-0.05 M $H_2C_2O_4$ scrub solution. Strip contacts with 0.05 M HNO_3-0.05 M $NH_2OH \cdot HNO_3$ show that only uranium, ruthenium, palladium, and technetium are not removed from the organic phase. Additional strip contacts, using 0.05 M HNO_3-0.05 M $H_2C_2O_4$ or 0.5 M Na_2CO_3 solution for these elements and the actinides, are shown in Table 2.[2] Uranium and ruthenium are efficiently stripped by carbonate; technetium is also stripped but less efficiently.

TABLE 2

Oxalic Acid and Sodium Carbonate Strip Data

	Distribution Coefficients	
Element	0.05 M Oxalic Acid - 0.05 HNO_3	0.5 M Na_2CO_3
Cm	0.20	--
Am	0.12	--
Pu	0.16	--
Np	7.5	--
U	0.095	0.006
Pd	0.8	--
Ru	11.0	0.05
Tc	--	0.58

Preliminary extraction distribution coefficients for various key elements from reduced synthetic LWR solution are shown in Table 3. For comparison, values obtained using 0.1 M $NaNO_2$ are listed in the far right hand column. Reduced synthetic LWR solution was 0.01 M $Fe(SO_3NH_2)_2$-0.02 M HSO_3NH_2. Ferrous sulfamate was prepared by dissolving stoichiometric quantities of ferrous ammonium sulfate and sulfamic acid in water. This solution was made free of SO_4^{2-} and Cl^- by passing it through a sulfamate anion exchange column. A new method of preparation[1] for a 1:2 molar ratio of $Fe(SO_3NH_2)_2$:HSO_3NH_2 involves the addition of a 1:4 mole ratio of iron filings to sulfamic acid. Care should be taken to protect this solution from oxygen, light, and heat.

[1] M. C. Thomson, Savannah River Laboratory, Aiken, South Carolina, Personal Communication.

TABLE 3

Distribution Coefficients For Key Elements From Reduced Synthetic LWR Waste Solution

Element	0.01 M $Fe(SO_3NH_2)_2$-0.02 M HSO_3NH_2	0.01 M $NaNO_2$
Mo	0.37	0.39
Nb	1.50	0.51
Tc	2.2	2.3
Zr	2.0	1.8
Pd	0.54	0.53
Ru	0.50	0.27
Ba	0.011	0.013
Cs	~0.0004	0.0005
Ce	5.8	5.8
Eu	2.9	2.9
Np	98	2.2

Experimental procedures for obtaining the data in Table 3 were the same as for Table 1. As expected, neptunium shows a much higher distribution coefficient when reduced to the quadrivalent state. Niobium and ruthenium also extracted to a greater extent under these conditions. Other elements to be measured are Pu, U, and Rh.

Experiments were run to see if neptunium would maintain a high distribution coefficient for several scrub contacts after being extracted from reduced synthetic LWR waste solution. Normal scrubs, two 1/5-volume contacts with 3 M HNO_3-0.05 M $H_2C_2O_4$, failed to maintain high distribution coefficients ($\bar{D}$< 5). Making the scrub 3 M HNO_3-0.05 $H_2C_2O_4$-0.02 M HSO_3NH_2-0.007 M $Fe(SO_3NH_2)_2$ maintained the distribution coefficient for the first and second scrubs at 70 and 22, respectively.

A conceptual flow sheet is being formulated for removing actinides from commercial LWR solution containing nitrite.

3.2 Extraction Mechanisms

Distribution coefficients for Pu(IV) between 30% DHDECMP in DIPB and various concentrations of nitric acid were determined. These data are shown in Figure 1 along with data from the last quarterly report. Plutonium was set in the quadrivalent state by adding 1 drop of 30% H_2O_2 to the nitrate tracer and taking it down to incipient dryness in concentrated nitric acid. The tracer was then taken up with the particular nitric acid concentration being studied and made 0.025 M in nitrite.

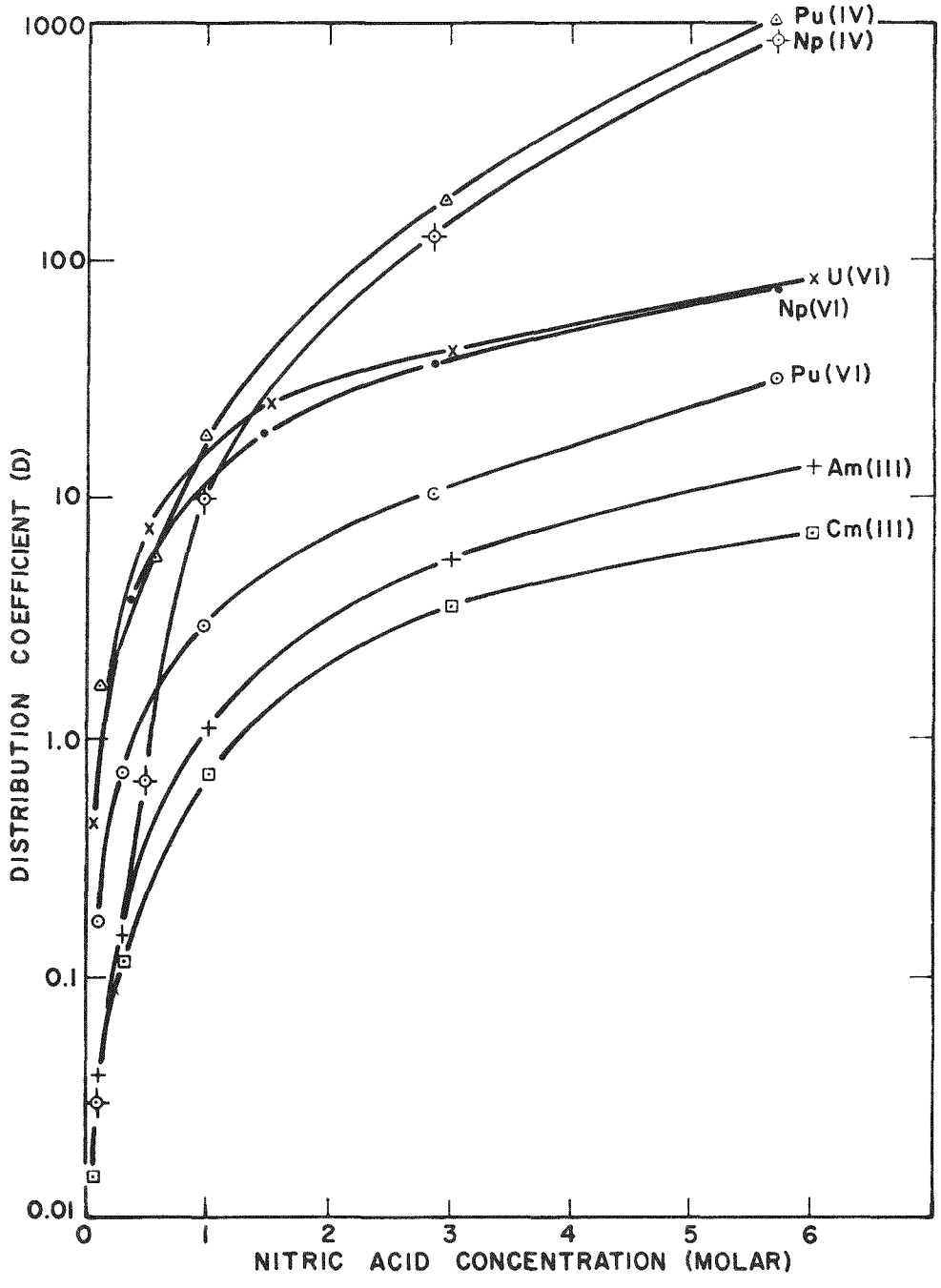

Figure 1. Distribution of Actinides Between Aqueous Nitric Acid Solutions and 30% DHDECMP in DIPB

The sample then was capped to prevent loss of NO_2, and allowed to set one hour. After this period, 1:1 extractions were made in the manner described in previous reports.

Efforts to determine distribution coefficients for Pu(III) using 0.025 M $Fe(SO_3NH_2)_2$ or 0.25 M sodium formaldehyde sulfoxylate ($NaCH_2OSO_2$) were successful up to 1 M nitric acid. Above that acid concentration oxidation to Pu(IV) readily occurred.

Other areas of interest that are basic to understanding the extraction capabilities of DHDECMP are being pursued. Additional studies will be made on how the variance in nitrate and hydrogen ion concentrations independently affect americium distribution coefficients.

The nature of the extracted complex also presents an interesting problem. Evidence in the literature[2] indicates that one of the methylene protons in DHDECMP could be acidic. Considering the similarity in structure of DHDECMP to acetylacetone about the methylene carbon, this is not too surprising. Acidic methylene hydrogens could have important roles in the ability of DHDECMP to form complexes. Loss of a methylene proton would allow neutral complexes of metals to be extracted into the organic phase.

In addition, aromaticity similar to metal complexes of acetylacetone might exist in these complexes:

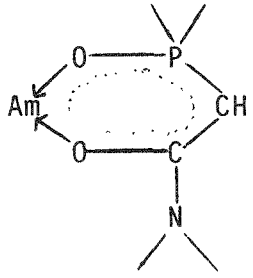

The correct number of π electrons (6) are available for this structure. Whether or not enough planarity exist for effective π orbital overlap is speculative. Efforts to obtain a metal complex of DHDECMP will be attempted. An NMR spectra of this complex should show a large down-field shift if aromaticity does exist.

The capacity of DHDECMP to load with rare earth elements was determined during this quarter. In this experiment, varying concentrations of La were extracted from 3.0 M HNO_3 into 30% DHDECMP-DIPB. These results are given in Figure 2, a plot of aqueous vs organic equilibrium La concentration. As expected, the D_{La}[3] is inversely proportional to its concentration in the extractant. The distribution coefficient dropped below one when the extractant was loaded to ~70% of its theoretical capacity. It should also be noted that when loaded to ~86% of its capacity the organic separated into two phases. In the actinide removal process envisioned for LWR Waste the extractant would be loaded to ~5% of its capacity. Hence, there would be no loading problem due to rare earth elements.

---

[2]M. R. Youinou, J. E. Guerchais, M. E. Louer, D. Grandjean, Inorganic Chemistry 16, p 872, 1977.

[3]In accordance with the ISEC-74, this notation will be used in all future reports. This notation replaces E_a^o.

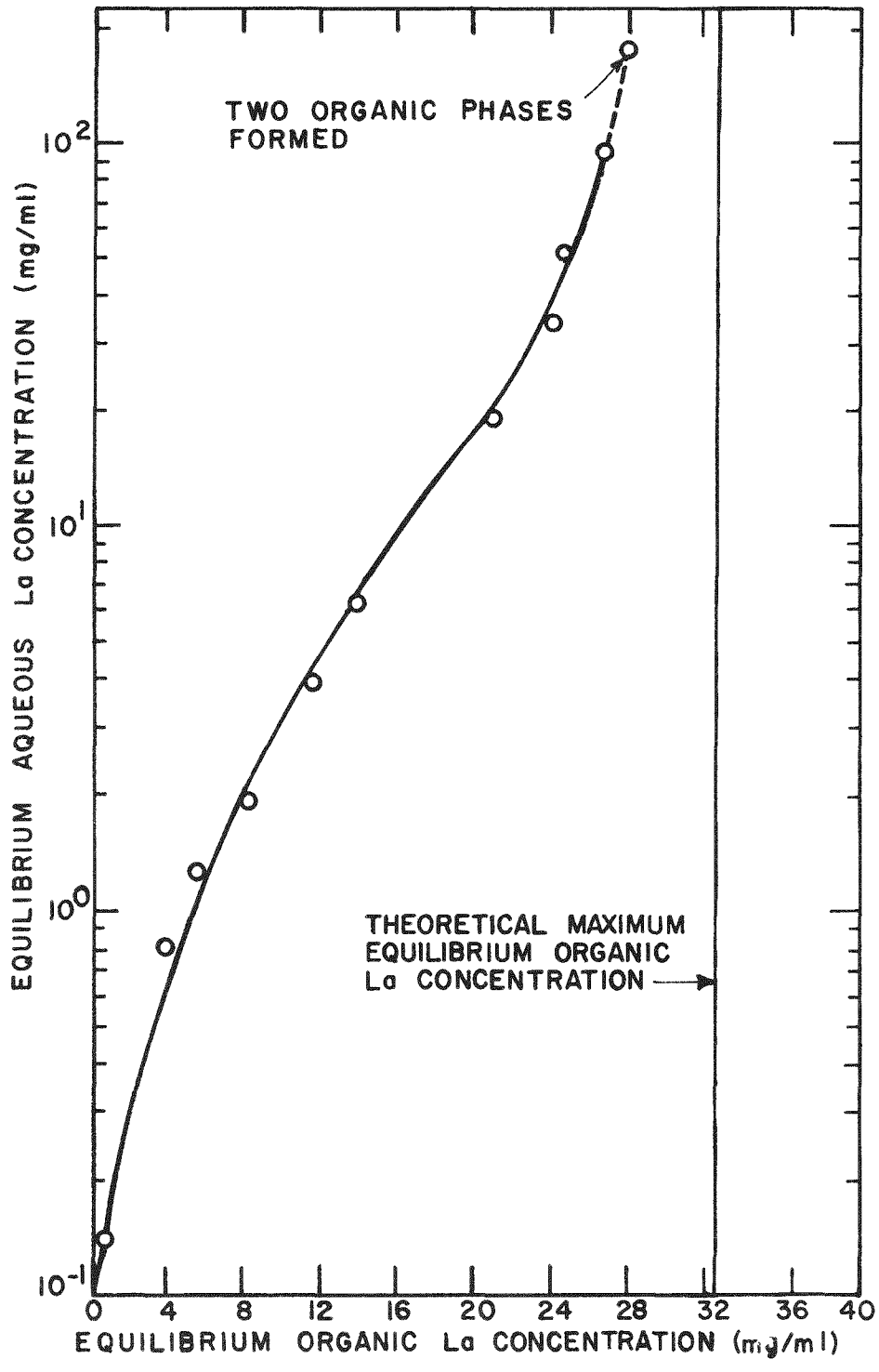

Figure 2. La Loading for 30% DHDECMP in DIPB

II. KRYPTON-85 STORAGE DEVELOPMENT

(R. Benedict, A. B. Christensen, L. T. Cole, M. Hoza, and D. A. Knecht)

1. Storage Alternatives and Testing

A contract was awarded to Fluor for A-E work on a conceptual design for installation of a hydrogen recombiner at the ICPP rare gas plant. Representatives of Fluor visited ICPP and reviewed our requirements. Zirconium dissolver off-gas composition was analyzed for O_2, F^-, I_2, and noble metals; calculations of the results are under way. Zeolite samples containing krypton or argon were placed on a gamma-radiation field at ≳100-200°C for preliminary long-term storage testing.

A revised draft of the report, "^{85}Kr Immobilization Prior to Long-Term Storage", was completed. The amounts of material required to immobilize ^{85}Kr produced in a year at 2000 Mg/yr (1 Mg = 1 metric ton) reprocessing plant are shown in Table 4 for various waste forms. Zeolite encapsulation and ion implantation/sputtering (shown for Ni and amorphous GdCoMo) appear to be the only methods which will give suitably large loadings (≳40 $cm^3 g^{-1}$).

2. Pressurized Cylinder Storage

Rubidium Corrosion - Pressurized cylinder material test specimens (hollow, notched, and C-ring) were put into a gamma-radiation field and rubidium environment for a ≳3-month test.

Conceptual Design of Storage Facility - A capital cost estimate (±30%) was completed for a krypton-85 storage facility (using pressurized cylinders) at a 2,000 Mg/yr commercial reprocessing plant, based on preliminary conceptual design by ACC in October 1976.[4] The cost estimate was made by Bechtel Inc. for ERDA as part of the Generic Environmental Statement for Commercial Wastes. The facility was assumed to be built in 10-year increments, at the following costs (mid-year 1976 dollars):

Head-End Plus Storage for 0-10 Years	$ 75,000,000
Storage for Each 10-Year Increment	$ 44,500,000
Total for 40-Year Storage	$208,500,000

Since storage of krypton at pressures greater than 3.4 MPa (500 psi) (which was used for the above estimate) is possible with commercial cylinders, there should be some reduction in cost due to the reduced number of storage positions required. An analysis of the heat load in a storage cell under accidental loss of cooling is required to assess the hazard of storing greater pressures per cylinder. The results of such a calculation are shown in Table 5 for the storage configuration used for the cost estimate.

---

[4] Technical Division Quarterly Progress Report, October 1 - December 31, 1976, ICP-1111, Idaho National Engineering Laboratory, Idaho Falls, ID, March 1977.

TABLE 4

ANNUAL REQUIREMENTS OF MATERIALS USED TO IMMOBILIZE ^{85}Kr[a]

Material	Kr Loading, Atom %[b]	Kr Loading, cm^3/g[c]	Volume Fraction[d]	Annual Volume,[e] m^3	Annual Weight,[e] Mg
Pressurized Cylinders:[f]					
3.4 MPa	100.0	---	29	6.5	8.3[g]
13.8 MPa	100.0	---	100	1.9	2.5[g]
Zeolite[h]	---	40	26[h]	7.3[h]	4.8
Nickel[i]	1.0	3.9	34	5.6	49
	5.0	20.1	179	1.1	9.5
	10.0	42.4	378	0.5	4.5
Aluminum	5.0	43.7	118	1.6	4.4
Glass[j]	---	$\lesssim 1$	$\lesssim 1$[j]	$\gtrsim 190$[j]	$\gtrsim 190$
Amorphous	30.0	127	888[k]	0.2[k]	1.5
$Gd_{0.11}\ Co_{0.73}\ Mo_{0.16}$					

[a]Annual production of 6% ^{85}Kr in krypton : 630 PBq, 191 M^3 at STP, or 0.71 Mg.

[b](100 x no. of atoms Kr)/(total no. of atoms).

[c](STP cm^3 Kr)/(g solid) basis unencapsulated solid.

[d](STP cm^3 Kr)/(cm^3 solid) basis unencapsulated solid; bulk density of pure material assumed unless otherwise specified.

[e]Does not include the encapsulated volume or weight (0.7 Mg) of krypton.

[f]Assuming DOT specifications 3AA-2400 cylinders at 49.6 L volume and 63 kg tare weight.

[g]Tare weight of cylinders.

[h]Assuming a bulk density of 0.65 g cm^{-3}.

[i]Values for iron are similar.

[j]Assuming a bulk density of 1 g cm^{-3}.

[k]Assuming a bulk density of 7 g cm^{-3}.

Pressurized carbon steel cylinders rated at 13.8 MPa (136 atm or 2000 psi) can withstand pressures up to 40.5 MPa (5900 psi) and temperatures up to 370°C.

TABLE 5

STEADY-STATE TEMPERATURES AND PRESSURES IN STORAGE CELL[a]

^{85}Kr Content, PBq	Initial Cylinder P, MPa	Cell Air T, °C	Cylinder T, °C	Cylinder P, MPa
4.74	3.4	84	125	4.8
9.03	6.9	107	175	13.6
11.0	8.6	117	196	20.4
12.9	10.3	126	215	29.1
16.4	13.8	142	248	52.7

[a]104-50 L cylinders containing 6% of ^{85}Kr in krypton, outside cell temperature at 45°C; 1 psi = 6.89×10^{-3} MPa.

Storage cost can be reduced by using higher pressures, but if a method for immobilizing ^{85}Kr can be developed for geologic storage, costs can be further reduced.

Heat transfer calculations for cylinders containing 6% ^{85}Kr in krypton were made using the Redlich-Kwong equation of state.[5] The resulting temperatures and krypton contents shown in Table 6 should be used to replace comparable values given in an earlier report[6] (which had used the ideal gas law). (The results in Table 5 were obtained using the more recent values.)

3. Zeolite Encapsulation Storage

Laboratory-Scale - Encapsulation experiments were run at various combinations of the following conditions: 410 and 510°C; 124, 159, and 193 MPa; and 0.5 to 24 h. The results obtained to date at 410°C and 159 MPa are shown in Figure 3 as a function of time. An empirical fit was obtained ($T \neq 0$) using the function

$$Y = 18.56 + 6.09 \ln(T)$$

for Y, the loading, and T, the time.

[5]J. M. Prausnitz and P. L. Chueh, Computer Calculations for High Pressure Vapor-Liquid Equilibrium, Prentice-Hall, Englewood Cliffs, N.J., 1968.

[6]B. A. Foster and D. T. Pence, An Evaluation of High Pressure Steel Cylinders for Fission Product Noble Gas Storage, ICP-1044, Idaho National Engineering Laboratory, Idaho Falls, ID, February, 1975.

TABLE 6

PROPERTIES AND FILLING RATES OF CYLINDERS CONTAINING ^{85}Kr[a,b]

Pressure, MPa	^{85}Kr Content, PBq	Heat Generation, W	Wall T[c] °C	Filling Rate, Cylinders/Yr	Total No. of Cylinders[d]
3.4	4.74	187	64	132.4	5295
8.6	11.0	434	98	57.1	2284
13.8	16.4	647	125	38.3	1533

[a]Assuming DOT specifications 3AA-2400 cylinders (49.6 L volume); 1 psi = 6.89×10^{-3} MPa.

[b]Annual ^{85}Kr production is assumed to be 630 PBq of 6% ^{85}Kr in krypton.

[c]Assuming natural convection cooling of vertical cylinder in air at 300 K.

[d]Total production during 40-year life of reprocessing plant.

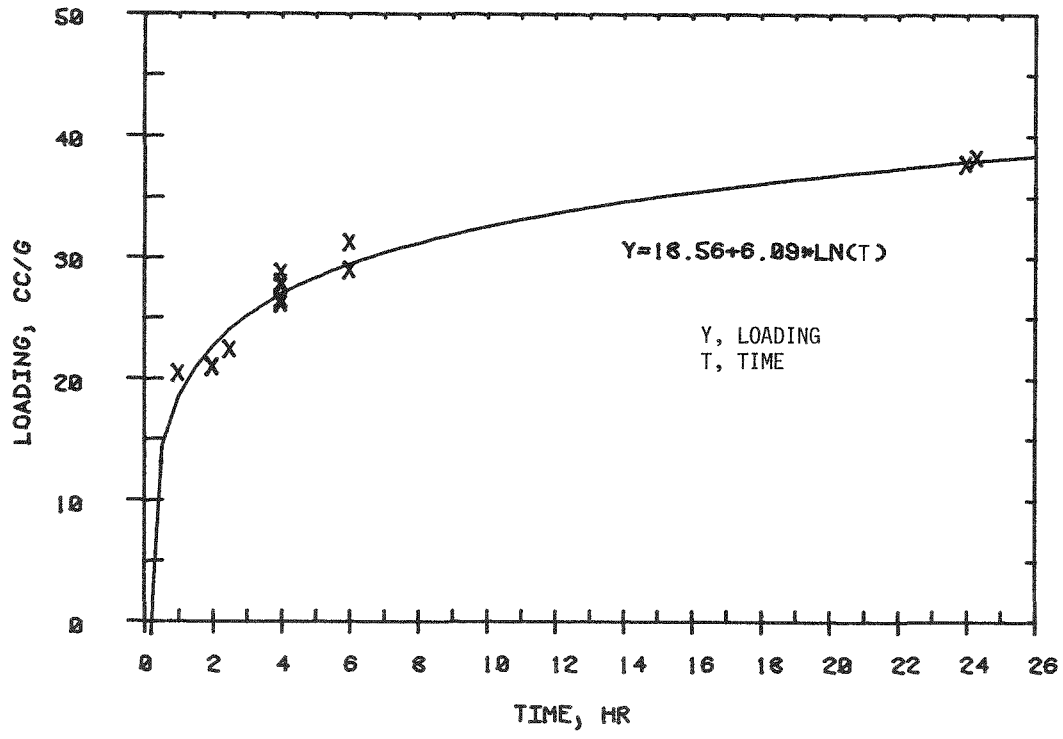

Figure 3. Krypton Loaded on Leached Sodalite at 410°C and 159 MPa as a Function of Encapsulation Time

The three 4-h runs shown in Figure 3 yielded an average krypton loading of 27.7 ± 1.4 $cm^3 \cdot g^{-1}$.

Encapsulation experiments (1 and 24 h) were also run at 510°C and 193 MPa (28000 psi) using zeolite, glass, quartz, silica gel samples, and aluminum powder. All samples except zeolite and Al were supplied by Battelle-Pacific Northwest Laboratory (BNWL). Krypton loadings are shown in Table 7. Some of the zeolites gave good loadings; aluminum and silica samples were not as good. Further experiments are planned to determine if additional silica outgassing will allow increased krypton loading.

TABLE 7

AMOUNT OF Kr ENCAPSULATED IN 24-H AT 510°C AND 193 MPa[a]

Material	Loading, $cm^3 \cdot g^{-1}$
Sodalite, Leached	34
Zeolite A, K-exchanged	67
Zeolite A, Rb-exchanged	57
Zeolite A, Cs-exchanged	43
Chabazite, Na-exchanged	59
Chabazite, K-exchanged	9
Erionite, K-exchanged	24
Aluminum powder	4
Six glass, quartz samples	0-6[b]
Three silica gel samples	0-3

[a] Calculated from weight gain; 193 MPa = 28000 psi.

[b] Most were <1 $cm^3 \cdot g^{-1}$ mass spectrometric analysis of one of samples showed 0.2 $cm^3 \cdot g^{-1}$ loading.

The mass spectrometric leakage measuring system was assembled and evacuation tests are in progress. The mass spectrometer will be connected when leaks have been repaired. Preliminary leakage tests of krypton from sodalite have been carried out using gas chromatrographic detection. The calculated activation energy of diffusion of krypton from sodalite was found to agree with the literature value.

Due to a breakdown of the thermal conductivity measurement apparatus, conductivity measurement of zeolite powder and granules will be discontinued for about 2 months. The results obtained so far are shown in Figure 4. It appears that the values are spanned by the two lines and

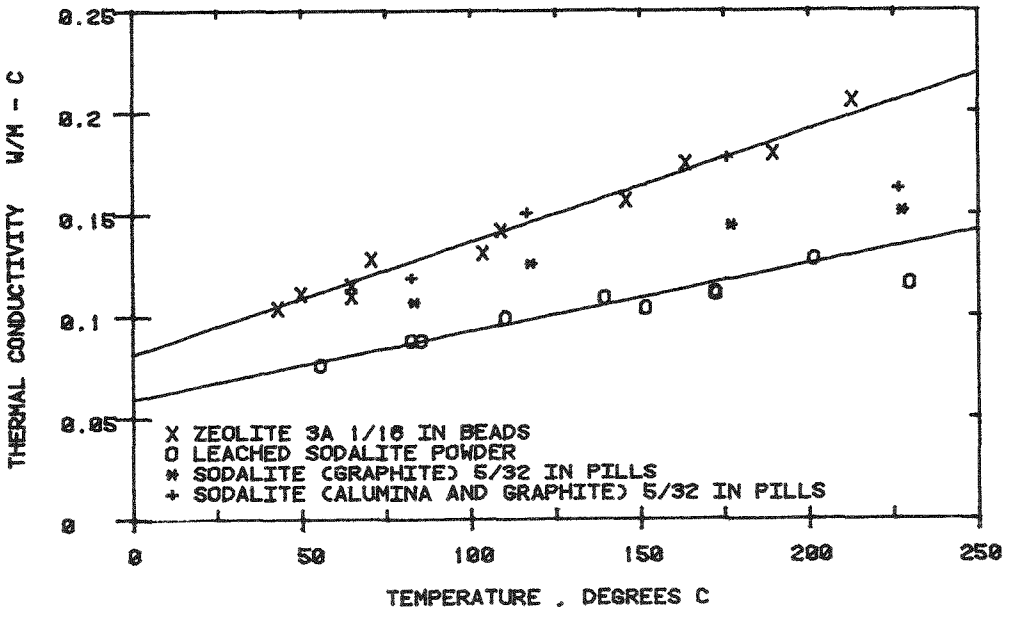

Figure 4. Thermal Conductivity of Unactivated Zeolite Samples

differences result more from physical form (powder vs. pellets) than from zeolite type.

A draft of the report on heat transfer considerations related to ^{85}Kr storage was completed. The report covers (1) physical properties of krypton, zeolite, and other potential storage media, (2) models and solutions for the required formulae, and (3) application of the models and solutions to heat transfer problems encountered in long-term storage and large-scale encapsulation of ^{85}Kr.

Pilot-Scale - The thermal conductivity of a packed bed of zeolite and krypton gas at high pressure was calculated[7-10] as a function of temperature and pressure (see Figure 5).

Using the data in Figure 5, the fractional extent of cooling (from encapsulation temperatures) in one or two hours of a 5- or 6-inch-diameter cylindrical high pressure vessel containing a packed bed of zeolite and

[7] R. Krupiczka, "Analysis of Thermal Conductivity in Granular Materials", Int Chem Eng., Vol. 7, pp. 122 and 144, 1967.

[8] E. J. Owens and G. Thodos, "Thermal-Conductivity-Reduced-State Correlation for the Inert Gases", AIChE Journal, Vol. 3, pp. 454-461, 1957.

[9] V. K. Saxena and S. C. Saxena, "Thermal Conductivity of Krypton and Xenon in the Temperature Range 350-1500 C", J. Chem. Phys., Vol. 51, pp. 3361-3368, 1969.

[10] R. Tufen, B. Le Neindre, and P. Bury, "Experimental Study of Thermal Conductivity of Krypton at High Pressures", C.R. Acad. Sci. Ser. B, Vol. 273, pp. 61-64, 1971.

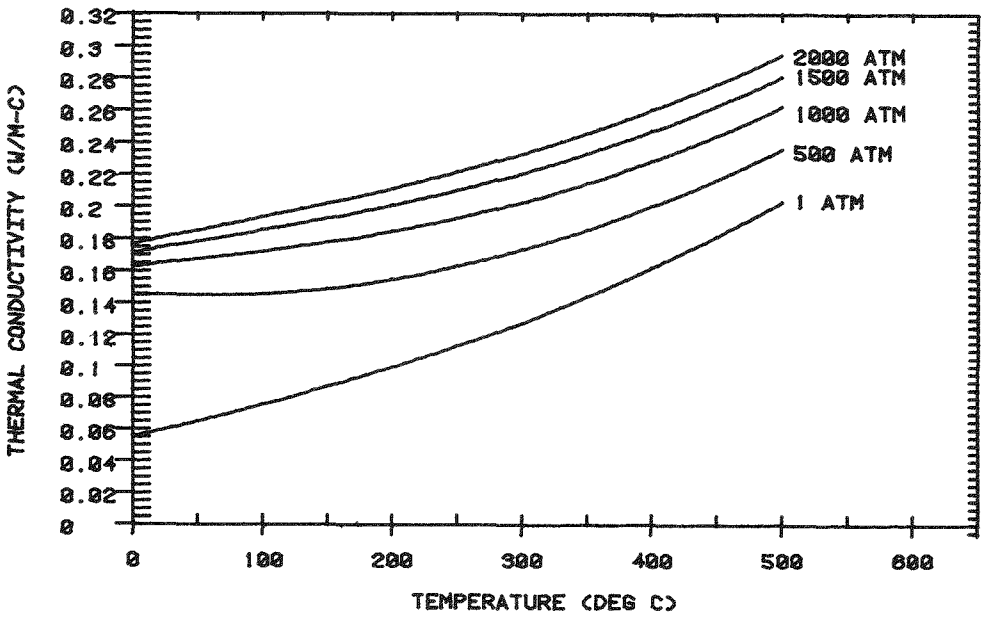

Figure 5. Thermal Conductivity of a Packed Bed of Zeolite and Krypton Gas as a Function of Temperature and Pressure, 1 atm = 0.1013 MPa

203 MPa (2000 atm) of nonradioactive krypton gas was calculated. The results are shown in Table 8.

These results show that cooling of large diameter zeolite beds during pilot-scale or commercial production-scale encapsulation could be a significant problem, even if the heat generation due to krypton-85 is not taken into account. Further calculations will be made for annular bed configurations with possible internal cooling.

An expenditure authorization for pilot-scale encapsulation system capital equipment funds was completed. Meetings were held with ERDA budget personnel to discuss funding of the proposed GPP facility to house the pilot-scale encapsulation system. It was decided that the facility could not be funded under GPP, and that the combined pilot-scale system and facility should be funded as a line item. Pilot-scale development will be deferred to make the ^{85}Kr Storage Development Program more compatible with the development progress of commercial fuel reprocessing. (A revised manpower and schedule 189 reflecting the program changes was submitted.) Pilot-scale system design criteria and related documents will be completed in FY 1977. A decision will be made by May 1978 on the approach which will be used for future pilot-scale development.

Plans for Next Quarter

A-E work on the conceptual design of the hydrogen recombiner will be completed, and capital equipment funds will be committed if the cost estimate is less than $800,000. Calculations of Zr off-gas composition will be completed. The Program Plan and a report on ^{85}Kr immobilization

TABLE 8

FRACTIONAL EXTENT OF COOLING OF A CYLINDRICAL VESSEL CONTAINING A PACKED BED OF ZEOLITE AND 203 MPa (2000 atm) KRYPTON AS A FUNCTION OF VESSEL RADIUS AND TIME

Time, h	Radius, cm	Fractional Extent of Cooling[a]
1	7.6	0.5
2	7.6	0.8
1	6.4	0.6
2	6.4	>0.9
1	5.1	0.9
2	5.1	>0.9

[a]Extent of cooling, γ, of centerline temperature relative to outside vessel temperature which is taken to be at the coolant fluid temperature

$$\gamma = \frac{T_c - T_o}{T_1 - T_o}$$

T_c = the centerline temperature (radius = o)
T_o = the initial temperature of the vessel
T_1 = the temperature of the vessel surface

methods will be issued. Radiation tests of pressurized cylinder materials in Rb and zeolites will be completed. Encapsulation and leakage experiments will continue. A report on heat transfer considerations in ^{85}Kr storage will be issued.

III. LWR OFF-GAS TREATMENT

(R. A. Brown, D. H. Munger, T. R. Thomas)

Work is continuing on a topical report of the NO_x-NH_3 reaction catalyzed by hydrogen mordenite.

Future Plans

The topical report will be completed and the program terminated by October 1977.

IV. ^{129}I ADSORBENT AND STORAGE DEVELOPMENT

(J. T. Nichols, L. P. Murphy, B. A. Staples, T. R. Thomas)

Recycle tests on a bed of silver-exchanged mordenite, Zeolon 900 (AgZ), in which airborne-elemental iodine is repeatedly loaded and stripped, are being conducted with simulated dissolver off-gas (DOG) streams. The experimental conditions are given in Table 9.

TABLE 9

Conditions for Recycle Tests

Experimental Parameter	Iodine Loading	Iodine Stripping
Bed Diameter (cm)	5	5
Bed depth (cm)	15	15
Particle size (mesh)	10-20	10-20
Superficial face velocity (m/min)	15	15
Bed temperature (°C)	150	500
Inlet pressure (mm Hg°)	700	760
Carrier gas	air	hydrogen
Iodine concentration at 21°C and 1 atm (mg/m^3)	1500*	7400
NO_2 concentration (%)	2	0
NO_2 concentration (%)	2	0
Dew point (°C)	35	nil
Iodine flux to and from bed ($mg/min\text{-}cm^2$)	1.5**	4.5

*Actual DOG concentration is anticipated to be about 380 mg I_2/m^3
**Actual DOG iodine flux would be about 0.4 $mg/min \cdot cm^2$

The AgZ test bed has been recycled five times. About 35 g of iodine is used for each loading; greater than 99% of the iodine is stripped at each regeneration. The loading tests are stopped when the decontamination factor is between 10^4 and 10^5. The results, along with the distribution of iodine from the top to the bottom of the bed, are given in Table 10.

The data indicate that the first 5 cm is in the saturation zone and the remaining 10 cm is in the mass-transfer zone. The average loading in the saturation zone is 187 mg I_2/g AgZ. The maximum loading in AgZ for complete conversion of Ag to AgI is 237 mg I_2/g AgZ. About 79% of the Ag

TABLE 10

Iodine Loading vs. Number of Recycles

Cycle	mgI_2/g AgZ in each 2.5 cm segment 1	2	3	4	5	6	Ave. Loading mgI_2/g AgZ
0*	179	174	164	132	60	7	119
1	182	170	161	127	71	10	120
2	212	201	178	147	76	13	138
3	192	192	180	150	70	5	131
4	194	189	179	145	67	8	130
5	191	180	176	147	80	10	131

*The AgZ was pretreated with H_2 at 500°C for the initial loading cycle.

is being used. No decline in iodine loading in the first 5 recycles is apparent; variations in the loadings are probably due to experimental error. The test bed will be recycled at least 15 times to check for loss of iodine-loading capacity.

An airborne-iodine concentration about four times greater than anticipated in actual DOG streams was used to shorten testing time. The iodine stripping rate is about ten times faster than the anticipated loading rate. However, the data given here are based on the initial 90% of iodine removed. Tests are being run to determine the tailing profile and average stripping rate based on 99% removal.

Iodine loadings of 400 mg iodine per gram lead-exchanged faujasite (PbX) have been obtained on PbX beds downstream of the AgZ bed during regeneration. The maximum iodine loading in PbX for complete conversion of Pb to PbI is 440 mg. About 90% of the lead is being used. The vapor pressure of iodine chemisorbed on PbX (PbIX) has been estimated. Samples of PbIX beads were placed in a heated optical cell and the vapor pressure of $I_2(g)$ vs. temperature determined from the absorption intensity of the $I_2(g)$ visible spectrum. Extrapolation of the data to room temperature indicated iodine-vapor pressures of less than 10^{-8} atm for PbIX in air, nitrogen, and hydrogen blankets. Beds of PbIX tagged with ^{131}I were immersed in hexane at room temperature for 16 hours to check for physisorbed iodine. Iodine in the hexane supernate was not detected. Previous tests have indicated that the water solubility of PbIX is less than that of PbI_2. The PbIX produced during the regeneration of AgZ is a dry yellow solid with a low iodine-vapor pressure and iodine-water solubility. Its physical properties and high iodine loading may make it an acceptable material for storage.

The final draft of a topical report entitled, "Airborne Elemental Iodine Loading Capacities of Metal Zeolites and a Method for Recycling Silver Zeolite", has been prepared. The process-flow diagram, which was used in the report, for full-scale application of AgZ recycle technology to iodine recovery is shown in Figure 6. Tables 11, 12, and 13 present the operational characteristics of an LWR fuel reprocessing plant, the laboratory data, and the design criteria, respectively.

The AgZ primary bed was sized for a 30-day loading operation. During the adsorption of iodine, the bed would attain some saturation loading of H_2O, NO_x, HNO_3, and ^{85}Kr. We have assumed an upper limit of 51 kg of H_2O and 36 kg of NO_2 for 0.65 m^3 of AgZ. During the 48-hr purge cycle, an average of 1.8 kg/h NO_x H_2O would be added to the 11.7 kg/h NO_x H_2O already present in the DOG. The combined load would increase the NO_x H_2O flow to the parallel AgZ primary bed (not shown in flow diagram) by about 13% over normal operation. The two parallel AgZ adsorbent trains permit continuous iodine recovery while one of the beds is being regenerated.

After the purge cycle, the AgZ bed is isolated from the DOG and opened to Streams 6-11. The air in the bed is purged off with nitrogen and vented just before the nitrogen inlet. Hydrogen is added to the nitrogen until the regeneration gas consists of 100% H_2. The AgZ primary bed is brought up to temperature, and the iodine stripped as hydrogen iodide. Any chemisorbed bromine would also be removed as HBr but at a rate 100 times faster than iodine. The desorbed iodine and bromine are chemisorbed as some form of lead halide on the PbX. Residual water on the AgZ and the PbX beds would be partially removed by the condenser. The regeneration process is a closed loop in which the H_2 is recirculated. Although 9 kg H_2/h would be recycled, only 4 kg H_2/y would be required to transport the halides as HI and HBr to the PbX.

The transfer of iodine to the PbX would be discontinued when iodine is detected in Stream 8. The self-contained cartridges in the PbX storage bed would be removed and placed in 0.2 cubic metre (55-gal) drums for storage. The PbX backup-bed cartridge would be repositioned at the top of the PbX storage-bed holder and new cartridges placed below it and in the backup-bed holder. This would provide a fresh backup-bed for every new set of cartridges placed in the PbX storage-bed holder.

After regeneration of the AgZ bed, it would be placed on standby status to remove iodine from the DOG after the parallel AgZ bed is saturated with iodine. With this design, the two AgZ beds would be regenerated five times a year.

Plans for Next Quarter

A study of the effect of dew point, NO_2, and NO concentration on the iodine loading of 15-cm-deep beds of AgZ will be completed. A topical report covering the laboratory effort from February to October 1977 will be drafted. The process-flow diagram for AgZ regeneration and recycle will be updated. The iodine adsorbent program will be terminated.

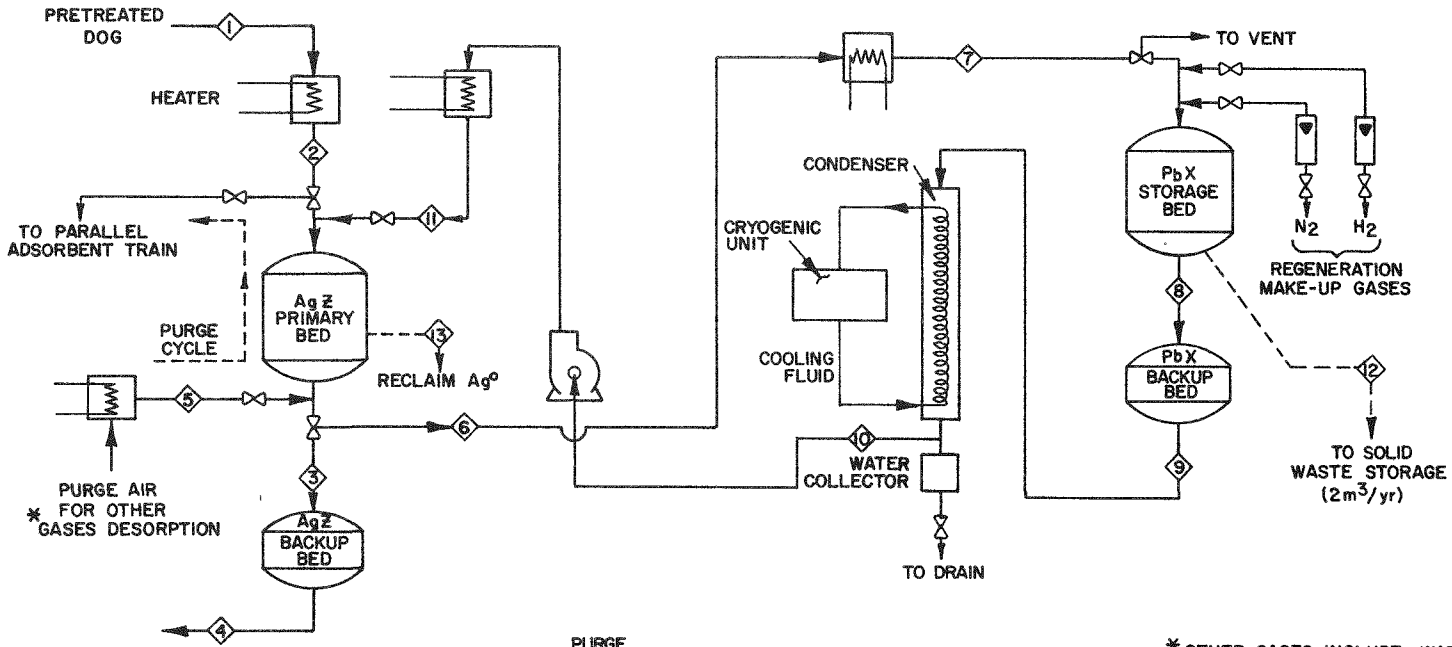

	LOADING CYCLE = 30 DAYS				PURGE CYCLE 2 DAYS	** REGENERATION CYCLE = 3 DAYS					
STREAM NO.	1	2	3	4	5	6	7	8	9	10	11
PRESSURE (atm)	1.0	1.0	0.8	0.75	1.1	0.94	0.94	0.87	0.85	0.85	1.0
TEMPERATURE (°C)	45	150	150	150	300	500	150	150	150	0	500
FLOW (m^3/h)	209	278	346	369	56	296	161	174	178	114	278
FLOW (kg/h)	233	233	233	233	38	9.6	9.6	9.6	9.6	9.6	9.6
NITROGEN	166	166	166	166	28	0	0	0	0	0	0
OXYGEN	51	51	51	51	9	0	0	0	0	0	0
OTHER GASES *	14.6	14.6	14.6	14.6	0.5	>0.6	>0.6	>0.6	>0.6	<0.6	<0.6
HYDROGEN	0	0	0	0	0	9	9	9	9	9	9
IODINE	7.1×10^{-2}	7.1×10^{-2}	7.1×10^{-4}	7.1×10^{-6}	0	0.26	0.26	2.6×10^{-3}	2.6×10^{-6}	2.6×10^{-6}	2.6×10^{-6}

* OTHER GASES INCLUDE: WATER VAPOR, NO_x, ARGON, AND KRYPTON AT 4.3, 7.4, 2.8 AND 0.09 kg/hr RESPECTIVELY.

** FLOWS FOR CLOSED LOOP. ABOUT 4 kg/yr H_2 NEEDED TO TRANSFER IODINE AS HI FROM AgZ TO PbX.

⟨12⟩ SPENT PbX TO WASTE STORAGE

⟨13⟩ LIFETIME OF AgZ UNKNOWN.

ACC-A-2622

Figure 6. Process Flow Diagram for the Recovery of Iodine From Dissolver Off-Gas

TABLE 11

Assumed Operational Characteristics
of an LWR Fuel Reprocessing Plant

1.	Plant capacity	2000 tonne/y
2.	Fuel burnup	28 700 MWd/tonne
3.	Cooling period	1.5 y
4.	Plant on-stream time	300 d/y
5.	Air flow through dissolver at 0°C and 1 atm press	2.83 m^3/min
6.	DOG pretreatment systems before iodine removal	H_2O/NO_x scrubber, de-entrainer, silica gel, and HEPA
7.	NO_x conc. after pretreatment	≤2%
8.	H_2O dew point after pretreatment	35°C
9.	Volatility of I_2 from dissolver	>99%
10.	Halide inventory from burnup	
	$^{127}I + ^{129}I$	470 kg/y
	^{81}Br	27 kg/y
	^{81}Br normalized to ^{129}I	43 kg/y
	total halides as ^{129}I	513 kg/y

TABLE 12

Fundamental Data from Laboratory Observations

1.	Iodine loading on AgZ	≥ 100 mg I_2/g AgZ
2.	Iodine loading on PbX	≥ 300 mg I_2/g PbX
3.	Dry density of AgZ	0.79 g/cm^3
4.	Dry density of PbX	0.85 g/cm^3
5.	Desorption rate of HI from AgZ at 500°C, 1 atm and 15 m/min face velocity	4.5 mg HI/min·cm^2 in pure H_2
6.	Pressure drop across AgZ at 150°C, 1 atm and 15 m/min face velocity	0.097 atm/m in air
7.	Pressure drop across AgZ at 500°C and 15 m/min face velocity	0.03 atm/m in hydrogen
8.	Pressure drop across PbX at 150°C and 11 m/min face velocity	0.02 atm/m in hydrogen

TABLE 13

Design Criteria for AgZ and PbX Beds

		face velocity (m/min)	diam (m)	length (m)	volume (m^3)	weight (Mg)	iodine loading (kg)
1.	AgZ primary	15	0.63	2.1	0.65	0.51	51
2.	AgZ backup	19	0.63	0.5	0.15	0.12	12[b]
3.	PbX storages[a]	11	0.55	3.2	0.76	0.64	192
4.	PbX backup	12	0.55	0.8	0.19	0.16	48[b]

[a]PbX storage bed consists of four self-contained cartridges designed to fit in 0.2m^3 (55 gal) drums. Number of cartridges needed per/yr = 10.6

[b]During normal operation the backup beds would not be loaded with iodine.

V. WASTE MANAGEMENT[11]

(B. E. Paige)

Liquid waste from spent nuclear fuels is concentrated to increase storage capacity and, thereby, reduce the cost of interim storage of the liquid waste. Nitric acid waste is produced from the tributyl phosphate extraction step during the reprocessing of either defense fuel or from several alternative fuel cycles currently being considered for power reactor fuel. In fuel reprocessing, liquid waste will generally be concentrated and placed in interim storage tanks as a nitric acid solution because neutralization increases the volume of waste and interferes with some solidification processes. The primary purpose of the current waste evaporation and storage project is to study factors which affect the rate of heat transfer as well as the service life of equipment in nitric acid waste solutions. Other waste solutions will be studied as they are identified in future reprocessing studies.

Factors being investigated include formation of solids, fouling of heat transfer surfaces, and the behavior of off-gas. These factors are particularly important in liquid waste generated from power reactors because they contain high concentrations of fission products resulting from the high burn-up attained prior to discharge of the spent fuel. Also, cladding is removed prior to fuel dissolution, thus eliminating dissolved metal salts which dilute the fission products in some liquid wastes.

[11]Part of the program Alternative Fuel Cycle Technology administered by Savannah River Operations and Savannah River Laboratory.

The behavior of materials of construction and the monitoring of corrosion in process equipment is also being investigated. A literature review of nitric acid corrosion[12] showed that very little information is available, even though failure of waste evaporators, especially reboiler tubes, has been a continual problem in nuclear fuel reprocessing. In current studies, particular attention is given to the investigation of the behavior of materials under process conditions.

Three types of simulated high level liquid waste (HLLW) solutions, which were patterned after HLLW solutions used in other waste studies[13], were used initially for the current program. Data from these solutions were compared to data from wastes simulating more recent estimates of acidic HLLW compositions[14]. Solids formation, physical properties, and corrosion behavior were found to be far more dependent on nitric acid concentration, total solids, and dissolved corrosion product concentration than on variations in the fuel or the process being simulated. The exception, however, is that high concentrations of iron, which can result from dissolution of fuel dissolver baskets, affect both corrosion and solids formation.

Current studies are continuing with a typical simulated HLLW expected from a tributyl phosphate extraction process. The HLLW contains gadolinium as nuclear poison and natural uranium as the actinides (uranium, thorium, and plutonium). Low levels of phosphate, which represent effective operation of solvent clean-up equipment and estimated levels of corrosion products from process equipment are added.

1. Evaporation

The evaporation studies for this quarter were performed in the small-scale thermosiphon evaporator unit. The unit was operated to identify operating problems with solutions containing solids, to investigate evaporation of HLLW from a tributyl phosphate extraction process, and to evaluate corrosion of a Type 304L stainless steel reboiler tube specimen. The corrosion results are reported in Section 3.0.

Figures 7 and 8 show the evaporator and auxiliary equipment which are located inside a 3-meter (10-feet) ventilated enclosure to permit use of actinides in waste solutions. Figure 7 shows the reboiler steam section, the preheater steam section, the recycle section, and the product and condensate collection system. Figure 8 shows the feed tank, the vapor head, the demister section, and the condenser. A sketch of the small-scale evaporator was published previously[15].

---

[12] M. W. Wilding and B. E. Paige, Survey on Corrosion of Metals and Alloys in Solutions Containing Nitric Acid, ICP 1107 (December 1976).

[13] LWR Fuel Reprocessing and Recycle Progress Report for April 1 - June 30, 1976, ICP-1101 (November 1976).

[14] LWR Fuel Reprocessing and Recycle Progress Report for January 1 - March 31, 1977, ICP-1116 (April 1977).

[15] LWR Fuel Reprocessing and Recycle Progress Report for July 1 - September 30, 1976, ICP-1108 (December 1976).

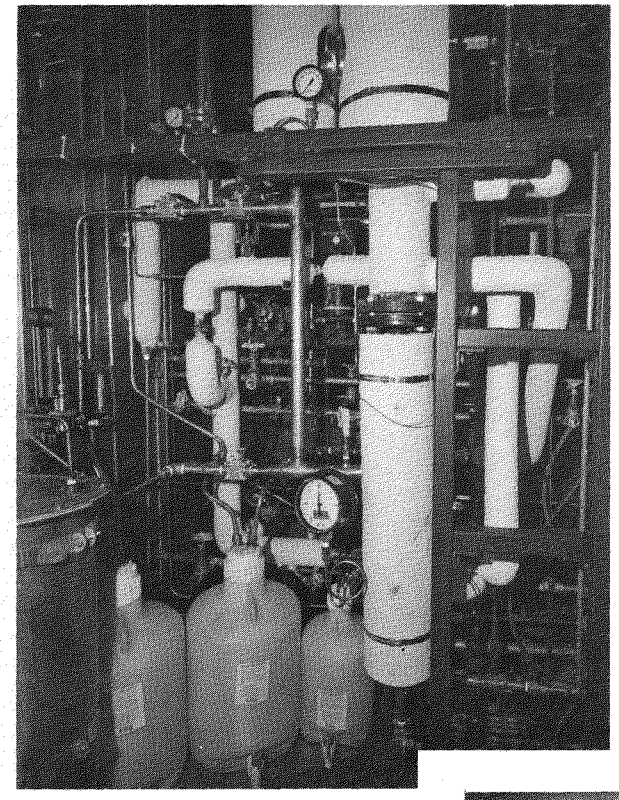

Figure 7. Lower Portion Thermosiphon Evaporator

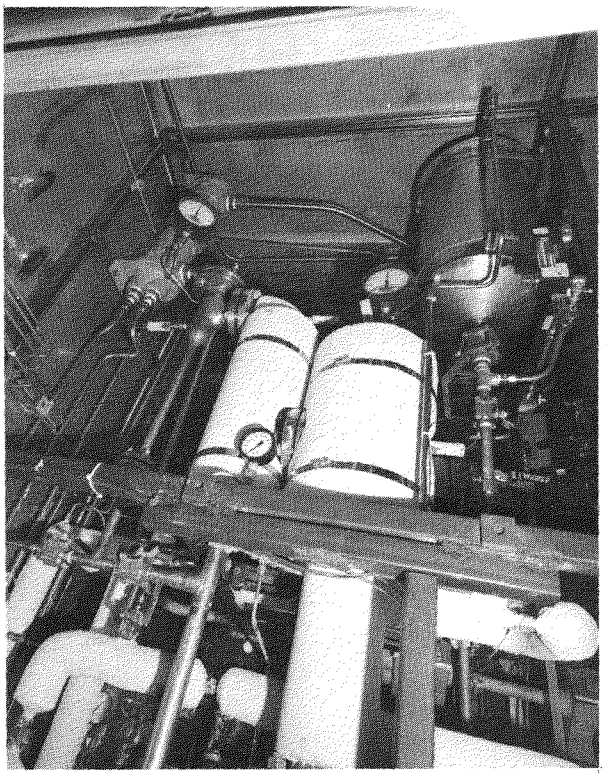

Figure 8. Upper Portion Thermosiphon Evaporator

The evaporator was operated with simulated HLLW and with nitric acid. Two levels of evaporation were selected for investigation. According to earlier laboratory evaporation of HLLW, 340 L/MTU (90 gal/MTU) represents the practical limit of concentration from the standpoint of total solids content. A concentration of 1380 L/MTU (365 gal/MTU) is estimated to be the concentration limit with respect to heat removal in storage tanks where in-tank cooling coils are the primary source for heat removal. Based on these limits, the runs were made at three operating conditions as follows:

(1) The evaporation of 20 litres of solution from 4900 L/MTU at 2.5 M nitric acid to 1380 L/MTU at 7.5 M nitric acid in 48 h.

(2) The evaporation of 20 litres of reconstituted solutions from Evaporation 1 from 4900 L/MTU at 2.5 M nitric acid to 340 L/MTU at 7 to 9 M nitric acid in 62 h.

(3) The recirculation of the solution from Evaporation 2 at 340 L/MTU for an additional 48 h while recycling all condensate.

A complete set of runs was first made with nitric acid to establish a baseline for the Type 304L stainless steel reboiler tube material. Evaporations were performed at the same conditions using simulated HLLW. The HLLW feed contained 6 g/L total fission products which represent extraction raffinate at 4900 L/MTU from fuel irradiated to 33,000 MWd/MTU and cooled for 150 days. The feed HLLW also contained 2 g/L uranium, 7 g/L gadolinium, 0.34 g/L phosphate and 0.01 g/L dissolved corrosion products.

The simulated HLLW solutions were prepared by combining stock solutions in an appropriate manner as to approximate the introduction of the components into an actual process solution. The advantages of using a series of stock solutions to prepare simulated HLLW are (1) the flexibility to rapidly prepare solutions of various concentrations of selected components, and (2) less undissolved solids in the simulated waste solution than when all reagents are added at once to a single vessel for dissolution[16]. Solution concentrations used to charge the evaporator were at the expected level of the evaporator product and were boiled during preparation to insure steady state conditions at the start of the run.

1.1 Operating Characteristics of Evaporator (G. R. Villemez, C. B. Millet)

The fast settling rate of the undissolved solids in the concentrated HLLW solution caused plugging during the operation of the thermosiphon evaporator. Most of the plugging problems were experienced at the higher concentrated solution level of 340 L/MTU as compared to a concentration level of 1380 L/MTU. Previously, laboratory evaporations have shown that there were 12% undissolved solids in HLLW solutions concentrated to 340 L/MTU. These solids settled within 10 minutes, but were easily suspended with gentle agitation.

---

[16] LWR Fuel Reprocessing and Recycle Progress Report for April 1 - June 30, 1976, ICP-1101 (November 1976).

In the thermosiphon evaporator, the feed line became plugged due to settled solids which collected below the recycle line in the area of the preheater. Air pressure applied to the feed line dislodged the solids easily. Unstable operating conditions occurred whenever the evaporator became plugged; an increase in the reboiler temperature and a decrease in HLLW recirculation resulted. The feed line is currently being connected directly below the reboiler tube to eliminate the pocket resulting from the pre-heater installation; this should minimize the plugging problem for future operations. An automatic control valve in the feed line will also be installed with a control signal from the evaporator head pressure to assist in maintaining a stable operating liquid level.

The thermosiphon evaporator operated very well in a total recycle mode for 48 hours with HLLW at the 340 L/MTU level.

1.2 Heat Transfer of Evaporator (G. R. Villemez, C. B. Millet)

The rate of heat transfer, q, is expressed as the product of three factors: the over-all heat transfer coefficient (U), the area of the heat transfer surface (A), and the temperature difference (ΔT). The relationship is

$$q = U \cdot A \cdot \Delta T.$$

The area is based on the inside diameter of the 1-inch reboiler tube. The reboiler tube exposed to the condensing steam was 30 cm (12-inches) in length; an additional 15 cm (6 inches) of the reboiler tube were exposed to the condensate. The apparent temperature difference was calculated from the condensing steam temperature and the measured saturated vapor temperature above the boiling liquid. The feed solution was preheated by steam to the temperature of the recirculated solution. The solution temperature was near the boiling point at the feed end of the reboiler section. This resulted in utilizing the entire length of the reboiler tube as a corrosion specimen.

The maximum allowable steam temperature in a waste evaporator is 130°C due to the explosion hazard of tributyl phosphate and nitric acid in actual process conditions. Within this temperature limit, the small-scale evaporator can be operated at a vapor velocity of 0.3 to 1.22 m/s (1 to 4 ft/s) using the steam control.

No data are available for the decomposition of nitric acid during evaporation.

The rate of heat transfer, q, was calculated as the product of the latent heat of evaporation of water at the saturated vapor temperature and the vapor rate at the atmospheric pressure of 84.7 kPa (12.3 psi) at 1585 metres (5200 ft) elevation. The calculated heat transfer rates should be within 10% of the actual value.

1.21 Rate

The apparent over-all heat transfer coefficient for current runs was calculated from operating data taken during steady-state conditions.

These preliminary data are shown in Figure 9 for nitric acid and HLLW during evaporation from 4900 L/MTU containing 2.5 M nitric acid.

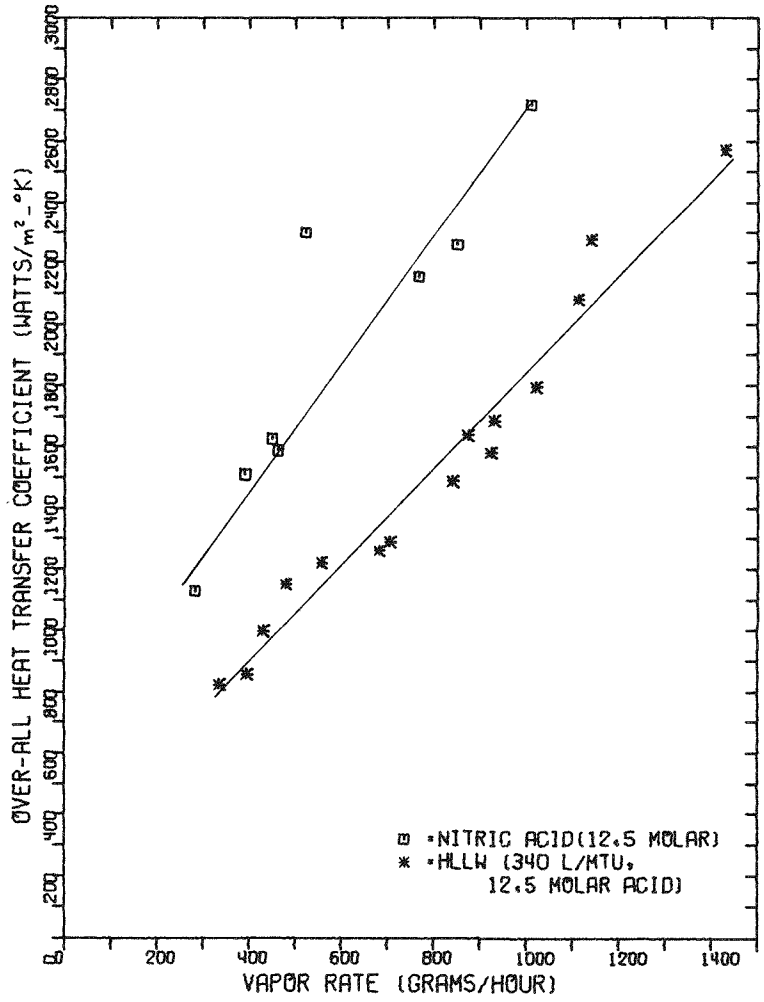

Figure 9. Heat Transfer Data for Initial Evaporator Runs

The over-all heat transfer coefficient increased as the vapor rate increased. The vapor condensate composition was in the range of 2 to 3 M nitric acid. A vapor rate of 300 g/h is equivalent to 0.3 m/s (1 ft/s) vapor velocity in the reboiler tubes assuming the vapor volume of water. The over-all heat transfer coefficients for the HLLW solutions were 70 to 80% of the base line nitric acid values. The coefficients varied from 760 to 2080 $W/m^2 \cdot K$ (134 to 367 $BTU/h \cdot ft^2 \cdot °F$) depending on the vapor velocities which varied from 0.3 to 1.22 m/s (1 to 4 ft/s). Since the heat transfer coefficients were similar for nitric acid and HLLW at lower solids content (1380 L/MTU and 7.5 M nitric acid), the lower heat transfer coefficients for HLLW solutions at the 340 L/MTU level may be due to the scale formed from the HLLW solution on the reboiler tube as well as to changes in the physical properties of the solution.

1.22 Scaling and Fouling

Scale was formed in the reboiler tube section during the evaporation of the simulated HLLW waste solution. Scale results in a fouling factor for the overall heat transfer coefficient during the evaporation process. Scale deposited on the feed end of the reboiler tube is shown in Figure 10. The scale deposit was thicker, as shown in Figure 11, in the top of the reboiler tube which was exposed to the steam and hence, the maximum temperature. This figure shows that scale did not form uniformly on the tube sheet.

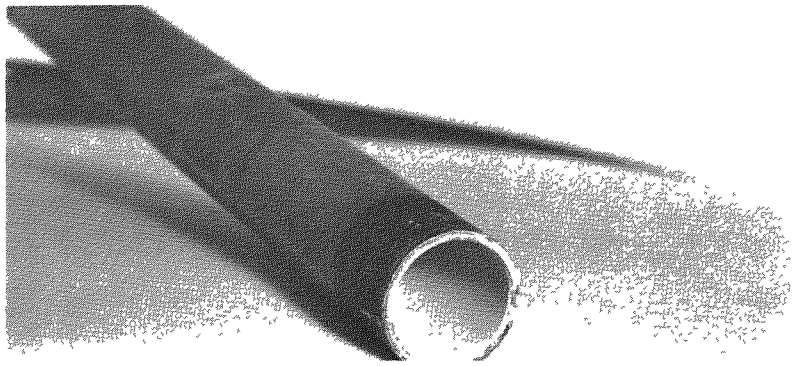

TYPE 304L S.S. REBOILER TUBE EXPOSED TO LWR WASTE SOLUTION - 1

Figure 10. Scale on Feed End of Reboiler Tube

1.23 Nature of Scale

X-ray diffraction patterns indicate that a major component of the scale consists of the hydrated zirconium-molybdenum compound which is also the major component in the precipitates from laboratory evaporations of HLLW. The X-ray pattern for the remainder of the material corresponds to the pattern for $Fe(UO_2)_2(PO_4)_2 \cdot nH_2O$. The latter compound was identified in scale deposits on the glass laboratory evaporator but not in the undissolved solids of the evaporated slurries. Examination of the scale by scanning electron microscope (SEM) shows that the solids are not definite crystals as have been precipitated from HLLW slurries evaporated in the glass laboratory evaporator. Additional examinations will be made to determine if similar scale has formed in other parts of the evaporator, and methods of descaling will be investigated.

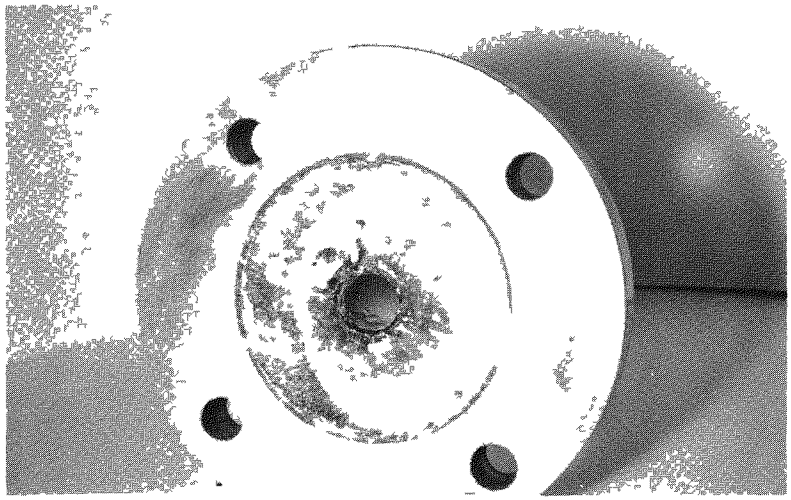

TYPE 304L S.S. REBOILER TUBE EXPOSED
TO LWR WASTE SOLUTION - 1

Figure 11. Scale on Tube Sheet and Top End of Reboiler Tube

2. Waste Storage

Studies are currently in progress to determine the behavior of HLLW solutions and slurries during interim storage. This information will provide the basis for improved and economical design of future liquid waste storage tanks. The data obtained will also permit more efficient and safer operation of existing liquid waste storage tanks.

During this quarter, the major effort has been expended in developing laboratory equipment and techniques which can adequately provide the desired information and data. In addition, long-term characterizations of simulated HLLW solutions are continuing.

2.1 Laboratory Storage Tank (P. A. Anderson)

A laboratory tank has been constructed for storage studies using simulated HLLW. The purposes are: 1) to develop techniques for laboratory waste storage studies, 2) to modify and improve the design of future experimental equipment, and 3) to obtain preliminary data on the behavior of stored HLLW slurries with respect to mixing, stability, heat transfer, scaling, and corrosion of materials exposed to HLLW.

2.11 Design of Equipment

The present experimental equipment, shown in Figure 12, consists of a 13.6 L(3.6 gallon) glass tank with a transparent plastic lid and a high

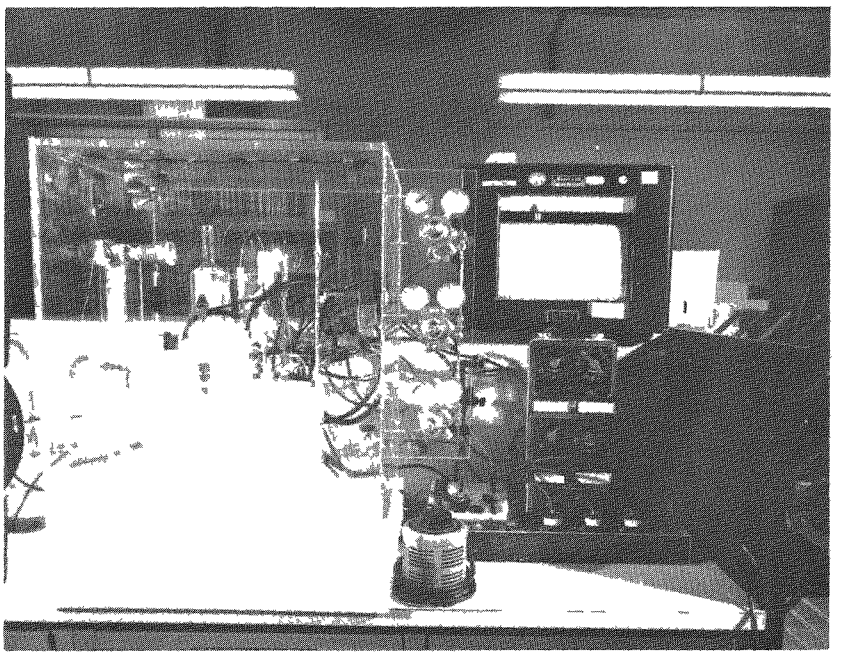

Figure 12. Laboratory Storage Tank

efficiency condenser. The tank is enclosed in a transparent plastic cubicle which is heated to the same temperature as the stored solution to prevent heat loss from the solution to the air. The cubicle air temperature is thermostatically controlled by a 110-V, 660-W resistance heater and a small circulating fan.

Fission product decay heat is simulated in the solution by a 110-V, 600-W immersed resistance heating coil. The heating coil can be either thermostatically controlled or operated to deliver measured amounts of heat from 0 to 680 W (2300 Btu/h) by a calibrated rheostat. The resistance of the heater was determined to be constant at 23.0 ohms over the temperature range of 40 to 60°C.

The Type 304L stainless steel cooling coil has an outside diameter of 0.63 cm (0.25 in.) and an inside diameter of 0.524 cm (0.206 in.). The total cooling coil surface area is 245 cm^2 (0.263 ft^2). The cooling water flow is regulated by a valved rotometer with an operating range of 0 to 8 cm^3/s. Accurate flowrate measurements are obtained by weighing timed increments of effluent cooling water. All inflowing water lines and the condenser are covered with foam insulation to minimize heat transfer to the cooling water from the heated air inside the cubicle.

Thermocouples are in the following locations: 1) in the inflowing and outflowing cooling water lines at the surface of the stored solution, 2) in the stored solution at points 5 cm from the top and 5 cm from the

bottom of the tank, and 3) in the transparent plastic cubicle both above and beside the tank. Temperatures are recorded at one minute intervals.

Mixing of the stored solution is obtained with two glass airlift circulators which are designed for continuous or intermittent operation. Two glass ballast tank agitators, powered by compressed air, are primarily designed to suspend undissolved solids which settle to the bottom of the tank; however, they also contribute to the mixing of the solution. The frequency of expelling solution from the ballast tanks is controlled by cyclic timers and three-way solenoid valves. Air which is displaced from the ballast tanks is vented into the storage tank.

The present experimental equipment is designed to simulate a typical large 1,100,000 litre (300,000 gallon) storage tank using a scale down factor of approximately 10^3. Table 14 shows the design criteria which were selected for the laboratory storage tank. These criteria are based upon the newest liquid waste storage tanks in the United States. The waste tank design is suitable for high-level heat generating wastes from different types of reactors. It is similar in design but more advanced than the stainless steel tanks used to successfully store acidic waste containing nitric acid and fluoride at ICPP.

TABLE 14

Design Criteria of Laboratory Storage Tank[a]

Discharge velocity of ballast tank nozzle		18 m/s (59 ft/s)
Ratio of total volume of ballast tanks to volume of solution		4.8×10^{-2}
Cooling coil water:	Flowrate per liter of stored solution	2.06×10^{-4} L/s
	Inflowing temperature (T_i)	35°C
	Outflowing temperature (T_o)	46°C
	Temperature of stored solution (T_s)	60°C
Ratio of cooling coil surface to solution volume		18 cm^2/L_2 (.072 ft^2/gal)

[a]Based upon the design of HLLW storage tanks described in Final Safety Analysis Report, Barnwell Nuclear Fuel Plant Separation Facility, Amendment No. 1, April 1, 1974, Sections 8 and 9.

Numerous improvements were made in the laboratory tank and equipment during the early operation with water as the stored solution. A more sensitive electronic thermostat was installed to maintain the cubicle temperature within one degree Celsius. Fluctuations in the cooling water

temperature were eliminated with increased insulation and by installing a constant temperature bath to regulate the temperature of the inflowing cooling water. A mechanical stirrer was installed to provide supplementary mixing when the airlift circulators are not operating. Plastic filings were put in the solution to aid visual observation of physical mixing during the equipment testing with water.

2.12 Heat Transfer

In order to verify the operating characteristics of the laboratory storage tank, heat transfer measurements were made using water at 60°C (140°F) and 49°C (120°F) with the heat source thermostatically controlled with known amounts of heat input. Heat transfer coefficients for the tank are shown in Figure 13 for various flowrates. The data points marked by asterisks were obtained at operating conditions which correspond to those expected in a typical large storage tank with respect to the flowrate, inflowing temperature, and outflowing temperature of the cooling water. The cooling coil water flow is entirely in the laminar flow range because turbulent flow could not be attained in the small tank at the selected design criteria. A Reynolds number of approximately 1000 is obtained at a nominal flowrate of 2.8 g/s.

2.13 Heat Balance

Heat balance measurements were also made for the laboratory storage tank. The rate of heat input was controlled by a calibrated rheostat on the solution heating coil. The rate of heat removal was determined from the increase in temperature of weighed quantities of cooling water. The solution was continuously mixed by both airlift circulators and ballast tank agitators.

As shown in Table 15, an average of 20 percent of the input heat is lost from the solution by means other than the cooling coil. Part of this loss may be attributed to evaporation into air discharged through the airlift circulators. Estimates made on the basis of the volume of air discharged indicate that airlift circulators emitting dry air at a rate of 23 cm^3/s (.049 ft^3/min) should remove approximately 13 W. However, comparison of the rate of solution temperature change with the airlift circulators operating to the rate of change with them turned off, indicates that heat is actually removed at approximately three times that rate. Other possible sources of heat loss which will be investigated include the evaporation of the solution into the air vented from the ballast tanks and the cooled condensate returning from the condenser.

2.2 Storage of Evaporated HLLW (P. A. Anderson)

Long-term storage studies of evaporated simulated HLLW slurries, at constant temperature and without agitation, are continuing. The slurries have been monitored at intervals of one to two months for stability with respect to quantities of undissolved solids. The data obtained from 18 samples, some stored up to 11 months, were analyzed statistically. The relationship between quantity of undissolved solids and length of time stored was significant at the 0.1 confidence level in 2 of the

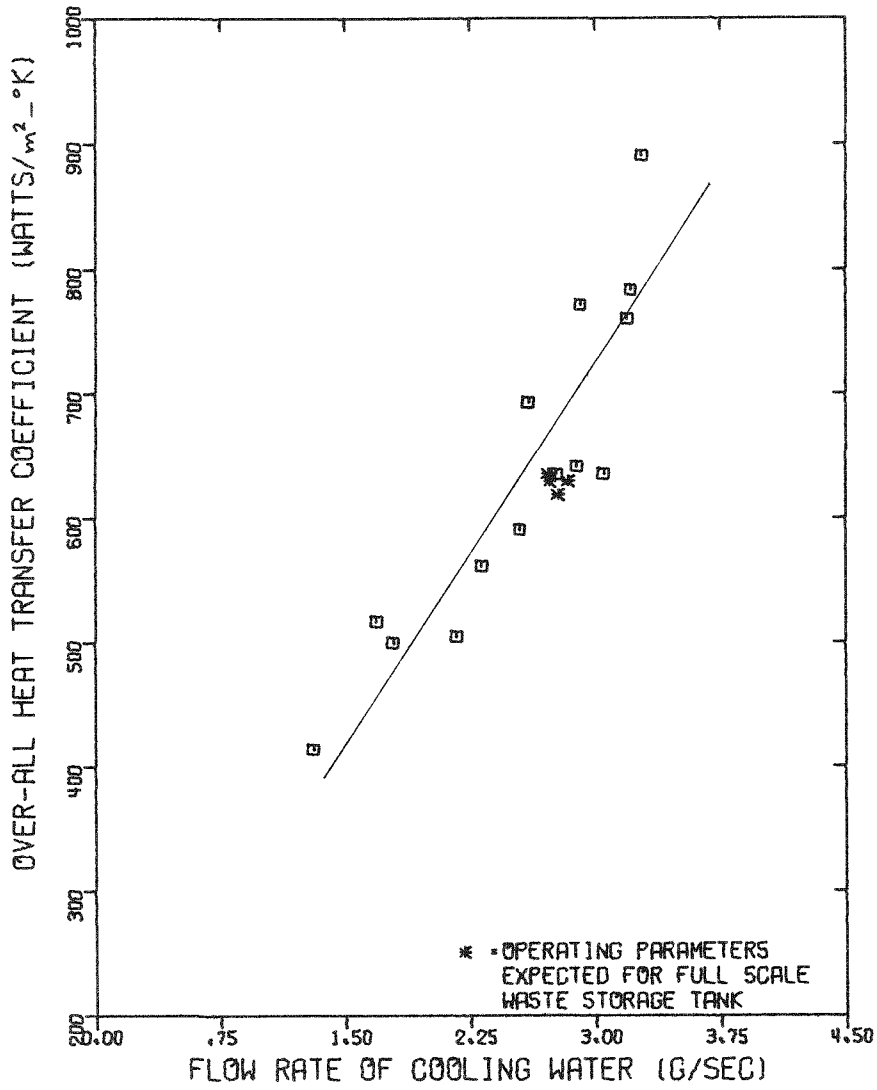

Figure 13. Heat Transfer Coefficients Obtained for Water in Laboratory Storage Tank

18 samples, but duplicates of these samples did not show significant changes. It is concluded that the quantity of undissolved solids in evaporated HLLW slurries has not changed significantly during interim storage for up to one year.

3. Materials and Corrosion

Materials and corrosion studies are being conducted in the laboratory and in small-scale equipment to establish the effect of waste composition and components on materials of construction and to investigate new materials for evaporators, waste tanks, and auxiliary equipment. In addition, methods for monitoring corrosion of waste tanks during interim storage of liquid waste are being investigated.

TABLE 15

Heat Balance in Laboratory Storage Tank

Heat Input (H_i) to Stored Solution, W	Heat Removed (H_o) via Cooling Coil, W	Percent of Heat Removed via Cooling Coil
185	122	66
185	120	65
185	121	65
202	173	86
302	326	108
315	250	79
331	323	98
372	258	69
440	348	79
501	401	80
645	530	82
645	538	83
680	533	78
		Average = 80

3.1 Monitoring of Storage Tanks (P. A. Anderson)

Microscopic examination of three electronic corrosion monitoring probes yielded no evidence of pitting or cracking in Type 304L stainless steel after four months of exposure at 60°C to simulated HLLW-0 (contains minimal process additives), HLLW-Fe (contains high iron), and HLLW-UP (contains high uranium and phosphate). There was visual evidence of general surface attack and very small amounts of scaling of solids on probe surfaces.

The evaluation of the Type 304L stainless steel monitoring probes is continuing with new HLLW slurries containing high levels of nitric acid and uranium as a simulant for total actinides. The present solutions contain palladium and rhodium, which were previously substituted, and gadolinium and ruthenium, which were previously omitted. A monitoring probe has also been installed in the laboratory storage tank.

3.2 Reboiler Tube Evaluation (G. R. Villemez, C. B. Millet)

A Type 304L stainless steel welded reboiler tube was evaluated for corrosion rates during the operation of the thermosiphon evaporator with

nitric acid and HLLW expected from a tributyl phosphate extraction process. Only general attack was visible in the reboiler tube after the scale was removed. The corrosion rate of the reboiler tube during 500 hours of evaporator service was 517 μm/yr (20.4 mils/yr) according to calculations from the weight loss and the total area of the reboiler tube. Based on the measured change of the inside diameter of the tube at the feed end, the corrosion rate was 523 μm/yr (20.6 mils/yr). The excellent agreement between these two values showed that the attack was uniform over the entire area of the reboiler tube.

Some weld decay occurred on the Type 304L stainless steel plate near the weld in the heat affected zone. Crevice corrosion can be seen in the outer area of the plate near the gasket location while general corrosion occurred on the face of the plate as shown in Figure 14.

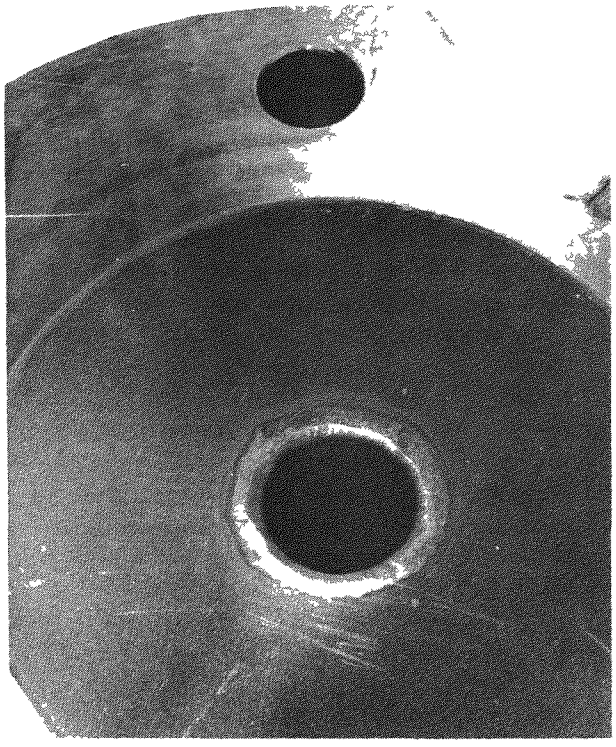

Figure 14. Crevice Corrosion and Weld Decay on Type 304L Stainless Steel Tube Sheet (Exposed 500 h to nitric acid and HLLW at boiling)

The evaporated solutions were analyzed for iron content to determine the quantity of corrosion products dissolved in each of the evaporator runs. Using the calculated exposed area, an average corrosion rate for the entire evaporator was calculated for the evaporated solution in each run. The average corrosion rate for all of the runs was 243 μm/yr (9.6 mils/yr); this indicates the reboiler tube experienced nearly twice the corrosion attack as the rest of the stainless steel evaporator surface.

The buildup of the corrosion product level in the solutions will limit the time that solutions can be used for evaporator tests because the corrosion rate of Type 304L stainless steel accelerates as the corrosion product level increases above 1 g/L[17]. In the thermosiphon evaporator, the corrosion product level increased faster in the HLLW solutions during evaporation than in the nitric acid solution, and the rate of increase depended on the acid concentration. During 68 hours of continuous operation, the corrosion products concentration increased from 0.2 g/L to 5.2 g/L in HLLW. However, the increase was only from 5.2 g/L to 6.2 g/L in 50 hours of operation in a recycle mode with the vapor condensate returning to the reboiler. This may have been due either to the formation of the scale on the evaporator surface or to the precipitation of the corrosion products.

These corrosion data are considered preliminary since this was the initial operation of the evaporator and some plugging occurred. More information on the effects of the stainless steel evaporator unit will be obtained using a titanium reboiler tube.

Plans for Next Quarter

The small-scale thermosiphon evaporator will be modified and improved to reduce plugging during operation with simulated HLLW solutions which are highly concentrated and contain considerable amounts of undissolved solid. The evaporator will be operated with a titanium reboiler tube specimen using nitric acid as a base line and several levels of HLLW as was done with the Type 304L stainless steel specimen. A comparison of heat transfer characteristics, scaling, and corrosion will be made between the two materials.

Laboratory corrosion tests will be performed to determine the effect of technetium, ruthenium, and cerium; the latter is the major component of commercial rare earth mixtures. Long term stability tests and evaluation of corrosion monitoring probes will continue.

The laboratory storage tank will be operated with nitric acid and simulated HLLW containing large amounts of undissolved solids to determine heat transfer and heat balance characteristics and to investigate the effect of scaling and mixing. The rate of loss of HNO_3 from the high efficiency condenser will be investigated.

[17] LWR Fuel Reprocessing and Recycle Progress Report for January - March 31, 1977, ICP-1116 (April, 1977).

VI. HTGR FUEL REPROCESSING

(L. W. McClure)

High temperature gas-cooled reactor (HTGR) fuel blocks consist of fuel particles in a graphite matrix. During reprocessing, the blocks are crushed and the graphite is burned to expose the fuel particles. The fuel particles are then crushed and burned in a secondary burner. During this step, fission products in the fuel will vaporize. Laboratory tests were conducted to identify which fission products will vaporize in the burner environment. These species will be tested for removal from the off-gas stream by a fluidized-bed condenser. The work is being done under subcontract to Oak Ridge National Laboratory.

1. Tube Furnace Experiments (K. L. Wagner)

Although vapor pressures of many of the elemental and oxide forms of the expected Fort St. Vrain Reactor (FSVR) fission products in an oxygen rich atmosphere have been calculated (Table 16), information on the carbide and chloride forms and the effects of a burning graphite environment have not been previously predicted.

The chemical form of the FSVR fission products when they enter the secondary fluidized-bed burner is not presently known. The commercially available elemental, oxide, and carbide forms of the fission products predicted to be present at more than 0.1 g per fuel element, were selected for study and comparison in these tests.

Chlorides of these selected fission products were also included in this study for comparison with the volatilities of the other fission product forms. Chlorides were included because most tracers are available only in the chloride form.

The experiments were conducted in a simple tube furnace apparatus. Samples of the various chemicals were mixed with crushed graphite in a quartz sample boat. Approximately a 1 to 5 ratio of sample to graphite was used. The sample boat, containing sample and graphite, was placed in a 2.5-centimetre-diameter quartz furnace tube and heated in stages to 900°C under 2.36 L/s (5 scfm) of dry air. The air inlet was attached to one end of the tube. The other end of the tube was connected to a modified fritted glass filter support which held a 5-cm-diameter glass fiber filter. The air stream was scrubbed before release into a fume hood.

Observations of volatility and condensation were made at 300, 500, 700, and 900°C temperature settings. At the conclusion of each experiment, the sample boat residue, if present, and the scrub solution were analyzed. The tube was cleaned and the deposits were analyzed. These analyses were used to determine a mass balance for the sampled chemical.

The percentage by weight of each species present in each part of the apparatus at the conclusion of an experiment is listed in Table 17. As Table 17 shows, the volatile species are Sb, Sb_2O_3, Sb_2O_4, Sb_2O_5, $SbCl_3$, Cd, CdO, $CdCl_2$.2-1/2 H_2O, CsO_2, CsC_6, CsCl, Mo, MoO_3, Mo_2C, $MoCl_5$, Rb_2O_4,

TABLE 16

VAPOR PRESSURES AT 1000°K AND 1500°K FOR FISSION PRODUCTS EXPECTED IN FSVR FUEL IN QUANTITIES GREATER THAN 0.1 g/FUEL ELEMENT

Element	Weight Expected Per FSVR Fuel Element(1) (g)	Melting Point (°C)	Boiling Point (°C)	Condensed Phase in 20% O_2 at 1000 K	Vapor Phase at 1000 K	Vapor(2) Pressure at 1000 K (atm)	Condensed Phase in 20% O_2 at 1500 K	Vapor Phase at 1500 K	Vapor(2) Pressure at 1500 K (atm)
Antimony	0.356	630.7	1750	$Sb_6O_{13}(s)$	Sb_4O_6	0.0073	$Sb_2O_3(l)$	Sb_4O_6	0.818
Barium	50.7	725	1640	$BaO_2(l)$	BaO	10^{-15}	BaO(s)	BaO	3.38×10^{-8}
Cadmium	0.699	320	765	CdO(s)	Cd	10^{-9}	CdO(s)	Cd	0.017
Cerium	99.2	795	3468	$CeO_2(s)$	CeO	10^{-37}	$CeO_2(s)$	CeO	10^{-21}
Cesium	76.9	28.4	678	$Cs_2O(l)$	CsO	7.3×10^{-4}	$Cs_2O(l)$	Cs	0.647
Lanthanum	41.0	920	3469	$La_2O_3(s)$	LaO	10^{-28}	$La_2O_3(s)$	LaO	10^{-15}
Molybdenum	105	2617	4612	$MoO_3(s)$	$(MoO_3)_3$	1.08×10^{-2}	$MoO_3(l)$	$(MoO_3)_3$	6.64×10^{-2}
Niobium	24.3	2468	4927	$Nb_2O_5(s)$	NbO_2	10^{-3}	$Nb_2O_5(s)$	NbO_2	10^{-17}
Neodymium	132	1024	3027	$Nd_2O_3(s)$	NdO	10^{-28}	$Nd_2O_3(s)$	NdO	10^{-15}
Palladium	15.9	1555	2927	PdO(s)	PdO_2	0.047	Pd(s)	PdO_2	0.248
Prasodymium	42.0	935	3127	$Pr_6O_{11}(s)$	PrO	10^{-31}	$Pr_2O_3(s)$	PrO	10^{-16}
Promethium	1.30	--Not Available--		$Pm_2O_3(s)$	PmO	10^{-15}	$Pm_2O_3(s)$	PmO	10^{-15}
Rubidium	18.6	38.9	688	$Rb_2O_2(l)$	RbO	5.45×10^{-3}	$Rb_2O(l)$	RbO	3.06
Rhodium	4.13	1955	3727	$Rh_2O(s)$	RhO_2	10^{-17}	$Rh_2O(l)$	RhO_2	5.47×10^{-7}
Ruthenium	47.5	2310	3900	$RuO_2(s)$	RuO_4	2.42×10^{-6}	$RuO_2(l)$	RuO_3	1.07×10^{-3}
Selenium	2.69	217	685	Se(g)	Se_2	1.0	--	--	--
Samarium	20.6	1072	1900	$Sm_2O_3(s)$	SmO	10^{-29}	$Sm_2O_3(s)$	SmO	10^{-16}
Strontium	39.2	769	1384	SrO(s)	SrO	10^{-19}	SrO(s)	SrO	10^{-10}
Silver	0.129	962	2212	$Ag_2O(s)$	AgO	10^{-15}	Ag(l)	Ag	3.37×10^{-4}
Technetium	22.6	--	--	$TcO_3(l)$	Tc_2O	10.48	$TcO_2(s)$	Tc_2O	0.121
Tellurium	18.2	450	990	$TeO_2(s)$	TeO_2	1.61×10^{-4}	TeO (l)	Te_2	7.7×10^{-3}
Tin	1.05	232	2270	$SnO_2(s)$	SnO	10^{-17}	$SnO_2(s)$	SnO	5.4×10^{-7}
Yttrium	21.3	1495	2927	$Y_2O_3(s)$	YO	10^{-35}	$Y_2O_3(s)$	YO	10^{-20}
Zirconium	139	1852	3578	$ZrO_2(s)$	ZrO_2	10^{-30}	$ZrO_2(s)$	ZrO_2	10^{-17}

(1) -6 year burnup - 1 year cooling

(2) -Calculated from UCRL - 12314

TABLE 17

WEIGHT PERCENTAGE DISTRIBUTION OF SPECIES AFTER HEATING WITH GRAPHITE

TO 900°C AND A FLOW OF 2.36 L/s DRY AIR

Species	% Remaining In Sample Boat	% in Tube Washings	% On The Filter	% Between Filter And Scrub	% In Scrub Solution	Comments
Antimony	1.4	25.8	39.8	0.0	0.0	Boat residue was $Fe_2Sb_2O_7$, filter deposit was Sb_2O_3
Sb_2O_3	25.5	5.6	24.7	0.0	0.0	Boat residue was Sb_2O_4, filter deposit was primarily Sb_2O_3 with Sb_2O_4 present
Sb_2O_5	55.2	1.2	18.6	0.1	0.0	Boat residue was Sb_2O_4, filter deposit was primarily Sb_2O_3 with Sb_2O_4 present
$SbCl_3$	0.0	1.1	24.7	12.3	60.9	Boat residue was $Fe_2Sb_2O_7$, filter deposit was amorphous
Barium	97.8	0.0	0.0	0.0	0.0	Boat residue was $BaCO_3$
BaO_2	95.3	N.M.*	0.0	N.M.	N.M.	Boat residue was $BaCO_3$
BaC_2	99.0	0.0	0.0	0.0	0.0	Boat residue was $BaCO_3$
Cadmium	78.7	27.3	1.8	0.6	0.4	Boat residue and filter deposit were CdO
CdO	76.0	N.M.	2.2	0.2	N.M.	Boat residue and filter deposit were CdO
$CdCl_2 \cdot 2\ 1/2\ H_2O$	0.1	71.8	56.2	0.0	0.0	Filter deposit was $CdCl_2 \cdot H_2O$
Cerium	99.1	N.M.	0.0	0.0	0.0	Boat residue was CeO_2
CeO_2	99.3	0.0	0.0	0.0	0.0	Boat residue was CeO_2
CeC_2	107.8	0.0	0.8	0.0	0.0	Boat residue was CeO_2, filter deposit was unidentifyable
CsO_2	85.1	1.1	1.3	0.0	0.0	Boat residue was amorphous, the sample reacted with the quartz
CsCl	0.5	52.1	46.1	0.0	0.0	Sample reacted with the quartz, filter residue was CsCl

TABLE T7 (Continued)

WEIGHT PERCENTAGE DISTRIBUTION OF SPECIES AFTER HEATING WITH GRAPHITE TO 900°C AND A FLOW OF 2.36 L/s DRY AIR

Species	% Remaining In Sample Boat	% in Tube Washings	% On The Filter	% Between Filter And Scrub	% In Scrub Solution	Comments
CsC_8	27.2	N.M.	0.0	0.0	0.0	Sample reacted with the quartz, boat residue was unidentifyable
EuO_2	95.2	N.M.	0.0	0.0	0.0	Boat residue was Eu_2O_3
La_2O_3	84.8	0.0	0.0	0.0	0.0	Boat residue was La_2O_3
Molybdenum	0.9	96.5	0.5	0.0	0.0	Tube crystals were MoO_3, filter deposit was probably MoO_3
MoO_3	0.2	57.5	27.6	0.2	0.0	Tube crystals and filter deposit were MoO_3
$MoCl_5$	0.1	0.6	15.6	9.7	29.1	Filter deposit was not identified
Mo_2C	0.9	30.6	53.4	0.0	0.0	Boat residue was unidentifyable, tube crystals were MoO_3, filter deposit was probably MoO_3
Palladium	100	0.0	0.0	0.0	0.0	Boat residue was Pd
Rb_2O_4	89.6	1.0	3.2	0.0	0.0	Sample reacted with quartz, boat residue was Rb_2O_2 with Rb_2CO_3 possibly present, filter deposit was RbCl with RbO_2 possibly present
RbCl	0.2	51.6	47.2	0.0	0.0	Sample reacted with the quartz filter deposit was RbCl
RbC_8	72.0	N.M.	0.2	0.2	0.0	Sample reacted with the quartz, boat residue was unidentifiable
Ruthenium on Carbon	57.5	0.1	1.4	0.0	1.9	Boat residue was RuO_2, filter deposit was amorphous

TABLE 17 (Continued)

WEIGHT PERCENTAGE DISTRIBUTION OF SPECIES AFTER HEATING WITH GRAPHITE TO 900°C AND A FLOW OF 2.36 L/s DRY AIR

Species	% Remaining In Sample Boat	% in Tube Washings	% On The Filter	% Between Filter And Scrub	% In Scrub Solution	Comments
RuO_2	---	---	---	---	---	Analyses pending
$RuCl_3$	---	---	---	---	---	Analyses pending
Selenium	0.4	No Method	19.8	0.0	No Method	Boat residue was unidentifiable, filter deposit was probably SeO_2, vapors escaped from the scrub solution
SeO_2	0.4	No Method	70.0	14.0	No Method	Filter deposit was H_2SeO_3 and SeO_2, vapors escaped from the scrub solution
Strontium	98.1	0.0	0.4	0.0	0.0	Boat residue was SrO with SrO_2 and $SrCO_3$ possibly present
SrO	99.6	N.M.*	0.0	0.0	0.0	Boat residue was SrO
$SrCl_2 \cdot 6\ H_2O$	67.8	5.4	0.4	0.0	0.0	Boat residue and filter deposit were $SrCl_2 \cdot 2\ H_2O$
SrC_2	93.2	0.0	0.0	0.0	0.0	Boat residue was SrO with SrO_2 possibly present
Silver	99.3	0.0	0.1	0.1	0.0	Boat residue was Ag splattered around the boat
Tellurium	N.M. Boat stuck in tube	No Method	52.9	0.0	No Method	Filter deposit was mostly amorphous with TeO_2 possibly present
TeO_2	27.8	No Method	18.7	0.0	No Method	Boat residue and filter deposit were not analyzed
$TeCl_4$	0.3	No Method	68.2	0.1	No Method	Filter deposit was amorphous
Tin	100	0.0	0.0	0.0	0.0	Boat residue was SnO_2
ZrO_2	99.9	N.M.	0.0	0.2	0.0	Boat residue was ZrO_2, filter deposit was amorphous

* N.M. - Not measured.

RbC_8, RbCl, Ru, RuO_2, $RuCl_3$, Se, SeO_2, Te, TeO_2, $TeCl_4$, CeC_2, and $SrCl_2 \cdot 6H_2O$. The species tested that were not volatile are Ba, BaO_2, BaC_2, Ce, CeO_2, Eu_2O_3, La_2O_3, Nb_2O_5, Sr, SrO, $SrOC_2$, Sn, SnO_2, Pd, and ZrO_2. Silver splattered from the sample boat but does not appear to be volatile to greater than 1% by weight.

As shown in Table 17, the chlorides of these species are generally more volatile than the elemental oxide or carbide forms of the same fission product. Any volatility studies with tracers should be conducted with the elemental, oxide or carbide forms rather than the readily available chlorides.

2. Deposition and Plate-Out Testing (G. O. Haroldsen)

A laboratory test system was set up to determine the deposition and plate-out characteristics of the semi-volatile fission products in a quartz burner. Quartz construction was selected for better visual observation of deposition and plate-out. Heating of the bed was by seven electric cartridge heaters inserted into the quartz vessel through nipples in the side of the vessel. Several check out runs were made with the apparatus, but satisfactory reproducibility was never achieved because of failure of the quartz at the nipples. A new model of the apparatus is being fabricated, which eliminates the use of internal cartridge heaters. Instead, external heating will be provided by placing the fluidized-bed section of the apparatus in a high temperature tube furnace.

3. Semi-Volatiles Condensing and Removal (G. O. Haroldsen)

A bench-scale fluidized-bed cooling and condensing apparatus has been designed and fabricated. The fluidized-bed concept for cooling and condensing was selected because of the high heat transfer rates achievable and because fluidized-bed operation is proven in remote operation. A schematic diagram of the laboratory unit is shown in Figure 15. It is a two-sectioned, bed-on-bed device. The bottom section is a heated fluidized bed that will volatilize the semi-volatiles. The fluidized-bed method was selected as a convenient way of volatilizing, and it is not intented to simulate fluidized-bed burner operation. The top section contains a fluidized bed that is cooled with an internal cooling coil. The two sections are joined with a flanged connection containing the distributor plate for the upper bed. Various distributor plates will be tested to identify the design that prevents plugging in the distributor itself and enhances cooling and quenching of the vapors in the bed.

The quenching apparatus was constructed of quartz for visual observation of deposition and quenching characteristics. Check-out runs have indicated good cooling characteristics in the quenching bed.

Plans for Next Quarter

Testing of the fluidized-bed semi-volatile removal device will begin. Various bed materials and alternate distributor plate designs will be tested.

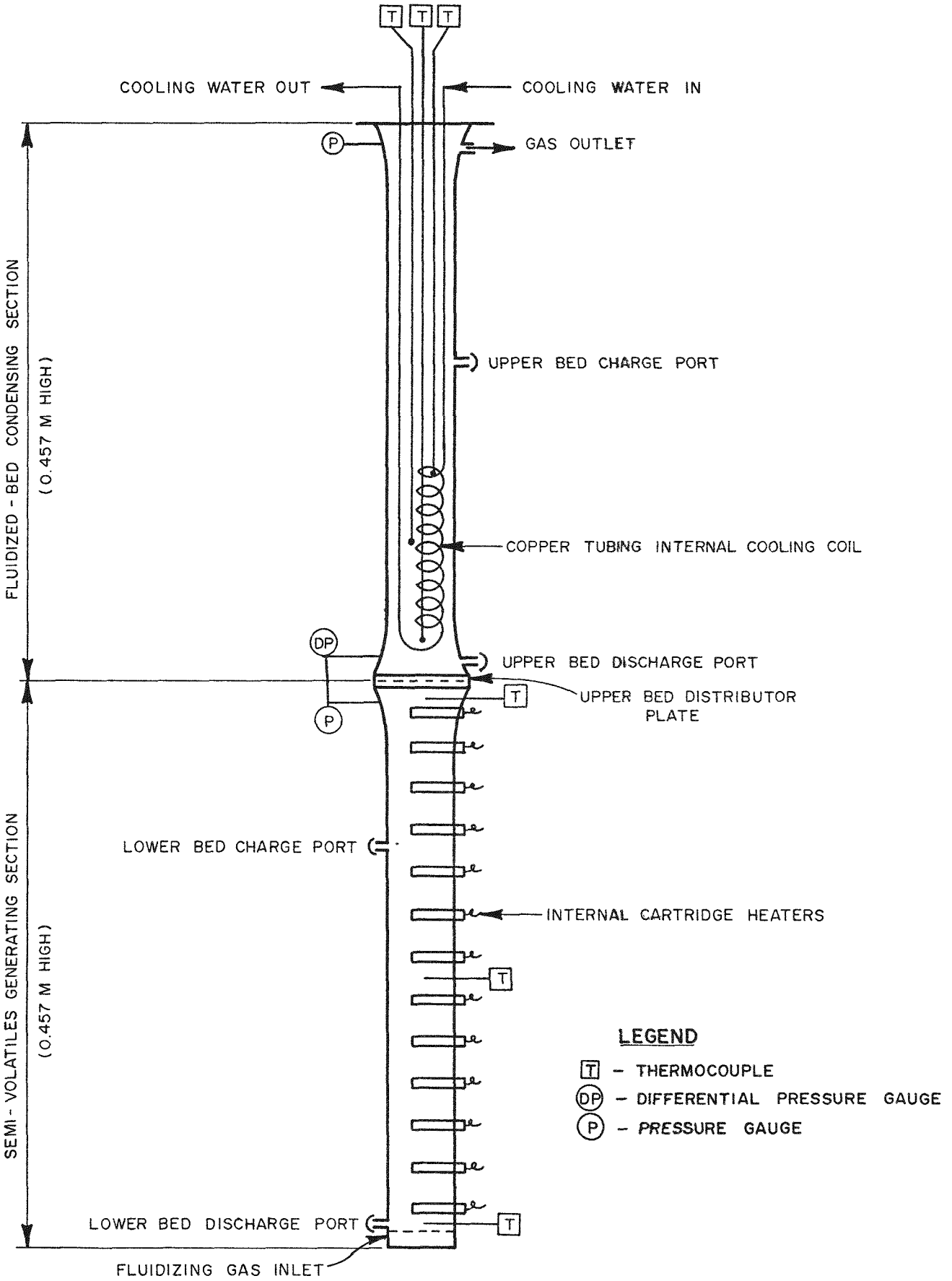

Figure 15. Fluidized Bed Quenching Apparatus ACC-A-2714

The experiments to determine the vaporization and condensation characteristics of the semi-volatiles in the redesigned lab scale quartz burner will be conducted. The chemical species found to be volatile in the tube furnace experiments will be tested.

VII. NATURAL FISSION REACTOR STUDIES (OWI FUNDING VIA LASL)

(W. J. Maeck, R. L. Eggleston, F. A. Duce, J. E. Delmore, R. A. Nielsen, F. W. Spraktes)

A unique approach to the study of the long-term behavior of waste containing fission products and the actinide elements in geologic environments is through the analysis of the remains of natural fission reactors. In 1972, the natural fission reactor at the Oklo pit in the Republic of Gabon was discovered. Initial studies conducted by both the French CEA and United States ERDA laboratories and reported at the IAEA Conference on the Oklo Phenomenon[18] showed that most of the fission products had remained in place for a period of ~2000 million years. Of particular importance was the high degree of retention of plutonium and the higher actinides in the vicinity of the natural reactor.

In May of this year, the IAEA in collaboration with the French Atomic Energy Commission announced the convening of an Experts Technical Committee Meeting on Natural Fission Reactor to be held in December 1977, to review the status of current research efforts, to review new results obtained in the past two years since the first Oklo symposium[18], and to discuss the general trends toward which future research should be directed. The following is a synopsis of our most recent research efforts which is being submitted for presentation at this meeting.

> Since the initial discovery of the natural occurrence of a sustained nuclear chain reaction at the Oklo site in Gabon, considerable speculation has been presented relative to the occurrence of other natural reactors. While it is now generally believed that the Oklo Phenomenon was not unique, the probability of detecting another such occurrence is less clear. For reactor sites which have remained intact, measurement of the U isotopic abundances generally provides the most direct evidence for the detection of a nuclear chain reaction. However, if the site had been subjected to geologic processes which resulted in the wide spread dissemination of the depleted uranium, sufficient dilution of this material with normal uranium will minimize to usefulness of uranium isotopic analysis. As an alternative and more sensitive technique, Roth and coworkers at the Libreville Oklo Symposium[18] suggested analyzing for the fission products elements selenium, ruthenium, palladium, and tellurium which are rare in nature but have relatively high fission yields. Of these, ruthenium is the most sensitive monitor, having a natural abundance in the earth's

[18] "The Oklo Phenomenon", Proceedings of an IAEA Symposium, Libreville, Gabon, (June 1975).

crust of ~1 part per billion, ppb, and an elemental fission yield of ~25%. Thus, the isotopic composition of natural occurring ruthenium could be significantly altered if contaminated with fission product ruthenium.

In a search for other possible natural reactors, ~30 selected samples obtained from various promising mine sites and from geologic libraries were analyzed to determine the uranium and ruthenium isotopic composition. Based on thermal ionization mass spectrometry, no obvious deviation from the natural abundance ^{235}U was observed.

Of the samples analyzed for ruthenium, all showed an isotopic composition which could not be attributed solely to natural ruthenium of that expected from ^{235}U thermal fission. After correction for natural ruthenium, the resulting isotopic composition varied from sample to sample, but in all cases was still significantly different from that producted by ^{235}U thermal fission. We now attribute the observed ruthenium isotopic composition to be the result of a mixture of ruthenium produced from ^{238}U spontaneous fission and induced ^{235}U thermal fission.

To determine the isotopic composition of the ruthenium produced by ^{238}U spontaneous fission, the results from the analysis of 16 unspiked and 20 spiked samples were subjected to a non-linear regression analysis. Knowing the isotopic composition of ruthenium produced by ^{235}U thermal fission, the best values for the isotopic composition of ruthenium produced by spontaneous fission were calculated. These results and those for ^{235}U thermal fission are given in Table 18. It is clearly demonstrated that the isotopic composition of natural ruthenium and that produced from ^{238}U spontaneous fission is significantly different from that resulting from ^{235}U thermal fission.

The ruthenium analysis technique consisted of leaching the ground ore samples for several hours in a boiling mixture of 9N HCl-3M HNO_3, filtering the sample, and for concentration measurements, removing weighed aliquots of the filtered samples and mixing with weighed aliquots of ^{96}Ru spike solution. The ruthenium is distilled as the tetroxide from a mixture of sulfuric acid and sodium bismuthate and collected in hydrochloric acid. The distillate is evaporated to near dryness and mounted on a pre-baked rhenium center filament for mass spectrometric analysis. In most cases, the amount of ruthenium placed on the filament and measured was 2-25 ng.

Although it is believed that the listed (Table 18) isotopic composition and fission yields for Ru produced from ^{238}U spontaneous fission are accurate to within the 5-10% range, additional studies are continuing. To minimize the effect of natural contamination and the contribution from induced ^{235}U

TABLE 18

RUTHENIUM COMPOSITION AND FISSION YIELDS

	Nat. Ru	U-th Fission		U-sp Fission	
Mass No.	Isotopic	Isotopic	FY,%	Isotopic	FY,%
96	5.5	---		---	
98	1.9	---		---	
99	12.7	35.6	6.16	24.0	6.0
100	12.6	---	---	---	---
101	17.1	29.4	5.08	28.4	7.1
102	31.6	24.3	4.23	31.2	7.8
104	18.6	10.6	1.84	16.4	4.1
			17.31		25.0
Isotopic Ratio					
99/101	0.743	1.210		0.845	
99/102	0.402	1.465		0.769	
99/104	0.683	3.358		1.463	
101/102	0.541	1.210		0.910	
101/104	0.919	2.774		1.732	
102/104	1.699	2.292		1.902	

fission, uranium ore samples having a moderate uranium concentration of 5-20% U and a high neutron poison content will be analyzed to provide a more accurate measurement of the isotopic composition of ^{238}U spontaneous fission produced ruthenium. Considering that these values are significantly different than those resulting from ^{235}U thermal fission and for natural ruthenium (Table 18), the possibility of using ^{238}U spontaneous fission produced ruthenium and the amount of uranium present in an ore sample as a method for determining the age of the uranium mineralization is being investigated. This method is based on the fact that ruthenium from spontaneous fission of ^{238}U depends only on: (1) the ruthenium fission yields from ^{238}U spontaneous fission, (2) the ^{238}U spontaneous fission half-life or fission rate, λsf, (3) the time-integrated amount of ^{238}U present, and (4) the length of time which spontaneous fission has been occurring (i.e., the age of the ore) and can be expressed as:

$$T = \frac{1}{\lambda} \ln \left(1 + \frac{Ru}{U} \frac{\lambda}{FY\ \lambda_{sf}}\right), \qquad (1)$$

where T is the age of the uranium ore, λ is the total decay constant of ^{238}U, Ru and U are the atoms of Ru and U present in the sample, FY is the fractional spontaneous fission yield of the ruthenium isotope measured, and λsf is the spontaneous fission rate of ^{238}U. Using the following values for the constants (1) $\lambda = 1.551 \times 10^{-10}\ yr^{-1}$ (2) $\lambda sf = 8.46 \times 10^{-17} \cdot yr^{-1}$, and (3) FY = 0.25 (mass 99 + 101 + 102 + 104) Eq. (1) simplifies to:

$$T = 6.45 \times 10^{9}\ \ln\left(1 + 7.33 \times 10^{6}\ \frac{Ru}{U}\right) \qquad (2)$$

Of the constants used, the largest uncertainties are associated with the ^{239}U spontaneous fission yields for the ruthenium isotopes and the ^{238}U spontaneous fission half-life. The fission yield values are based on results given in Table 18, and the $^{238}U_{sf}$ half-life is the result of a rigorous evaluation[19] of the half-life measurements reported to date.

Although the occurrence of ruthenium in a uranium ore body can result from three distinct sources; (1) ^{238}U spontaneous fission, (2) ^{235}U induced fission, and (3) natural ruthenium, the fraction from each source can be identified. Identification of the natural component can be based either upon the abundance of mass 96 or 100, neither of which occur as a result of fission. After subtracting the natural component, the fraction of ^{235}U induced fission and ^{238}U spontaneous fission can be determined using the ruthenium isotopic ratio data given in Table 18.

To date, approximately 20 rich uranium ore samples have been dated using this technique. All of the samples gave ages which are in reasonable agreement with the estimated age of the deposits. Triplicate analyses for one ore sample gave an age equal to $1.35 \pm 0.07 \times 10^{9}$ yr, where the uncertainty is the random error associated with measurement. For this sample, the uranium content was $\sim$40% and the amount of ^{238}U spontaneous fission produced ruthenium was $\sim$6 ng per gram of sample. For all of the samples analyzed, the fraction of ruthenium produced by ^{238}U spontaneous fission was greater than that from ^{235}U induced fission and the natural component was 25% or less of the total ruthenium.

This age dating technique is especially attractive because the natural abundance of ruthenium in the earth's crust is very low ($\sim$1 part in 10^{9}) and the formation of the stable measured product is almost instantaneous with no intermediate highly soluble elements with long half-lives in the decay chain. The major question which remains is whether the uranium-ruthenium system is closed. That is, do each behave geochemically in the same manner. To further evaluate this technique several samples from a large "reference sample" which has been dated by the U-Pb couple, and which is considered to be representative of a closed system will be analyzed.

[19] K. E. Apt, LASL, Private Communication, April 1977.

A paper relative to the age dating method will be a combined INEL-LASL presentation.

Current laboratory efforts are being devoted to a continuing study of this new age dating technique. Samples from outside of the Oklo reactor zones are being analyzed to determine if ruthenium has migrated any significant distance and to determine, if possible, the age of the deposit.

A recent communication from R. Naudet, Saclay to G. A. Cowan, LASL, indicates that remains of another natural fission reactor may have been found in the Oklobondo mine about a mile from the Oklo mine. This observation is based on the analysis of an ore sample by the French which gave a ^{235}U abundance of $\sim$0.67%. At this time, we know little more, but speculate that the Oklobondo pit is of the same geologic origin as that of Oklo and is perhaps an extension of the same mineralization.

A short summary of the ruthenium ^{238}U spontaneous fission yield data has been submitted to the IAEA Nuclear Data Section for inclusion in the third edition of "Progress in Fission Product Nuclear Data", INDC(NDS)-86.

RESULTS

SPECIAL MATERIALS PRODUCTION

I. LONG-TERM MANAGEMENT OF ICPP HIGH-LEVEL WASTES

1. Post Calcinaton Treatment of ICPP Wastes

1.1 Pelletization of ICPP Wastes (K. M. Lamb)

A pelleted waste produced from ICPP calcine is being developed to improve on-site waste storage characteristics. Pelleted waste reduces chances for dispersion and improves leach resistance of the waste. Also, retrieval from storage bins is simplified.

Studies of techniques to pelletize ICPP calcines continued. Four "Spray Systems" flat spray nozzles were tested for spray angle with viscous liquids on the 41-centimetre (16-inch) disc pelletizer. The highly viscous phosphoric acid solution used as a pellet binder tends to spray in solid streams causing off-size and irregular pellets to form. The nozzles were tested over the concentration range of 40-65 vol% (7 M - 11.2 M) H_3PO_4 to determine if useful spray patterns could be produced within a practical flow and pressure range. Normal pelletizer operation requires no more than 50 mL/min of liquid spray. None of the flat spray nozzles tested met the desired criteria. The acid would spray at pressures above 480 kPa (70 psi), but excessive dusting and misting occurred.

Using the Spraying Systems Conejet Nozzle, which was supplied with the 41-centimetre- (16-inch) diameter disc pelletizer, a study was made to determine concentrations of H_3PO_4 that could be sprayed. The experiments determined a range of concentrations of H_3PO_4 solutions which can be sprayed at practical pressures and flow rates using the 1X nozzle (Figure 1). Solutions containing between 10 and 30 vol% H_3PO_4 (1.7 M - 5.2 M) sprayed reasonably well at flow rates between 45 to 55 mL/min. This H_3PO_4 concentration range may still be high enough to impart good green strength and reduced leachability to the pellets. Similar results may be expected for the flat spray nozzles using H_3PO_4 concentrations in the 10 to 30 vol% (1.7 M - 5.2 M) range.

Two 100-h calciner runs in the 10- and 15-cm-diameter calciners were made to determine the effects of adding pellet binders to the liquid wastes prior to calcination. Boric acid was added to make the calcine $\sim$6 wt% in B_2O_3 and zinc oxide was added at $\sim$5 wt%. The ZnO should help compensate for reduced phosphate content (sprayed on during pelletization step) in the pellet as it binds well with phosphates. Evaluation of run data is not complete. The precalcination addition of pellet binders will form a more intimately mixed calcine and will simplify pelletizing by eliminating addition of solid binders permitting the use of low concentration liquid sprays. The product from these runs will be used to verify this pellet formation concept.

A two-day course on theory and operation of the 41-centimetre- (16-inch) diameter disc pelletizer was completed. Much useful information including proper start-up procedures and the effects of changing pelletizer

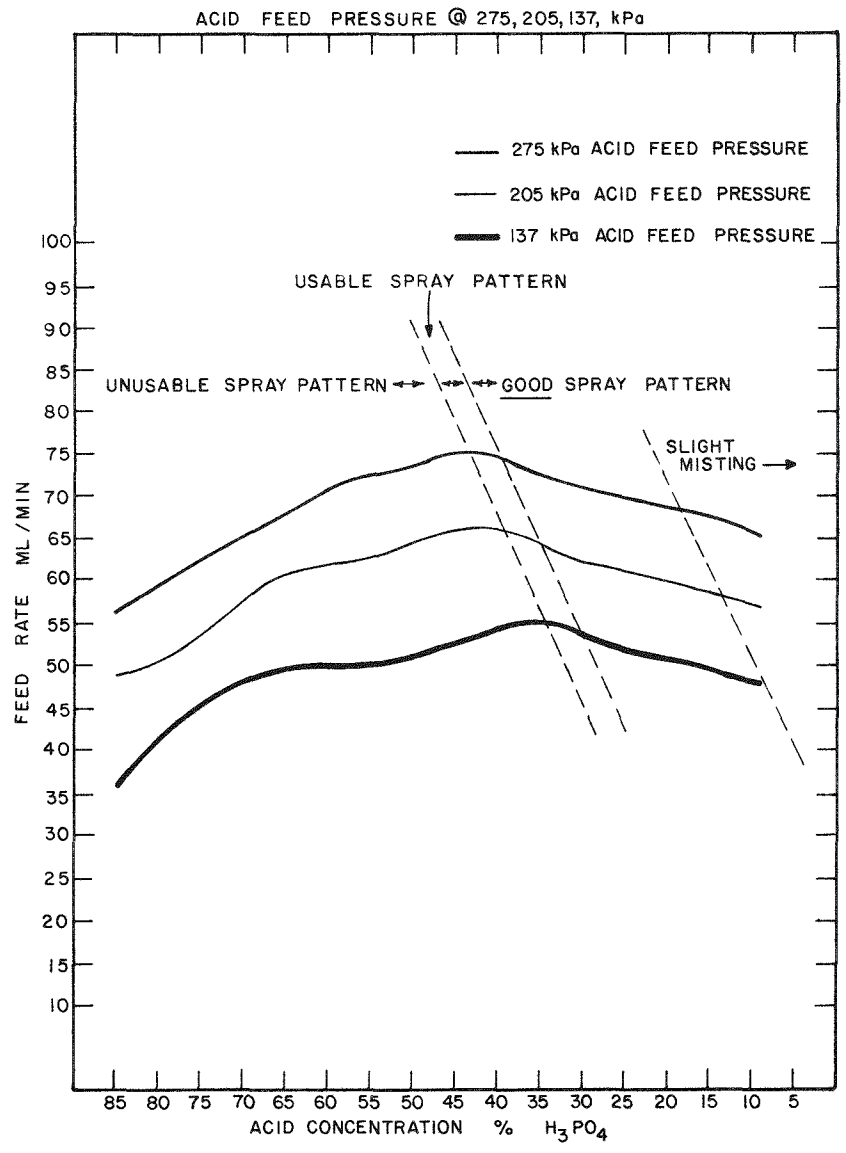

Figure 1. Spray Pattern and Flow Rates of IX Conejet Nozzle vs. Phosphoric Acid Concentration at Three Pressures

parameters such as disc speed, solid and liquid locations, etc., was gathered.

1.2 Characterizations of Waste Forms (H. S. Cole)

1.21 Pelleted Waste Form

Waste form characterization continued on thirteen pelleted waste formulations prepared on the 41-centimetre-diameter rotating disc pelletizer using boric acid, metakaolin and calcium hydroxide as solid binders, and mixtures of H_3PO_4, HNO_3, or H_2O as liquid binders.

Compression strength of the pellets was measured by placing the pellets individually between two flat steel plates and applying a measured force, as specified in ASTM-382-72. Table 1 shows that the dried pellets had greater compression strength than the heat-treated ones. Assuming the pellets were uniform spheres tightly packed in a bed, a vertical column of 1-cm^2 cross-sectional area would resist the pressure indicated in the last column in Table 1.

TABLE 1

COMPRESSION STRENGTH TEST OF PELLETS

Sample		No. Pellets Tested	Pellet Mean Diameter, cm	Compression Strength N	Compression Strength kPa[a]
P-2	H.T.[b]	25	.63±.11	136±93	4370
P-3	H.T.	79	.67±.08	113±31	3200
P-7	Dried[c]	25	.68±.06	99±24	2730
P-7	H.T.	23	.62±.07	28±10	940
P-8	Dried	25	.56±.08	87±32	3540
P-8	H.T.	25	.47±.06	62±25	3560
P-8A	Dried	24	.57±.07	155±41	6070
P-8A	H.T.	25	.53±.05	76±29	3420

[a]Force (in kPa) of a vertical column 1 cm^2 in cross-sectional area through the bed

[b]Heat treated at 750°C for 1 h

[c]Dried at 200°C for 18 h

Both dried and heat-treated pellets should be strong enough for transport and storage with minimal breakage.

Cesium and strontium are the major long-lived fission products in ICPP calcine. Cerium is used as a stand-in for the actinides in the simulated calcine, although it is also present in actual waste as a fission product. Experiments to determine the leach resistance of pellets which had been heat treated one hour at 750°C, or two hours at 800°C were conducted. Pellets were Soxhlet leached in distilled water for 100 h at 95°C and the leach solutions analyzed for Cs, Ce, and Sr. Analytical values indicate that about 2% of the strontium present could be removed in 100 h by leaching while essentially none of the cerium was removed (less than 0.05 μg/mL which is equivalent to 0.032 wt% of the cerium present). Cesium leach rate variations were very large indicating basic insufficiencies in the detection method. Plans are being made to reanalyze using neutron activation, which could increase the accuracy.

Radioactive pellets of waste (either dried or heat treated) will be stored at elevated temperature due to radioactive decay heat. Table 2 shows the loss of volatiles and of nitrates due to storing dried (non-heat treated) pellets at 450°C. The data indicate that most of the volatiles are lost within the first day, but even after 38 days, slight losses were still being observed. For the nitrates, in spite of high initial losses, 9 to 44% remained after 38 days of heating. Dried pellets should be satisfactory for bin storage, but additional heating to the treatment temperature is necessary if pellets are to be stored in sealed containers or put into a metal or concrete matrix.

TABLE 2

VOLATILES AND NITRATE LOSS ON STORING NON-HEAT TREATED PELLETS AT 450°C

Cumulative Storage Time, Days	P-3		P-7		P-8		P-8A	
	Weight %							
	Volatiles Lost	Total NO_3 Content	Volatiles Lost	Total NO_3 Content	Volatiles Lost	Total NO_3 Content	Volatiles Lost	Total NO_3 Content
0[a]	---	2.69	---	0.48	---	0.36	---	3.89
1	3.54	.58	1.61	0.28	1.33	0.25	2.48	0.78
2	3.65	.62	1.70	0.33	1.39	0.23	2.68	0.90
9	4.11	.48	1.95	0.23	1.53	0.18	2.91	0.56
38	---	---	2.75	0.21	2.00	0.16	3.53	0.36

[a]Samples dried at 200°C for 16 h

1.22 Glass Waste Form

Fifteen different waste glass compositions were prepared; composition of the glass fluxes used is shown in Table 3. Leach-rate values (total weight change) obtained to date are shown in Table 4. Soxhlet leaches were run on ~5 g samples of glass which had been ground to -10 to +60 mesh; 150 mL of boiling distilled water refluxed continuously through the sample for 100 h. Brine[11], acid, and caustic leaches were performed on ~4 g samples of the glass ground to -10 to +60 mesh; 100 mL of the appropriate solution was continuously stirred during the 19 h test at ambient temperature. Leach rates were exceedingly low in the four brine and caustic solutions. The acid leach rates were somewhat higher, but probably still acceptable. Surprisingly, the distilled water leach rates were generally higher than expected, perhaps due to loss of material from the extraction thimbles.

Glass samples (7, 8, 9, and 10) were heated for 48 h at 650°C to determine if the glass would devitrify over long-term heating. X-ray diffraction examination of the "before and after heating" specimens indicated some slight undetermined crystallinity changes and the formation of $Ca_5(PO_4)_3(OH)$. Effects of the crystallinity changes have not been determined.

[11]Brine compositions were supplied by Sandia Laboratories.

TABLE 3

GLASS FRITS TESTED

Compound	Formulation No. (Wt% of Compound) #1	#2	#3	#4	#5	#6	#7	#8	#9	#10	#11	#12
SiO_2	57.0	57.0	57.0	57.0	57.0	57.0	58.6	56.0	56.0	56.0	56.0	56.0
Na_2O	10.0	4.0	10.0	10.0	10.0	10.0	12.4	20.0	20.0	20.0	20.0	20.0
B_2O_3	14.0	14.0	14.0	14.0	14.0	14.0	10.0	14.0	14.0	14.0	14.0	14.0
ZnO	7.0	4.0	7.0	7.0	7.0	7.0	--	--	5.0	5.0	--	2.5
CaO	12.0	3.0	--	3.0	9.0	6.0	6.0	--	--	5.0	--	--
MgO	--	6.0	3.0	--	--	--	--	--	--	--	--	--
P_2O_5	--	12.0	6.0	6.0	3.0	6.0	6.0	5.0	5.0	--	5.0	5.0
Li_2O	--	--	3.0	3.0	--	--	4.0	5.0	--	--	5.0	2.5
TiO_2	--	--	--	--	--	--	3.0	--	--	--	--	--

TABLE 4

LEACH RATES FOR VARIOUS WASTE GLASS FORMULATIONS

Glass Frit No.	Ratio Frit to Calcine	Wt% Loss or Gain in: Brine Solutions A	B	C	Acid pH 3.5	Caustic pH 9.5	Soxhlet 100 h @ 95°C
1	3:1	+0.047	-0.019	-0.012	-6.83	-0.032	-3.33
7	2:1	-0.122	-0.025	-0.031	-0.559	-0.044	-3.63
9	2:1	+0.05	-0.023	-0.11	---	---	-2.66
10	2:1	-0.059	+0.365	+0.030	---	-0.040	-3.69
11	2:1	-0.015	-0.005	-0.092	-1.50	-0.078	-3.84
12	3:1	-0.054	-0.050	-0.093	-1.04	-0.056	-3.52
12	2:1	+0.04	-0.006	-0.002	-1.62	-0.071	---
12	1:1	-0.017	-0.033	-0.019	-3.27	-0.047	-3.21
12	3:2	-0.002	-0.047	+0.024	-5.00	-0.012	-2.31

1.3 Conceptual Design Studies for a Post-Calcination Treatment Pilot Plant (S. J. Priebe)

The conceptual design for a post-calcination treatment pilot plant incorporates processes for both glass melting and pelletizing of simulated ICPP wastes. The specific processing stages involved for each waste form are discussed in the following sections.

1.31 Pelleted Waste Formation Process

Calcine and solid binder will be screw fed from hoppers to the pelletizer. Liquid binder is fed under constant pressure to the pelletizer. The solid binders may include metakaolin, silicates, and borates. The liquid binder can be colloidal silicas or a combination of HNO_3 and H_3PO_4. Some of the binders may be incorporated in the feed to the fluidized-bed calciner.

A 41-centimetre- (16-inch) diameter rotating disc pelletizer will form spherical pellets approximately 3-6 mm in diameter. Throughput will be up to 23 kg/h. The pelletizer will be enclosed to facilitate venting off-gas which may contain some dust and NO_x.

The pelletizer will produce moist pellets which will be continuously dried in a microwave or radiant-heated dryer. Drying temperature will be 150-200°C. Dried pellets will be screened, if necessary, to remove all pellets over twice the desired diameter. The oversize pellets will be ground to the desired diameter and recombined with the main pellet flow.

To produce leach-resistant pellets, heat treating at 800-900°C for ~2 h is necessary. The most promising method to accomplish this is a rotating tray heater. Radiant heating will be used, and the number and rotational speed of the trays will establish the residence time. Forced air will remove the off-gases from the heat treating stage.

Finally, the pellets will be stored in bins.

1.32 Glass Melting Process

Glass melting can be done in two ways as described below.

(1) In-can melting--Calcine and glass frit are fed directly to a canister in a furnace which does both melting and annealing. The canisters will be 1-1.25 m long by 15-25 cm in diameter. The furnace is a split-half three-zone type furnace.

(2) Ceramic-melter melting--This is the glass formation method preferred for ICPP wastes, because of the waste volumes to be handled. Therefore, this process will be tested in the pilot plant. A ceramic-lined melter, heated by electrodes, melts the calcine and frit. The melter will have a capacity of ~0.1 m^3. Molten glass can be drained continuously or in batches into the canister for annealing.

In both cases, the same hoppers and screw feeders as used in pelletizing will be available.

An experimental plan was developed to answer questions in processing, including pellet screening, microwave pellet drying, and heat treating of pellets. Microwave drying experiments were begun to determine drying time. Table 4 shows results of microwave drying experiments using simulated pellets. These were previously dried pellets which were then soaked in distilled water for 27 h. Since a commercial home microwave oven was used, the actual microwave power output is not known. These results indicate that while a higher power requires less drying time, a larger amount of other volatiles are lost. Components lost through volatilization will be determined.

TABLE 5

Microwave Drying of Pellets

Power Setting	Initial wt. of H_2O in Pellets (g)	Total wt Loss on Drying (g)	% of Total Loss That is H_2O	Drying Time (min)
1 (highest)	21.1	31.4	67.4	10
2	21.2	30.7	69.1	12
3	20.6	28.9	71.3	15
4 (lowest)	21.5	27.4	78.5	20

Plans for Next Quarter

Additional pellet formulations will be prepared on the 41-cm-diameter disc pelletizer and their properties compared with previously prepared compositions. Cesium leach rates, using chemical and activation analysis, will be measured. Fluoride volatility during preparation of waste glass will be determined. Glass samples will be analyzed by x-ray diffraction both before and after attempts to devitrify them at 550-850°C. Devitrification effect on leach rate will be determined.

The specially prepared calcine will be pelletized and the effects of precalcination addition of boric acid and zinc oxide will be determined. Pellet screening experiments will be done with wet and dry pellets to determine the screen effectiveness and also the necessity of drying before screening. Microwave pellet drying will be tested on a larger scale.

A mockup of the rotating tray heat treater will be built and tested to study the physical problems associated with such a system. The most efficient throughput mechanism will be determined.

2. Actinide Removal From ICPP Wastes (L. D. McIsaac, J. D. Baker, J. F. Krupa)

During the preceding quarter, equilibrium distribution coefficients for selected actinides between aqueous HNO_3 solutions and DHDECMP were determined. Lanthanum loading capacity and the distribution of HNO_3 for

DHDECMP were measured. Also, distillation by means of a thin-film molecular still was shown as a viable method to purify DHDECMP in quantities (~100 L) necessary for engineering pilot-plant studies.

Plotted in Figure 2 are typical data for the equilibrium distribution at 22°C of selected +3, +4, and +6 actinides between aqueous HNO_3 solutions and 30% DHDECMP in diisopropyl benzene. The 30% DHDECMP-DIPB used to obtain the results shown in Figure 2 was prepared from vacuum-distilled (86% purity) DHDECMP and was sequentially washed with 0.5M Na_2CO_3 and water prior to use. Equal volume portions of aqueous and organic phases were shaken for five minutes. Adjustments of Pu(IV) and Pu(VI) oxidation states were made with 0.025M $NaNO_2$ and 0.025M $NaBrO_3$-0.001M $Ce(NH_4)_2(NO_3)_6$, respectively. Neptunium(IV) and neptunium(VI) states were adjusted with 0.024M $Fe(NH_2SO_3)_2$ and 0.025M $NaBrO_3$-0.001M $Ce(NH_4)_2(NO_3)_6$, respectively. Erratic results, not shown here, were obtained for the distribution of Pu(III) between HNO_3-$Fe(NH_2SO_3)_2$ solutions and 30% DHDECMP-DIPB extractant.

Distribution of HNO_3 between aqueous HNO_3 solutions and 30% DHDECMP-DIPB has been measured over the acidity range of 0.15-10M HNO_3. A distribution coefficient of ~0.2 was observed over the entire HNO_3 range.

A centrifugal molecular still, ordered from CVC Products, Inc., Rochester, NY, was received and placed in operation. This apparatus is presently used to purify DHDECMP in hundred gram quantities. It is felt that once this system is optimized, a liter of DHDECMP per day can be distilled. During the first two distillation runs, the product purity was ~90%.

Mercury, used in the Al fuel dissolving process, extracts into DHDECMP. Once extracted, the Hg does not strip by conventional methods. Thus, the mercury tends to build in the organic and eventually reduces the extraction coefficient of the extractant for actinides.

Mercury appears to interact with the extractant differently than other elements. Mercury extraction, from preliminary studies, appears to be a function of extractant purity and extraction time, dependencies which were not evident with the other elements of interest. This, combined with the fact that mercury does not complex strongly with oxygen, suggests that the mercury-extractant interaction is different from the complexes formed with other elements. One thrust of investigations this next quarter will be elucidating this interaction in terms of structure and kinetics.

The mercury has been successfully stripped from the extractant electrolytically and by using caustic cyanide. Both these methods will be examined parametrically and in terms of a practical actinide removal flowsheet. Other methods of mercury removal will be investigated as they are suggested from our investigations and literature research.

DHDECMP has been difficult to obtain, because the only manufacturer was a small company which made this organic on a custom basis. Eastman Organic Chemicals, Rochester, NY, has now agreed to produce DHDECMP in 120 L batches.

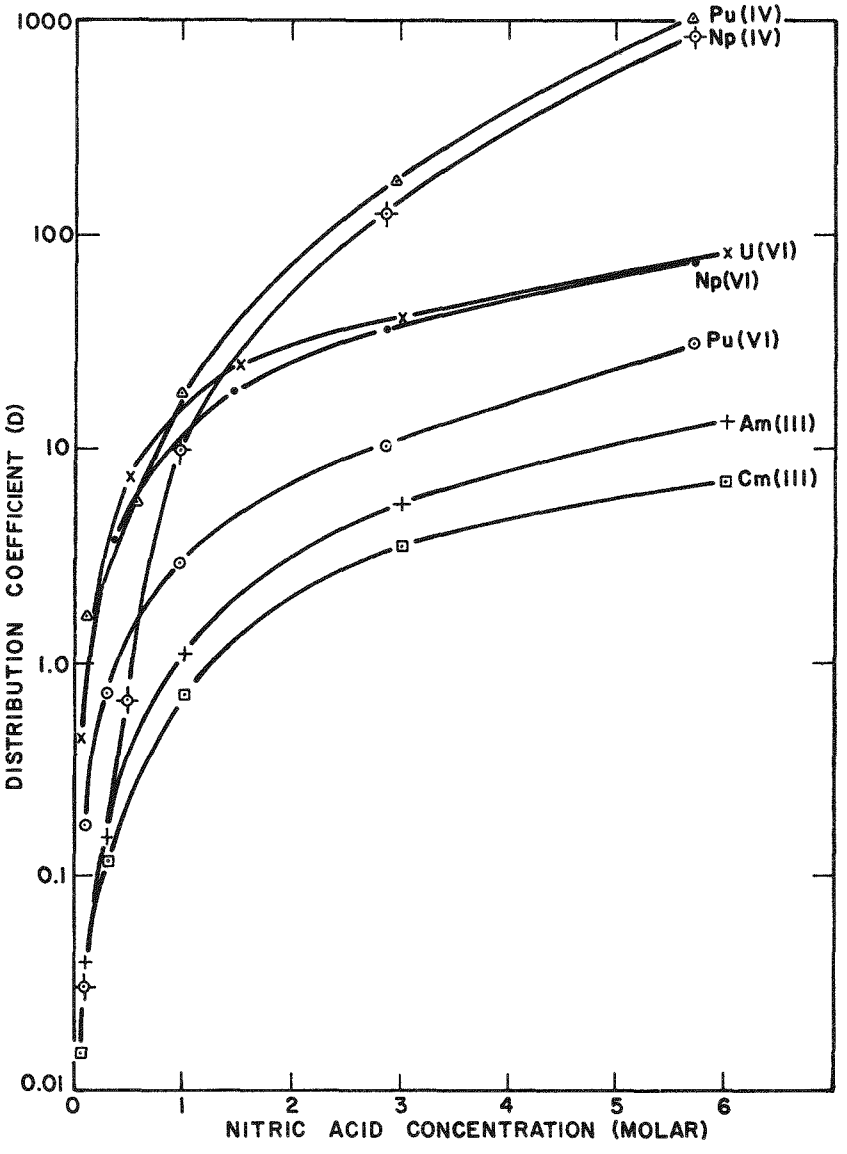

Figure 2. Actinide Distribution Coefficients

This should simplify purchase of this extractant. Eastman expects the purity of their material to be at least 50%. An order for 120 L of DHDECMP was placed with Eastman. This organic will be purified by vacuum distillation for future engineering pilot plant experiments.

ICPP intermediate level liquid waste has been simulated. The macro constituents and their concentrations in this solution are given in Table 6. Extraction of the actinide elements from this matrix will be investigated the next quarter.

The second annual Actinide Removal Workshop, hosted by ARHCO at Richland, Washington, was attended by L. D. McIsaac and J. D. Baker. At this workshop, the ERDA sites which are participating in actinide removal studies discussed the progress of the preceding year.

TABLE 6

ICPP Simulated Intermediate-Level Liquid Waste

Element	Concentration (M)
H^+	1.40
Al^{+3}	0.56
Zr^{+4}	0.00011
Fe^{+3}	0.011
Na^+	1.6
F^-	0.00065
NO_3^-	4.4
B	0.0057
Cl^-	0.032
PO_4^{-3}	0.020
SO_4^{-2}	0.035
Hg^{+2}	0.0050
K^+	0.24
Mn^{+2}	0.024

Plans for Next Quarter

DHDECMP purification techniques will continue to be investigated. Methods of Hg removal from DHDECMP will be studied. A minimixer settler experiment will be conducted to test a mixed diluent, i.e., decalin-diisopropyl benzene, an acidic scrub stream and a dilute exalic acid strip.

3. Calcined Solids Retrievability and Handling (J. S. Schofield, J. A. Hendricks)

The calcined solids retrieval program has been redirected to place initial emphasis on sampling of stored radioactive calcine and development of cold prototype retrieval equipment.

Samples of cold zirconia and alumina calcine were maintained at 90 kPa mechanical loading pressure and 450°C and 600°C, respectively, for 1500 h. No signs of agglomeration were visible; very minor lumping of material, which would break up upon touching was noted.

Design work has started on a process and associated equipment for the bin sampling project. Bins 3 (alumina calcine) and 7 (zirconia calcine) in Bin Set 2 have been selected for sampling. A commercially available hydraulic drilling unit has been selected for the actual sampling operation. Shielding calculations have been made for various sizes of sample shielding containers.

Upgrading of the existing solids retrieval testing equipment is currently underway. When completed, an in-depth calcine retrieval nozzle development program will be started to delineate the parameters directly affecting nozzle performance. Various nozzle designs have already been fabricated for testing.

Preliminary project plans have been prepared and issued. A detailed plan is being written.

Plans for Next Quarter

A detailed program plan for calcined solids retrieval will be issued in August, 1977.

Design work should be completed for the bin sampling process and all the capital equipment items ordered. A safety review document for the bin sampling program will be started.

A set of design bases for the cold prototype retrieval equipment will be issued and an A-E selected for the conceptual design and performance specification writing.

Nozzle testing should be completed for the existing commercial retrieval nozzle and all of the presently available test designs.

4. ICPP Defense Waste Document (R. L. Nebeker, N. A. Chipman)

A Defense Waste Document (DWD) which discusses alternatives for the long-term management of ICPP High-Level Solid Waste was completed. The DWD describes the existing technology for treating and disposing of ICPP wastes. Costs and risks associated with the various alternatives are presented.

The document discusses disposal in terms of storage location and waste forms. Three location options are discussed:

(1) Storage at the INEL

(2) Storage at a Federal Repository

(3) Removal of the long-lived actinides from the waste with subsequent storage of the actinides at a Federal Repository and storage of the actinide-free waste at the INEL

The waste forms which are considered are:

(1) Calcine

(2) Pellets

(3) Sintered glass-ceramic

(4) Metal matrix

Costs for each alternative were estimated from preliminary design and expected operating costs. Risks, defined as probabilities times consequences, were estimated for each phase of each alternative. These phases include calcine retrieval, calcine dissolution (where applicable), post-calcination treatment, shipment, and storage. The risks were converted to a risk cost by assuming a value of $1000 per man-rem. This risk cost then was added to the capital and operating cost to produce a total alternative cost.

The analysis showed that the least expensive and least risky alternative is to leave the calcine in the existing bins. All other options result in both increased cost and increased risk. Most of the risk is associated with routine operations from additional waste handling during processing. Accidental risks, because of the low probabilities of occurring, are relatively minor.

II. ICPP PLANT PROCESS IMPROVEMENT

1. Uranium Accountability Measurements (E. E. Filby, R. L. Hand, M. A. Wade)[a]

This report outlines some of the results which have been obtained in the uranium accountability measurements system by the Radiochemistry and the Production Support and Analytical Branches. Progress has been made in a number of areas in the system, including the methods used for routine chemical separations, work in the Mass Spectrometry Lab, and in general development.

1.1 Chemistry and Related Procedures

A new procedure, Method U-Sep-2 (tentative), was used during the most recent plant processing campaign. As will be shown later in this report, the use of this new method, along with the other improvements which have been made in the total measurements system, has resulted in noticeably better performance. During the course of the development work on improving the chemical separation method used, two other alternative procedures have also been found.[2] All three procedures start with the same remote operations involving the extraction of the complexed uranium into hexone. Method U-Sep-2 (tentative) and one of the alternatives use an anion-exchange resin for later cleanup. The third alternate employs the "liquid anion exchange" material, tri-isooctyl amine (TIOA). Future development work will exhaustively compare these three so the best can be selected for routine use.

Another modification was made in remote pipetting and weighing. For each IFU and control, a comparison was made between the volume delivered by

---

[2]S. D. Reeder (this report, page 115)

[a]The authors wish to acknowledge the contributions by the Shift Lab analysts, the Mass Lab operators, and by J. E. Delmore, S. Kelly, S. D. Reeder, F. W. Spraktes, D. R. Trammell, G. W. Webb, and N. R. Zack.

the pipetter (as determined by previous calibration) and a value calculated from the measured sample weight and density. While the measured weight was the only value used for subsequent calculations for concentration, this cross check has two valuable results. First, the need to obtain agreement in the cross check ensures greater consistency among the various analysts in the way they do these operations. This tends to minimize some of the possibilities for analyst-related variations in the overall results. A second advantage is that any sudden changes in instrument characteristics can be detected immediately and necessary corrective measures can be instituted. Representative data from earlier in the run are shown in Table 7.

TABLE 7

Data for Volume Cross-Check

	Initial Performance		After Familiarization	
	In[a]	Out[a]	In	Out
Biased[b] Analysts	8 (35%)[c]	15 (65%)	17 (77%)	5 (23%)
Other Analysts	50 (78%)	14 (22%)	58 (82%)	13 (18%)
All Analysts	58 (67%)	29 (33%)	76 (82%)	17 (18%)

[a] "In" means that the calibrated volume and the calculated volume differed by less than 0.75%, "Out" differed by more than this.

[b] Composite set for three analysts whose initial performance differed from the others.

[c] The parenthetical percentages refer to the fraction In or Out for a set.

The value of 0.75% used for comparison was based on the inherent reproducibility of the pipetting/weighing system. Except for the three analysts whose particular techniques differed noticeably from that of the others, the data clearly show the degree of consistency attainable. Also, after the initial period, all of the analysts attained a very consistent level of performance. Moreover, preliminary evaluation of comparison data for later in the plant run indicates that an even higher level of consistency has been attained.

1.2 Mass Spectrometry Lab

A number of changes have been made in the procedures used in the Mass Lab. To better define what is meant by "bad running" behavior for the instrument, the operators were given a list of codes which covered most of the "typical" kinds of behavior. Some of these kinds include:

(1) Strong, but unstable (noisy) beam

(2) Weak and unstable beam

(3) Weak, but stable beam

(4) Beam strength decreases rapidly during running

A similar set of criteria also were established to better define poor filament-loading behavior. Use of these criteria have allowed a comparison between certain sample characteristics and the loading and running behavior. Studies using these codes are under way at the present time.

Analysis of a large amount of raw mass spectrmetry data also has resulted in a more objective criteria for what constitutes "good" running in the instrument. This criteria is based upon the set of individual standard deviations derived by the instrument computer for the isotopic peaks. These values are printed out along with the atom percent numbers calculated for a given series of scans. It has been found that a set of mean standard deviations for a reasonable number of analyses does reflect how well the group of samples ran. Table 8 shows the data obtained for a sampling of the 1976 Zirconium-type plant samples and from the more recent plant run, which began with zirconium fuel processing.

TABLE 8

Basis For More Objective Running Criteria

Sample Type & Plant Processing Period	Mean Std. Dev. for U-233[a]	Mean Std. Dev. for U-235[a]	Fraction of Std. Dev. >0.05	Fraction of Std. Dev. >0.08
Zirconium (1976)	±0.077	±0.060	37.5%	18.8%
Coprocess (1977)	±0.048	±0.042	20.1%	7.3%
"Good"[b] (1977)	±0.038	±0.035	13.3%	2.8%

[a] U atom percents, typical values are 25-35% for U-233 and 55-65% for U-235.

[b] The "good" sample type denotes a more recent period in the Coprocess run during which the overall behavior of the samples in the instrument was quite good--it represents about 100 consecutive analyses.

The data for the 1976 zirconium run represents about 50 samples, and it is apparent that the higher mean standard deviations (and the corresponding larger percentage of outliers) does correlate with the very poor running behavior for which that run was noted. The set listed for Coprocess represents a mix of about 110 straight zirconium and Coprocess samples during the early stages of the 1977 plant run; a period during which the

samples were found to run quite well, but still with an occasional poor one. Finally, the last set represents about a week's work (around 100 samples) during a time when the samples appeared to be running exceptionally well. It is apparent that these mean standard deviations do reflect the overall behavior of a set of samples.

These mean standard deviations have been used to establish a rejection limit for comparison with any given sample as it is being run in the mass spectrometer. The rejection criteria says that the standard deviations printed out for a scan set must be less than 0.05 for all of the major peaks (generally, U-233, U-235, and U-238). If these limits are not met, a new scan set must be taken. The use of this criteria is modified for those cases where a sample is running so poorly that acceptable data cannot be obtained. In these cases, the operator must take a minimum of five scan sets. If no two sets of data meet the 0.05 limit, it is assumed that the group of five is the best that can be done, and no further effort is justified. A second filament is loaded from those samples and run when time permits. This criteria thus gives the operators an objective measure of how well a sample need run, along with an established procedure to follow when a sample does not run well. It, therefore, provides a reasonable trade-off between analysis time and acceptable data quality.

A study also has been made of the dependence of filament loading behavior upon the sample acidity at a particular uranium concentration. Some of the observations made for an approximately 1 g/L solution are given below.

0.5M HNO_3: Two large drops loaded fairly easily, and a quite acceptable yellow-orange residue was left on the filament upon drying.

0.75M HNO_3: Two large drops loaded reasonable well, but the residue left was neither as large nor acceptable in form or color.

1.0M HNO_3: Could not load sample, the second drop slipped down and hung from the bottom of the filament. Two loadings were attempted unsuccessfully.

1.5M HNO_3: Two small drops were loaded with great difficulty, and the resulting residue was very poor.

The results indicate that the acidity strongly affects the loading behavior at this particular concentration of uranium. On the other hand, further work seems to show that the acidity dependence is closely tied in with the variation in uranium concentration. Additional study is needed to further define this apparent inter-dependence.

1.3 Quality Control Results

The Quality Control data generated during the most recent plant run indicate that the overall system has improved since the last run. Table 9 lists the results for precision from duplicates and from the control samples. These data cover approximately two-thirds of the run, including the period of familiarization early in the run.

TABLE 9

System Precision For Concentration

	Rel. Std. Dev. From Duplicates Data	Rel. Std. Dev. From Control Data	Statistically[a] Significant Difference?
1976 Zirconium Run	0.63%	0.60%	No
Present Zirconium Run	0.48%	0.52%	No
Aluminum Dissolver	0.40%	0.51%	No
Coprocess Solutions	0.48%	0.23%	Yes

[a]The "f" test was applied to each pair. Also, the "f" test showed that the difference between the values for the 1976 Zirconium Run and the present Zirconium Run is statistically significant.

It is apparent that the overall performance of the system has improved noticeably compared to the 1976 run. In general, the system performed at a 0.5% level during this period versus around 0.6% for the previous zirconium run. The low value shown for the coprocess controls is probably a statistical anomaly resulting from the relatively small data base for the control data. A complete analysis of the QC results for the run may clear up this difference.

1.4 Total System Definition

Another area of work during this time involved the definition of the total system (administrative as well as technical) for the uranium accountability measurement. A wide variety of documents have been collected, and pertinent SOPs have been identified and examined. A complete system description is being compiled from these and other inputs.

One result of this examination of the total system is a better understanding of how the measurement practices impact on the ICPP accountability material balance. A key number associated with that balance is the limit of error (LE) for the BPID, the "Book-Physical Inventory Difference". A breakdown of the contributions to the LE for a previous balance was made. Table 10 lists the contributions which have been identified.

TABLE 10

Breakdown of Contributions to the BPID-LE[a]

	From Uncertainties in Measurements				From Uncertainties in Estimates	Total
	Analytical		Operations			
	rand.	syst.	rand.	syst.		
Input	12.9	9.7	3.2	28.7	---	64.5
Final Product	0.6	5.4	---	---	---	6.0
Inventories[b] & Waste	15.6	0.3	6.8	---	---	22.7
Holdup	---	---	---	---	6.8	6.8
TOTALS	29.1	15.4	10.0	38.7	6.8	100.0

[a]BPID-IE stands for the Limit of Error on the Book-Physical Inventory Difference.

[b]Includes both Beginning and Ending inventories. "rand." and "syst." denote random and systematic uncertainties.

The breakdown shown is, of course, for a single particular plant balance. Some of the relative contributions will be different for a different system; nevertheless, the general features probably hold for most systems. The measurements shown for Operations are the tank volumes used in the inventory calculations. Obviously, the uncertainties for input volume measurements are the largest single contributor to the LE. But the analytical measurements also are a substantial part, and improvements in this area would have a worthwhile impact upon the overall LE. One somewhat surprising feature highlighted by this breakdown was the significant contribution of the uncertainties for the plant Inventories to this particular calculation. These measurements contributed over a fifth of the overall LE. However, the uncertainties in these measurements were only estimated, and the estimates used were probably conservatively high.

Past evaluation of the overall measurements system has been handicapped by the fact that no real guidelines exist for how well analyses must be done. The only guide appeared to be that the results should be "as good as possible". This handicap still applies, but this evaluation of the total system has at least identified what appears to be a kind of upper limit on the acceptable limit of error. This value is 0.7% which, according to the ERDA-ID Nuclear Materials Control Survey No. ID-76, appears in the document 10 CFR 70 as a maximum allowable LEMUF for chemical processing plants. (The "LEMUF" is equivalent terminology for BPID-LE.) Since the LE is defined as twice the relative standard deviation versus the input quantity of uranium, this would indicate a maximum allowable relative standard deviation of 0.35%. The fact that the previous balance showed a value of 0.24% indicates that, while the present system is safely

under that maximum limit, there really is not any "slack" there. Consequently, there is every reason to work to improve the capability of the system, and to learn more about the system so it can at least be maintained reliably at its present level for all kinds of plant throughput.

2. Zirconium Fuel Recovery Process (M. L. Gates)

For the reporting period, efforts were exclusively in chemical and engineering verification studies for the Fluorinel process to be installed at ICPP.

The Fluorinel headend system will be installed in a new building and will consist of several dissolvers, several complexing and surge tanks, and a liquid feed clarification system. Auxiliary equipment required to support the headend process includes facilities for fuel storage and handling, off-gas cleanup systems, several casks, improved analytical systems, and various safety and control systems. Existing facilities at the ICPP will be used to extract uranium from the dissolver product.

2.1 Entrainment Velocity and Velocity Gradients in Proposed Fluorinel Dissolver (K. F. Childs)

Tests were made to determine the velocity of the liquid sparge required to suspend typical process solids in the proposed inverted dish design for the Fluorinel dissolver bottom. The velocity profile between sparge lines was estimated.

The proposed design for the Fluorinel dissolver bottom is an inverted dish with three sparge tubes located around the circumference of the bottom. These tubes will be allowed to fill with solution before being pressurized with nitrogen to force the solution out. This pulse of liquid will serve to agitate and suspend the various solids that are expected in the Fluorinel process.

The liquid sparge velocity required to suspend solids in the proposed dissolver was estimated by two methods: (1) calculation of a minimum fluidization velocity for the solids, and (2) assuming that turbulent flow in a toroidal volume would provide adequate suspension. The major assumptions made in using the two methods are as follows:

Fluidizing Velocity	Turbulent Flow
- Equation for minimum fluidization velocity holds for liquid-solid systems.	- Turbulent flow in toroidal channel approximately 20.3 cm (8 inch) diameter imposed in vessel bottom is sufficient to suspend solids.
- Sparge flow distributed optimally for fluidization.	- Sparge liquid momentum is transferred to vessel liquid without losses.
- Fluidization cross-section approximately 0.46 m^2 (4.9 ft^2) (see calculations.)	- Solids density approximately 9728 kg/m^3 (600 lb/ft^3).

Fluidizing Velocity (contd.)	Turbulent Flow (contd.)
- Solids diameter approximately 100μ .	- 30% solids by wt in toroidal channel.
- Liquid density approximately 1524 kg/m^3 (94 lb/ft^3).	- Liquid density approximately 1524 kg/m^3 (94 lb/ft^3).
- 91.4 cm (36 inch) diameter vessel, 1/2 inch, Sch XX sparge tubes.	- 91.4 cm (36 inch) diameter vessel, 1/2 inch, Sch XX sparge tubes.

Both methods indicate that a liquid velocity in the sparge tubes of approximately 1.83 m/s (6 ft/s) is required to produce the circulation required to suspend solids in the bottom of the proposed dissolver vessel. Approximately 2.07 x 10^5 Pa (30 psig) nitrogen would be required to drive the liquid sparge at this velocity. Nitrogen consumption (for three sparge tubes, assuming a 6 second minimum sparge cycle) would be roughly 3.63 x 10^{-3} L/min (0.13 ft^3/min) at 2.07 x 10^5 Pa (30 psig).

The velocity gradient between sparge tubes was estimated using equations for a turbulent-free jet. It was assumed that the equations are valid for estimating liquid systems as well as gaseous systems. The velocity profile tends to confirm that the momentum transferred to the vessel liquid is sufficient to create turbulent flow [0.008 m/s (0.026 ft/s)] over the majority of the flow channel assumed.

2.2 Agitation in the Proposed Fluorinel Dissolver Charge Chute (K. F. Childs)

A study was made to determine the agitation created in the charge chute of the proposed fluorinel dissolver due to thermal gradients and hydrogen evolution during the dissolution of the fuels.

Heat generation was calculated to be 152 KW (5.2 x 10^{-5} Btu/h). Hydrogen generation was calculated to be 0.79 m^3/min (28 ft^3/min). These estimates were based on the following assumptions:

(1) Acid addition rate of 550 L/h of 6.8M HF

(2) $Zr + 4HF \longrightarrow ZrF_4 + 2H_2$; $\Delta H = -5.86 \times 10^5$ J/mol (-140 kcal/mol)

(3) HF reacts completely and instantaneously

It was concluded that the hydrogen generated would cause extreme agitation[3] in the dissolver charge chute and create a gas lift circulation[4] between the chute and the dissolver annulus of approximately 7.34 x 10^4 L/min (1800 gal/min). The agitation and circulation would provide such rapid mixing that thermal gradients would be negligible.

---

[3] IDO-14562, Mixing and Evaporation in a Packed Vessel, G. K. Cederberg and J. A. Buckham, September 20, 1961.

[4] HW-37432, Operational Characteristics of Submerged Gas-Lift Circulators, M. W. Cook and E. D. Waters, 1955.

2.3 Erosion Due to Process Solids (K. F. Childs)

A series of tests were carried out in bench-scale apparatus to determine the erosion effects of sparge jets using ZrO_2 in simulated complexed dissolver product (CDP) slurries on Hastelloy C-4[2] (as would be encountered in the proposed Fluorinel dissolver bottom design). The system was designed so that a timer cycled the sparge gas on for 0.5 s, at 10-s intervals. The gas drives the slurry out of the sparge tube at roughly 0.9 m/s (3 ft/s) onto the Hastelloy test coupon. The sparge tube was vented to the atmosphere between the 10-s pulses to allow the tubes to refill. Test conditions are outlined below:

Hastelloy C-4 Coupon[a]	Temperature (°C)	Slurry (Wt%)	Number of Cycles
KCC	20	1% ZrO_2 in H_2O	37,560
KCA	20	1% ZrO_2 in CDP	40,140
KCB	65	1% ZrO_2 in CDP	38,880

NOTE: CDP composition same as used in filter corrosion tests. (See following Section 2.4).

No visual evidence of erosion was seen with any of the coupons. Coupons KCA and KCB, however, showed weight losses corresponding to rates of 0.91 and 18.6 μm/mo (0.036 and 0.732 mil/month) respectively. These rates are roughly equal to the rates from corrosion only, estimated from previous data, of 7.62 and 14.7 μm/mo (0.3 and 0.58 mil/month) respectively. It was concluded that sparger erosion is not significant at these velocities.

A series of tests were carried out in bench-scale apparatus to determine the erosion effects on transfer lines of ZrO_2 - complexed dissolver product (CDP) slurries flowing in these lines. It was assumed that 11.4 L/min (3 gal/min) flowing in a 1-inch line, or a Reynolds number of 5150, would represent typical Fluorinel flows. Test conditions were as follows:

304L ss Tube Element	Temperature (°C)	Slurry (Wt%)	Reynolds Number	Run Time (h)
C	20	1% ZrO_2 in H_2O	3240	96
A	20	1% ZrO_2 in CDP	5554	96
B	45	1% ZrO_2 in CDP	5554	96

NOTE: CDP composition same as used in filter corrosion tests.

No visual evidence of erosion was seen with any of the test elements. Elements A and B showed weight losses corresponding to rates of 0.51 and 1.02 μm/mo (0.02 and 0.04 mil/month) respectively. This compares with the rates from corrosion only, estimated from previous data, of 0.19 and 1.27 μm/month (0.0075 and 0.05 mil/month) respectively. It was concluded that erosion at these velocities is not significant.

[a]Stellite Division, Cabot Corporation, 1020 W. Park Ave, Kokomo, IN 46901

2.4 Filter Element Corrosion (K. F. Childs, C. A. Buckham)

During the dissolution of fuel in the Fluorinel Process, miscellaneous insoluble solids are produced. The majority of these solids must be removed before the solution reaches the ICPP extraction system to prevent column upsets. Filtration is being investigated for removing these solids.

Two filters appeared to be suitable during scoping studies. They were the Mott cross-flow sintered-metal filter[5] and the Vacco etched-disk filter[6]. Samples of three sintered metal filter elements and an etched-disk filter element were tested for corrosion effects in complexed Zr dissolver product. The sintered-metal test samples were approximately 1.3 cm in diameter by 17.8 cm long. The etched disks making up the filtering portion of the element were roughly 20% of the complete element by weight. The elements were suspended in CDP for testing. The composition of the CDP was:

F	Zr	Al	NO_3	H^+	SO_4	Cd	
3.07	0.60	0.42	2.45	2.10	0.21	0.16	molar

Test results are shown in Tables 11 and 12.

TABLE 11

Corrosion of Filter Elements in Complexed Dissolver Product

Temperature 60°C - Exposure Time 24 h

Element	Material	Initial Weight (g)	Weight Loss (g)	% Weight Loss
Sintered Metal	Monel	15.3646	Dissolved	---
Sintered Metal	Type 316 Stainless steel	13.4247	2.0363	13.0%
Sintered Metal	Hastelloy C	15.6089	2.0363	13.0%
Etched-disc	Type 304L Stainless steel	601.8301	0.6083	0.1%

[5]Mott Metallurgical Corporation, Farmington Industrial Park, Farmington, Connecticut 06032

[6]Vacco Industries, 1035 Vacco Street, South El Monte, California 91733

TABLE 12

Confirmatory Corrosion Test of Filter Elements
Temperature 40°C - Exposure Time 168 h

Element	Material	Initial Weight (g)	Weight Loss (g)	% Weight Loss
Sintered Metal	316 stainless steel	28.8671	3.8179	13.23%
Etched-disc	304L stainless steel	601.2218	1.9426	0.32%

The two elements from Test 2 were bubble tested by the vendors after corrosion testing to determine pore size changes associated with the reported weight losses. In both cases, results (unexpectedly) showed no change. It was felt that this was due to a lack of forced flow through the elements during testing. It was concluded from the above results that:

(1) Type 316 stainless steel was significantly better than Hastelloy C, and Monel was totally unacceptable for the sintered metal elements.

(2) The etched-disc Type 304L stainless steel element was far superior to the sintered metal Type 316 stainless steel element.

2.5 Evaluation of Proposed Fluorinel Dissolver Chute Design (K. F. Childs)

The proposed design of the Fluorinel dissolver charging chute was evaluated with respect to the number and location of the slots required. The design of the chute has been determined to have a significant impact on the heat transfer and fluid circulation characteristics of the dissolver.

From this evaluation the following recommendations were made:

(1) The total cross-sectional area of the slots should be equal to or greater than the charge-chute cross-sectional area.

(2) The slots should be located approximately 25 cm (approximately 10 inches) above the highest product overflow line.

This design would prevent the excessive carryover of foam into the dissolver annulus while maximizing the liquid circulation rate. The elimination of foam from the dissolver annulus will improve the performance of both dissolver level instrumentation and the product overflow lines.

Maximizing the circulation rate in the dissolver will improve the heat transfer to the cooling coils and thereby reduce the liquid evaporation rate in the dissolver.

Plans for Next Quarter

Design verification studies for the Fluorinel process will continue. Studies that are to be completed during the 4th Quarter include:

(1) Solids separation system performance evaluation

(2) Dissolver sparging studies

(3) Corrosion testing of the proposed materials of construction with each of the Fluorinel process flowsheets

(4) Solids dissolution flowsheet development

III. ADVANCED GRAPHITE FUELS REPROCESSING

(L. W. McClure)

The Rover processing equipment, currently being installed at ICPP, will serve as the headend process for recovering uranium from the Rover Nuclear Rocket graphite fuels. In this process, the bulk of the graphite fuel matrix is converted to CO_2 in a primary burner. The residual graphite is then burned in a secondary burner to produce an ash consisting of U_3O_8, Nb_3UO_{10}, and Nb_2O_5. This ash is then dissolved, leaving 60% of the Nb_2O_5 as a solid residue. These undissolved solids are removed by a continuous solid bowl centrifuge, and the clarified solution is fed to the existing ICPP solvent extraction system. Current pilot-plant work consists mainly of verification of process designs which have been specified for the Rover facility and recommendations for rectifying design deficiencies.

1. Solids Transport Systems Testing (H. S. Meyer)

Tests were made to verify that the jet ejectors installed in the Rover plant will perform adequately to pneumatically transfer solids during Rover fuel reprocessing. Experiments were also made to determine: (1) alumina bed material attrition during transport and (2) erosion of jets, elbows, and deflector plates during transport of alumina and simulated ash.

1.1 Verification of Pneumatic Transport System

Scoping tests of the operability of the plant solids transport system were completed using a pilot plant test loop. Penberthy ejectors were used to transport alumina (Al_2O_3) and simulated burner ash through a 1-inch-diameter piping transport system. The tests showed that the system installed for pneumatic transport of Rover solids is adequate.

The effect of pressure in the receiving vessel on transfer rates was determined. The solids flow rate varied inversely with pressure differential across the filters in the receiving vessel at various motive gas operating pressures supplied to the jet. The solids flow rate at 13.75 kPa (55 inches H_2O) and the extrapolated pressure differential for no solids flow are shown in Table 13.

TABLE 13

Rover Solids Transport Scoping Tests Through a 1-Inch Piping Transport System

Jet	Material Being Transported	Vibrator Used on Vessel Being Emptied	Solids Transfer Rate At 13.75 kPa (55 in. H_2O) Across Filters (g/min) Operating Pressure (kPa) 140	257	415	Estimated Pressure Differential for No. Solids Being Transferred (kPa) Operating Pressure (kPa) 140	257	415
63A	Primary Burner Ash	No	400	1200	1800	18	35	52
63A	Primary Burner Ash	Yes	375	800	1400	20	36	58
63A	Al_2O_3	No	---[a]	1400	---	---	27	---
62A	Secondary Burner Ash	No	450	1600	1900	18	64	123
62A	Secondary Burner Ash	Yes	---	1400	---	---	N. C.[b]	---
LL1	Primary Burner Ash	No	---	1800	2500	---	40	59
LL3/4	Secondary Burner Ash	No	---	1400	1700	---	41	68

[a]Not measured.

[b]Data does not correlate to give no solids flow.

1.2 Al_2O_3 Attrition Tests

Tests to determine if excessive attrition would result from transporting Al_2O_3 to and from the burners have been completed. The tests show that excessive attrition should not be experienced. The apparatus for the experiments is shown in Figure 3. Transfers were made by a Penberthy Model 63A jet operated at 550 kPa (80 psi). A 10 kg sample of Al_2O_3 was split into two test charges. Prior to testing, a screen analysis was performed on each charge. One solids charge was transferred through a system having six 1.57 radian (90°) elbows; the other charge was transferred through 10 elbows.

The material was periodically screened to determine attrition. The results of these tests are shown in Figure 4. The changes in the mass mean

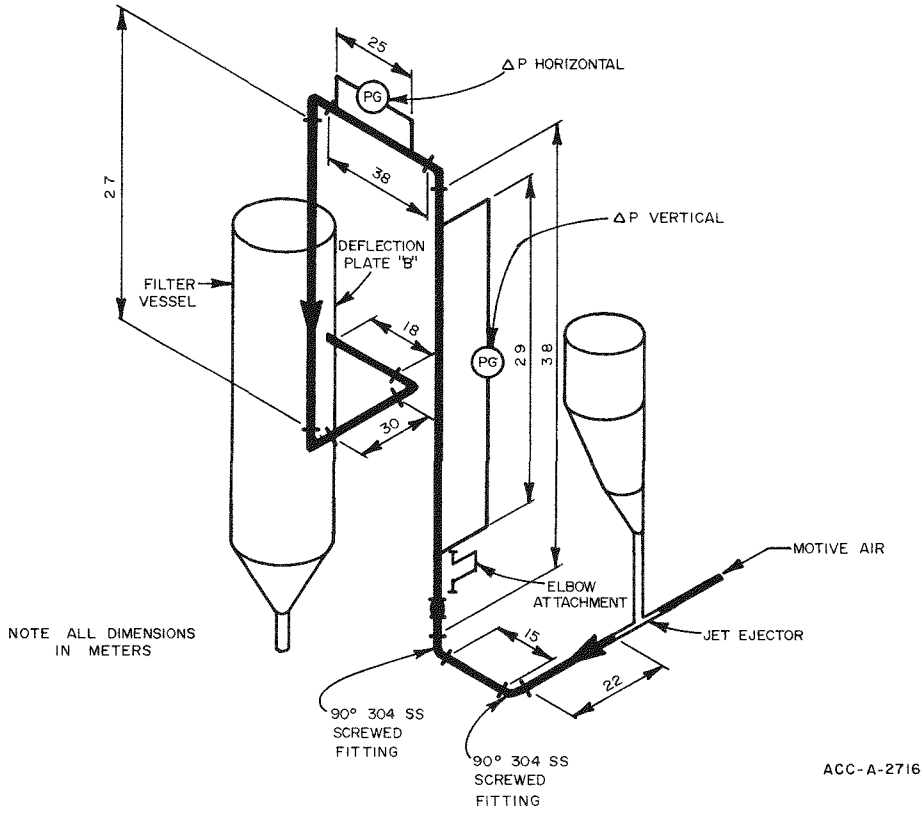

Figure 3. Equipment Arrangement for Al_2O_3 Attrition Tests

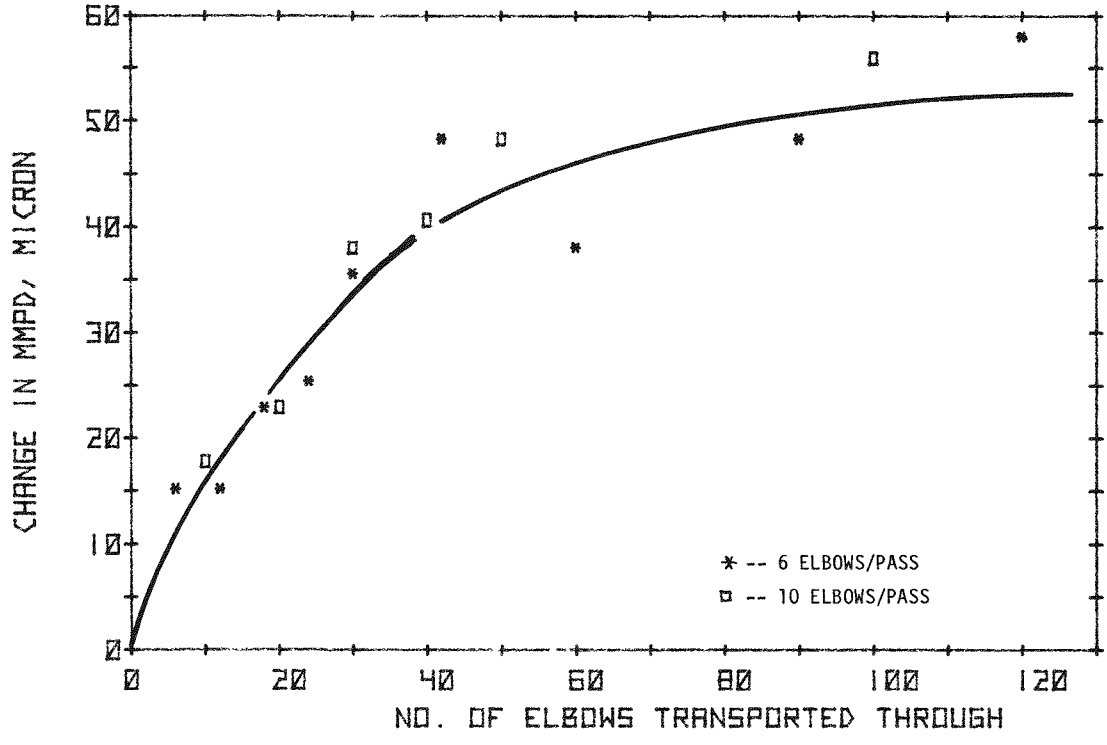

Figure 4. Change in Diameter (MMPD) of Alumina During Transfer

particle diameter (mmpd) represent a change in d (the mean weight mesh size) from 50 mesh for fresh Al_2O_3 to 60 mesh after passing through 120 elbows. Examining the Al_2O_3 under a 10x microscope showed the sharp corners of the particles were being removed. The results for the two systems, with 6 and 10 elbows respectively, correlate very well.

During transfers 12 through 15 for the 6 elbow system, the outlet to the jet was only partially opened resulting in lower transfer rates. These runs were used to evaluate the Scarpa ultrasonic flowmeter and the pressure differential gages used as flow meters and flow indicators.

The results of the tests are shown in Figure 5. The Scarpa meter or pressure gages could be used for a flow indicator, while the pressure gages were better as flow meters.

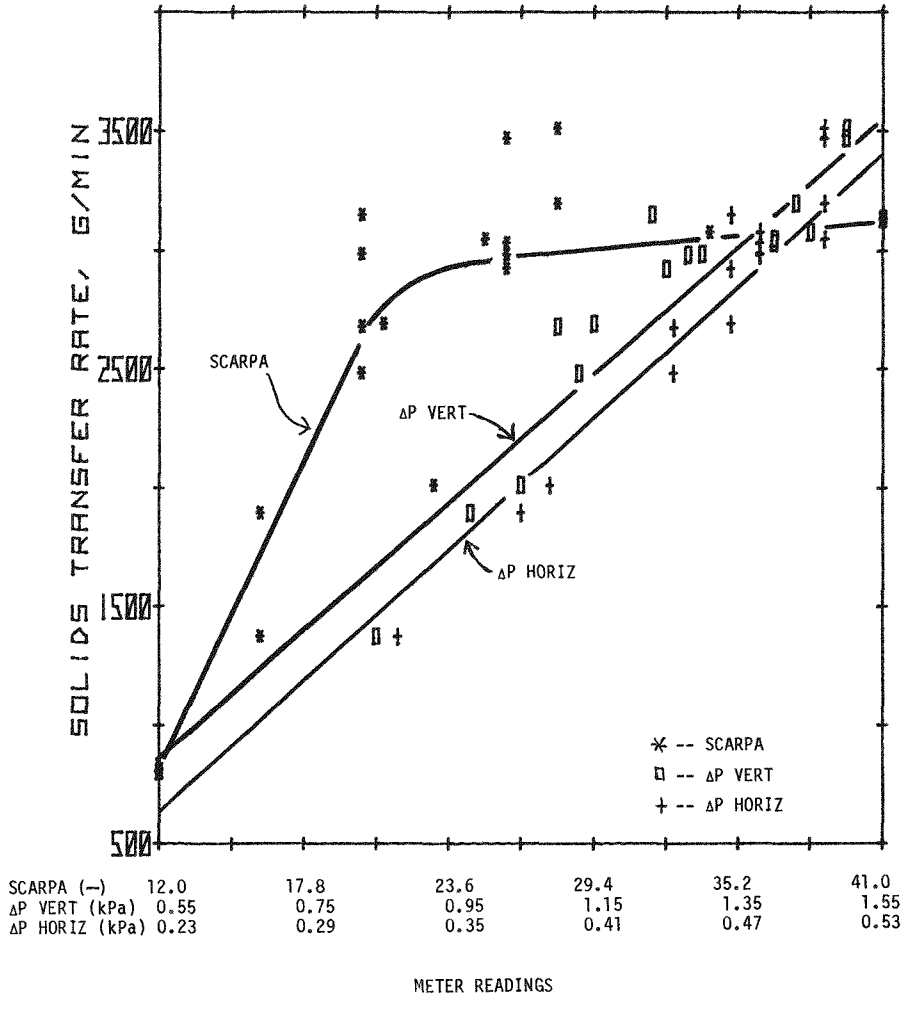

Figure 5. Calibration of Flow Meters

After these tests were completed, erosion measurements were taken on the elbows. Ultrasonic thickness measurements showed that the first elbow, located 22 cm from the jet, lost up to 23% of its wall thickness; and the second elbow, located 15 cm downstream of the first elbow, lost about 8% after 55 minutes of transferring.

1.3 Erosion by Al_2O_3

Scoping tests of erosion to elbows and a filter deflection plate by Al_2O_3, simulating transfers from the bed storage vessel, were completed. The tests resulted in erosion to failure of an elbow after four hours of transferring.

The Al_2O_3 from the attrition tests was recirculated through the transfer loop shown in Figure 6. A Penberthy Model 63A jet was used with 550 kPa (80 psi) motive air to make the transfers. Ultrasonic thickness measurements were made on the stainless steel elbows during the test to measure erosion.

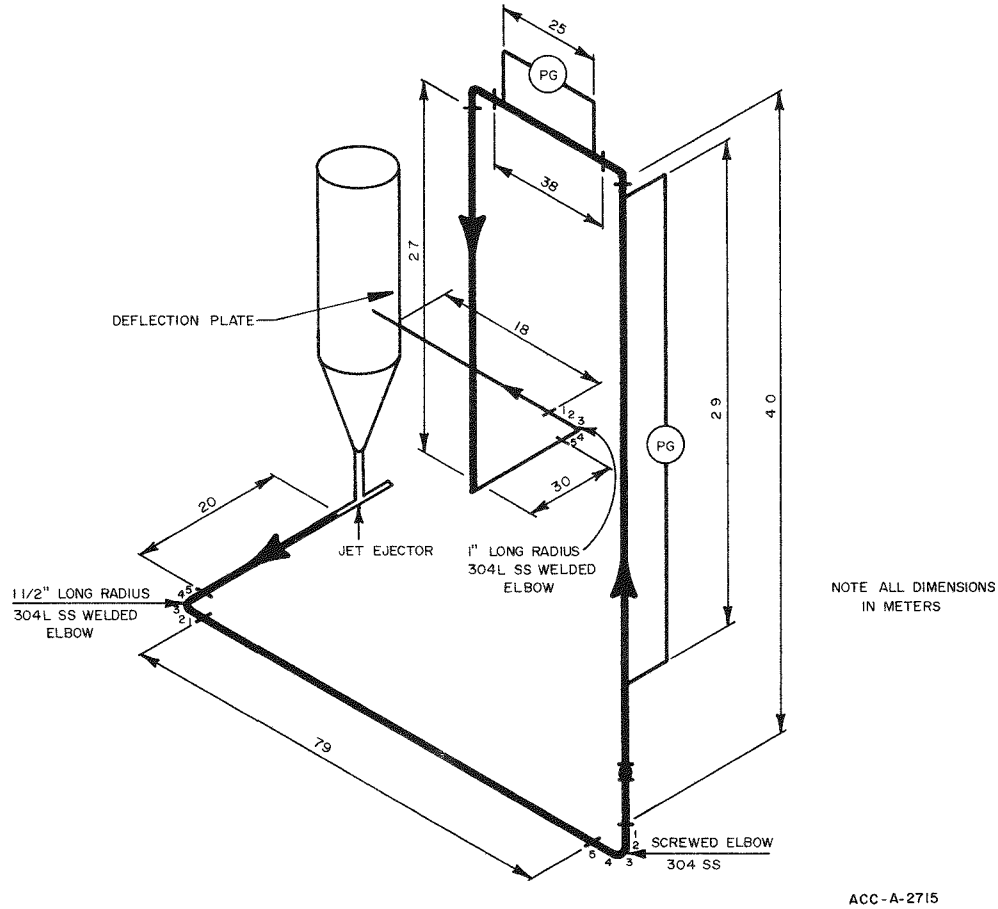

Figure 6. Equipment Arrangement for Erosion Tests

The following observations were made during the test:

(1) During solids transferring, the surface temperature of the elbow rose to about 45°C. When the solids flow was stopped, the temperature dropped to ambient, indicating the temperature rise was the result of the transfer of the energy from the particles to the elbow.

(2) The Scarpa flow meter was difficult to calibrate compared to its use in the attrition tests. There was no change in the meter reading with or without solids flow.

(3) Pressure differential measurements were good indicators of flow or no flow. Readings changed from 0.18 to 0.38 kPa with no solids flowing to 0.49 and 1.25 kPa with solids flowing for pressure drops measured on horizontal and vertical lines respectively.

(4) After about 3-3/4 h of transferring, a small bump formed on the outside center of the elbow. The bump became larger, and after about four hours, a pinhole opening broke through the wall.

The results of this test were:

(1) The wear rate at the center of the elbows is shown in Figure 7. The 1-1/2 inch welded elbow formed a hole after four hours. The 1-inch welded elbow wear was probably due to acceleration of the particles caused by the smaller pipe diameter. The 1-1/2-inch screwed elbow had negligible losses. This was probably due to most of the energy loss occurring in the first elbow, or it could be the result of the larger internal cross-sectional area.

The shape of the curve in Figure 7 is probably due to the smoothing of the particles seen in the attrition tests. At the end of the 4-h test, the mean weight mesh size was 80 with a MMPD of 167 μ (0.0066 inches), and the particles were very smooth. For a non-recirculating system, which will be experienced in the plant, the particles will be sharper and larger and should erode the elbows at a more constant rate.

(2) The filter deflection plate was removed from the filter vessel after a total time of five hours. An indentation of about 125 μ (5 mills) was observed.

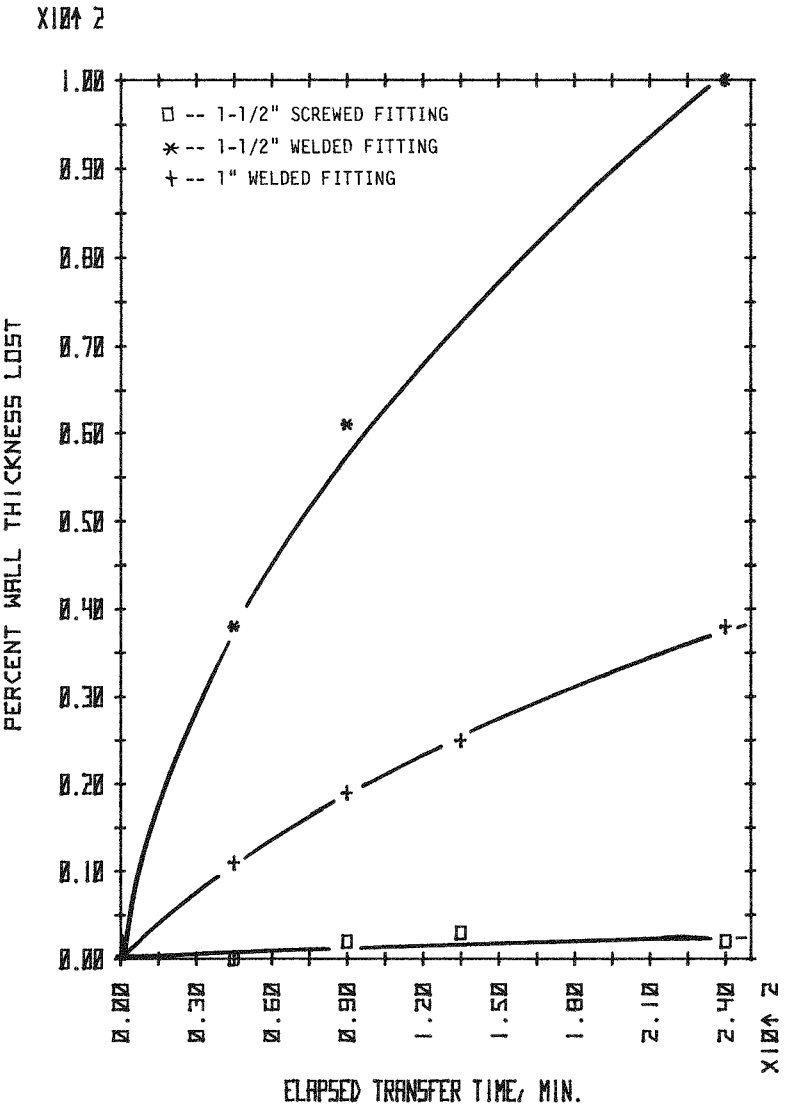

Figure 7. Wear Rates of 90° Elbows Caused By Transporting Al_2O_3

1.4 Erosion by Simulated Primary Burner Ash

Scoping tests with simulated primary burner ash, modeling transfers from the primary burner collection vessel and the secondary burner weight hopper, were completed. The results show that the simulated ash is not as erosive as Al_2O_3. The ash causes an erosion rate of about 25μ (1 mil)/h.

The apparatus was arranged as shown in Figure 6. The simulated ash was comprised of:

Al_2O_3	-	2.2%
Graphite	-	41.4%
Iron Powder	-	24.6%
Soda Ash	-	31.8%

The following observations were made during the test:

(1) No temperature rise was observed in the first elbow.

(2) Sufficient material was charged to the vessel to allow the vibrating level probes to cycle on and off during transport. No problems were experienced with the probes.

(3) Pressure gages gave similar readings as reported in the Al_2O_3 erosion testing. The Scarpa flow meter was not tested.

The results of the test are:

(1) After eight hours of transfer, the percentage of wall loss was 4, 12, and 2% for the 1-1/2-inch-welded, 1-inch-welded, and 1-1/2-inch-screwed elbows respectively.

(2) The maximum erosion of the deflection plate was about 100μ (4 mils).

1.5 Erosion of the Transfer Jet

Upon completion of the erosion testing, the 63A jet was examined for erosion. Measurements were not taken on the jet when new. However, the bodies for the model 63A and Model 163A jets are the same, and therefore, the 163A jet with little usage was used for comparison. The 63A was visibly worn. A comparison of the two bodies is given in Table 14. The performance tests show a transfer efficiency of only 50% of original flow due to the erosion of the jet.

TABLE 14

Comparison of Jets 63A and 163A

					Performance		
Jet Body	Body Condition	Wt. (g)	Discharge Dia. (mm)	Throat Diam (mm)	Operating Pressure (kPa)	Transfer Rate (g/min)	Vacuum Produced With Closed Suction (kPa)
63A	Worn	394	20.6	14.3	275	547	36
					415	688±135	53
					550	563±50	58
163A	Fairly New	450	14.3	12.7	275	1173	51
					415	1310	58
					550	1213	58

1.6 Conclusions of the Erosion Tests

These tests, which verified the expected service life of certain piping configurations in the as-built plant, indicated that either periodic replacement of critical elbows and jets or changes in line configuration may be required. In the interpretation of these test results it should be noted that in the actual process, solids transfer in a given line occurs for only a small fraction of the total operating time.

2. Rover Pilot-Plant Centrifuge Erosion Testing (A. G. Westra)

The Rover pilot-plant centrifuge was started on May 13 for erosion tests of the auger which had been overlaid with Tribaloy 700.[a] Tribaloy 700 is a hard-facing material with a composition of 50% nickel, 32% molybdenum, 3% silicon, and 15% chromium. The pilot-plant centrifuge is the same type as the one installed in the Rover plant (a 6-inch Bird continuous centrifuge).

A slurry of 0.65 g/L graphite, 2.57 g/L Al_2O_3, and 7.28 g/L Nb_2O_5 in water was gravity fed to the centrifuge at 3 L/min. This is the same solids concentration and flowrate expected in the feed to the Rover plant centrifuge. The solids discharged from the centrifuge were reslurried with the supernate and recycled to the centrifuge feed tank. The centrifuge has been operated at 243 radians/s (2320 RPM) for 160 h. Since recycling the solids through the centrifuge grinds the solids to very fine particles, fresh slurry is made up periodically.

A solids discharge line with a flat plate simulating a closed diverter valve was installed on the centrifuge to determine if the solids can be washed through the line and the valve kept clean with water sprays. The solids discharge line has the same dimensions as the line in the Rover plant (4 inch Sch 40) with a spray nozzle located at the same relative position. An additional nozzle was installed to spray directly on the simulated diverter valve to insure it is kept clean and will operate. Spraying water through these nozzles has successfully washed the solids through the 0.56 m of line and kept the simulated diverter valve clean.

3. Rover Support Dissolver (A. G. Westra)

A cost estimate and expenditure authorization for the installation of a support dissolver have been prepared. The dissolver will be made of Kynar-lined pipe and will be a small-scale version of the plant dissolver. Fabrication and installation is scheduled to begin in October.

Plans for Next Quarter

Further solids transport system erosion testing will be done to: (1) evaluate the effect of the percentage Al_2O_3 in the ash, (2) test plugged tees as replacements for elbows, and (3) test the effect of increased distance from the jet to the first elbow.

---

[a] DuPont trademark

Erosion testing of the Tribaloy 700 overlay on the centrifuge auger will be completed. A reducing elbow on the feed line to the Rover plant centrifuge will be evaluated in the pilot plant to determine if it could plug.

Procurement of materials for the pilot-plant dissolver will be completed.

Calibration of the neutron interrogator will proceed. Standards to be used for periodic recalibration during plant operation will be prepared.

IV. WASTE TRANSFER SYSTEMS

(B. E. Paige, D. W. Siddoway)

Underground transport of radioactive liquid and solid wastes via pipelines is common throughout the nuclear industry. Previously, little effort has been expended to standardize designs from one location to the next or to evaluate various pipeline design alternatives to maximize personnel and public safety while minimizing the total facility cost. The goal of this project is to evaluate various pipeline design alternatives and to publish those evaluations in the form of proposed guidelines to be used in the development of future piping standards. Included in this program are: (1) determination of soil corrosion resistance of pipeline materials, especially stainless steel; (2) laboratory and field evaluation of commercial pipeline coatings applied to stainless steel secondary containment pipe; (3) evaluation of the use of cathodic protection to protect stainless steel piping from soil corrosion; and (4) studies of general piping design (e.g., seismic stability, encasement design, etc).

1. Coatings Evaluation (D. W. Siddoway, R. E. W. Birch)

Corrosion has long been understood to be an electrochemical phenomenon which occurs when anodic and cathodic locations exist on the same structure (piping, tanks, etc.) in contact with a common electrolyte (soil, sea water, etc.). Cathodic protection involves applying opposing currents to nullify the corrosion currents flowing in the structure. In cathodic protection, a rectifier or galvanic anode provides the protective current. The principle is the same as that used in the recharging of an automobile battery. The level of current necessary for protection is directly proportional to the metal surface exposed to the electrolyte. The use of coatings having high electrical resistances can decrease the amount of surface requiring protection to 1%-2% of the original pipe surface and can decrease protective current requirements by the same degree. This can reduce the capital and operating costs for the cathodic protection system by significant amounts.

Long-term field and short-term laboratory testing of pipeline coatings applied to Type 304L pipe have been initiated. Coal tar epoxy, hot applied coal tar tape, fusion bonded epoxy, extruded polyethylene, and polyethylene tape have been selected as the most promising of the commercially available coatings and will be tested. Table 15 lists positive

TABLE 15

COMPARISON OF COATINGS

Coating	Advantage	Disadvantage	Cost/ft²	Cost/m²
Hot applied coal tar	(1) Long service experience	(1) Decreasing availability	$ 0.30-0.35	$ 3.23-3.77
	(2) Field or factory applied	(2) Subject to cold flow		
	(3) Low cost	(3) Low service temperature		
		(4) Low puncture resistance		
Coal tar	(1) Moderate to high service temperature	(1) High cost	$ 0.40-0.60	$ 4.31-6.46
	(2) Hard coating	(2) Poor impact resistance		
		(3) Decreasing availability		
Polyethylene	(1) Field or factory application	(1) Poor resistance to field bend damage	$ 0.30-0.40	$3.32-4.31
	(2) Moderate cost	(2) Limited service temperatures		
Extruded polyethylene	(1) Moderate cost	(1) Factory applied only	$ 0.30-0.40	$ 3.23-4.31
	(2) Primer increases premature resistance	(2) Limited service temperature		
	(3) Readily available			
	(4) Good field bend quality			
Fusion Bonded epoxy	(1) Moderate cost	(1) Factory applied only	$ 0.35-0.45	$ 3.77-4.84
	(2) High impact resistance	(2) Vulnerable to electrical disbonding		
	(3) Good field bend quality			
	(4) High service temperature			

and negative aspects of each coating along with relative costs. Ability of coatings to adhere to the pipe is the major unknown in evaluating the feasibility of coating stainless steel pipe. Other characteristics (flexibility, resistance to impact, water permeability, electrical resistivity, etc.) should be the same as observed and reported for the coating of carbon steel and will not be evaluated in this project.

1.1 Specimen Preparation (R. E. W. Birch)

Laboratory and field specimens were both prepared in the same manner using ASTM G8-72 as a guide. Each field sample was 45.72 centimetres

(18 inches) long; laboratory samples were 22.86 centimetres long. Each sample was prepared by cold soldering an electrical test lead to the inside of the pipe, plugging each end with a rubber stopper, and sealing with silicone rubber sealant. Final testing was performed to insure that the specimens were water tight. Each of the coated specimens then had a 6.35 mm (1/4 inch) hole drilled in the coating. The degree of disbonding will be determined by measuring the increase in the size of the hole over the duration of the test. Figure 8 shows specimens of each of the 5 types of coatings.

1.2 Laboratory Disbonding Tests (R. E. W. Birch)

Disbonding of coatings occurs when hydrogen evolves at the cathode (the pipe sample) and loosens some of the material around the hole in the coating. Specially designed platinum electrodes were received and are in use in the laboratory disbonding tests. A special laboratory testing apparatus has been set up, as described previously[7], to enable accelerated disbonding of pipeline coatings in the laboratory. Laboratory findings will be correlated to field evaluations and will be used to interpret field pipe-to-soil potential readings.

1.3 Field Laboratory Disbonding Tests (R. E. W. Birch, D. W. Siddoway)

The coated specimens were buried near an anode in the ICPP yard to obtain a high potential similar to that which is sometimes encountered at ICPP due to the large amount of current needed to cathodically protect bare pipe lines. These field samples will be pulled for evaluation at 3, 6, 12, and 24 month intervals. The pipe-to-soil potentials indicate the degree of over-voltage being applied to the specimens, and they will be measured throughout the program. A pipe-to-soil potential in excess of -1.5 volts may create a situation where weakly bonded coatings will begin to disbond.

The placement of the specimens in a 76-centimetre-deep trench is shown in Figure 9. Current density will be measured and correlated with visual disbonding in the laboratory. As the field readings are taken, the increasing current requirements of each sample can be used to estimate the disbonding occurring underground.

After samples were buried in the trench, initial values of pipe-to-soil potential were taken. These are shown in Figure 10. The highest readings were obtained directly over the anode. Six sections of bare pipe, buried as controls, can be seen as sample numbers 1, 2, 23, 24, 45, and 46. A greater potential drop on these pipe sections occurred compared to the coated specimens. This drop is indicative of the lower resistance of bare metal. Each set of readings becomes gradually lower on either end of the plot due to the greater distance from the anode. Some of the readings were beyond the range of the meter and an estimated curve (dashed line) is inserted on Figure 10.

[7]ICPP Technical Quarterly Report # ICP-1117 dated January 1977-March 1977.

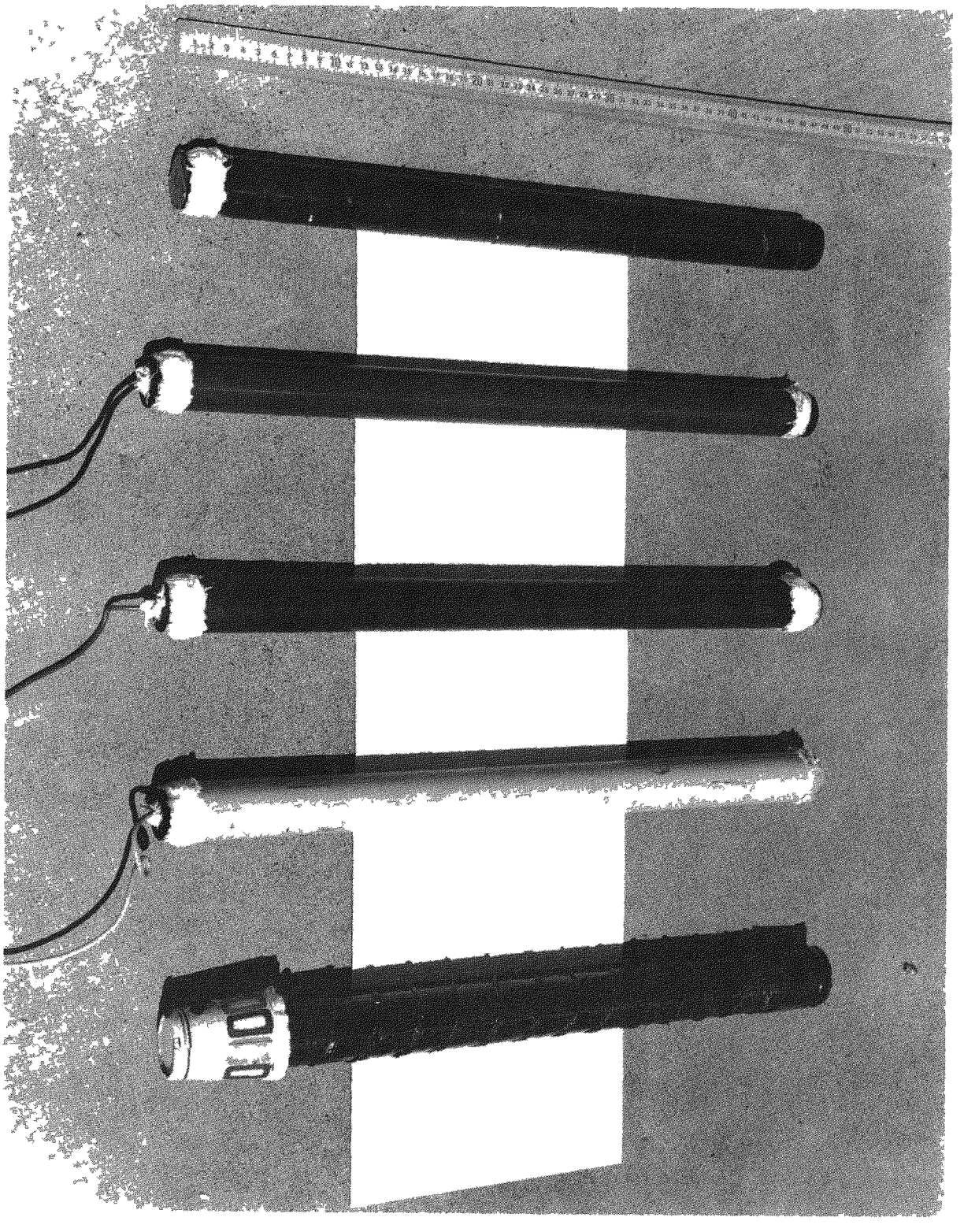

Figure 8. Coated Pipe Specimens for Field Tests

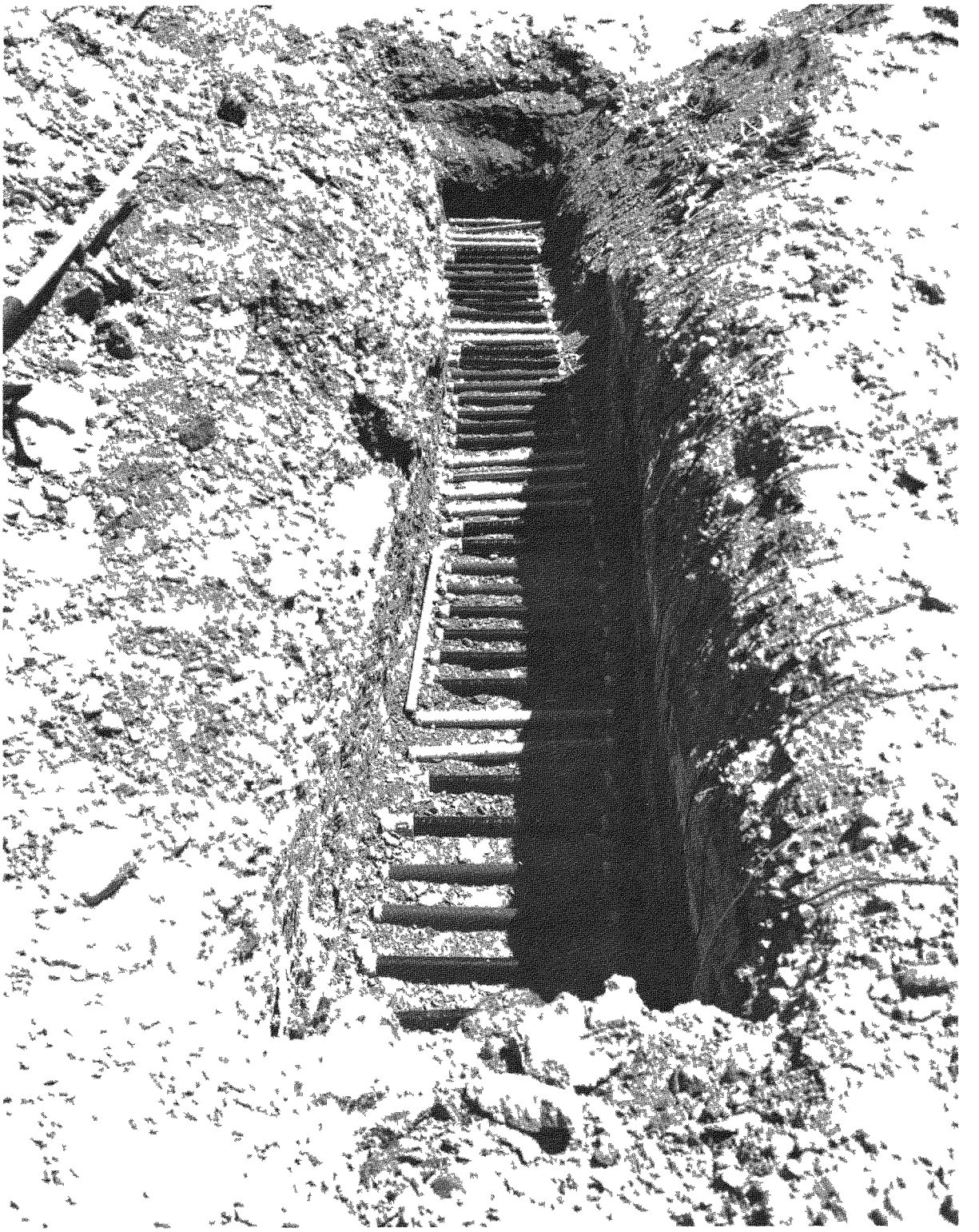

Figure 9. Coated Specimen Field Laboratory

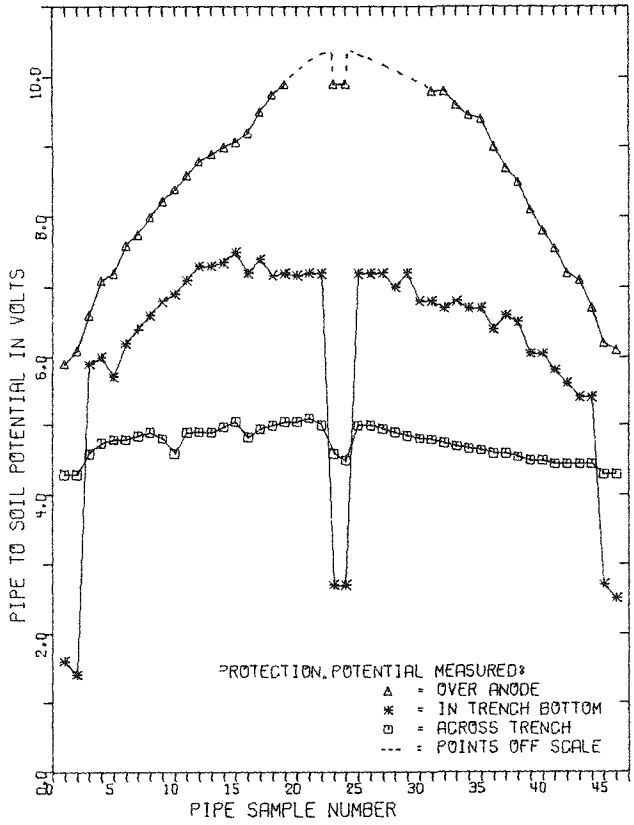

Figure 10. Pipe-To-Soil Potential For Various Pipe Specimens

2. Metal Corrosion Testing

Metals testing is conducted to evaluate:

(1) Effect of coupling dissimilar alloys (e.g., patching a Type 347 stainless steel pipline with Type 304L stainless steel pipe). This practice may lead to galvanic corrosion and premature pipe failure.

(2) The relative corrosion rates of various types of stainless steel pipe in acid soil (typical of eastern United States) and basic soil (typical of western United States, e.g., CPP).

2.1 Laboratory Metal Corrosion Tests (R. E. W. Birch)

Electronic corrosometer probes are in use in the laboratory to obtain a corrosion rate of four metals in CPP soil. Types 316, 347, 304L stainless steel, and carbon steel probes are in use. These probes allow the total amount of corrosion to be determined directly. As corrosion progresses, the surface area of the exposed metal probe decreases and the resistance increases. To insure that all four metals are in a similar as possible environment, moisture-temperature sensors are in the containers with the probes. These sensors measure the amount of water in

the soil, the soil temperature, and enable uniform conditions to be maintained throughout the tests.

2.2 Field Metal Corrosion Tests (D. W. Siddoway, R. E. W. Birch)

Several 46-centimetre (18-inch) sections of Type 304L, 316L, and 347 stainless steel pipe were placed in a field test tank containing alkaline CPP soil. Galvanic couples were also placed in the field tank to determine if different types of stainless steel welded together will cause galvanic corrosion. The four metals will also be placed into a tank containing an acid Judkins soil. Use of an acid soil will allow data obtained from this program to be used in predicting piping feasibilities in the eastern United States where nearly all soil is acid. The tanks permit isolation of the test specimens from other stray DC currents flowing in the CPP soil (due to cathodic protection, etc.) and allow evaluation of soil corrosion without interference from other sources. Samples pulled from the tanks at 1, 2, 4, 8, and 20 years will be evaluated for corrosion and compared to accelerated data obtained in the laboratory tests. Tank layouts are shown in Figure 11.

Figure 11. Field Laboratory Tanks for Bare Metals Testing

3. Encasement Design

All high-level radioactive waste lines installed at CPP are encased in a secondary pipe to help insure that waste will not enter the environment directly from a leaking primary waste line. The integrity of the secondary containment must also be insured because it serves as a monitor for leaks in the primary line. Whereas, the primary waste lines are vulnerable to the corrosiveness of the waste streams themselves, the secondary encasement is subject to soil stresses and soil corrosion. Of specific concern is the ability of the secondary encasement to maintain integrity in the event of an earthquake or comparible soil stress situation. Seismic evaluation of common secondary encasements has therefore been included as part of this program.

3.1 Seismic Evaluation (D. W. Siddoway)

Seismic evaluations of various encasements including (1) stainless steel pipe, (2) fiberglass-reinforced plastic pipe, (3) stainless steel-lined concrete trough, and (4) stainless steel-lined walk-in manway have been completed by EG&G Applied Mechanics. All encasements were evaluated for seismic accelerations of 0.1, 0.3, and 0.5 g (equivalent to greatest acceleration experienced in California earth tremors) and for soils of hard, medium, and soft consistencies. Soil hardness is represented by the shear wave velocity which the soil will transmit in a seismic disturbance. Soft soils were represented in the calculations by shear wave velocities of 152.4 m/s (500 ft/s), medium soils by velocities of 274.32 m/s (900 ft/s), and hard soils by velocity of 396.24 m/s (1300 ft/s). These values are selected to be on the conservative end of realistic scales.

Axial and bending stresses for varying seismic acceleration and soil conditions were calculated for encasements made of stainless steel or fiberglass reinforced plastic (FRP) pipe. The summed total of these two stresses was then compared to the allowable design stress for the pipe itself. Tables 16 and 17 show the ratios of total seismic stress (σT) to the allowable design stress (σ all) under various soil accelerations and soil hardnesses. A ratio greater than 1 indicates that the encasement pipe, under those conditions, is exceeding allowable design stresses. This does not necessarily mean, however, that the pipe would fail in those conditions, since all values used for calculations are intentionally selected to give a conservative design. Only FRP pipe withstood all accelerations and soil hardness combinations without exceeding the selected allowable design stress. Increase in pipe diameter from 15 to 25 cm had no effect on seismic stability.

Concrete encasements lined with stainless steel (see Figure 12) and concrete walk-in tunnels (see Figure 13) were evaluated for their seismic stability. The approach of this portion of the evaluation was to design the concrete encasements to withstand maximum earthquake conditions without crumbling or loss of pipe protection. Reinforcing rebar was positioned and sized to accept the total tensile loading of the encasement. The stainless steel liner will remain intact even though the concrete cracks, and therefore, no loss of containment will occur.

TABLE 16

Seismic Data For Stainless Steel (Type 304L)
Pipe Encasements

Seismic Acceleration	Soil Hardness	Ratio of Total Seismic Stress to Allowable Design Stress $\sigma T/\sigma All$[a] 6" and 10" Sch 10, 304L
0.1 g (98.04 cm/s^2)	Soft	0.73
	Medium	0.40
	Hard	0.28
0.3 g (294.13 cm/s^2)	Soft	2.18
	Medium	1.21
	Hard	0.83
0.5 g (49.0.22 cm/s^2)	Soft	3.63
	Medium	2.01
	Hard	1.39

[a]Allowable design stress for Type 304L stainless steel pipe (10" and 6") is 15,711 psi.

TABLE 17

Seismic Data For Stainless Steel (Type 304L)
Pipe Encasements

Seismic Acceleration	Soil Hardness	Ratio of Total Seismic Stress to Allowable Design Stress $\sigma T/\sigma All$[a] 6" and 10" Sch 10, 304L
0.1 g (98.04 cm/s^2)	Soft	0.18
	Medium	0.10
	Hard	0.07
0.3 g (294.13 cm/s^2)	Soft	0.53
	Medium	0.29
	Hard	0.20
0.5 g (440.22 cm/s^2)	Soft	0.88
	Medium	0.49
	Hard	0.34

[a]Allowable design stress for fRP pipe (10" and 6") is 3200 psi.

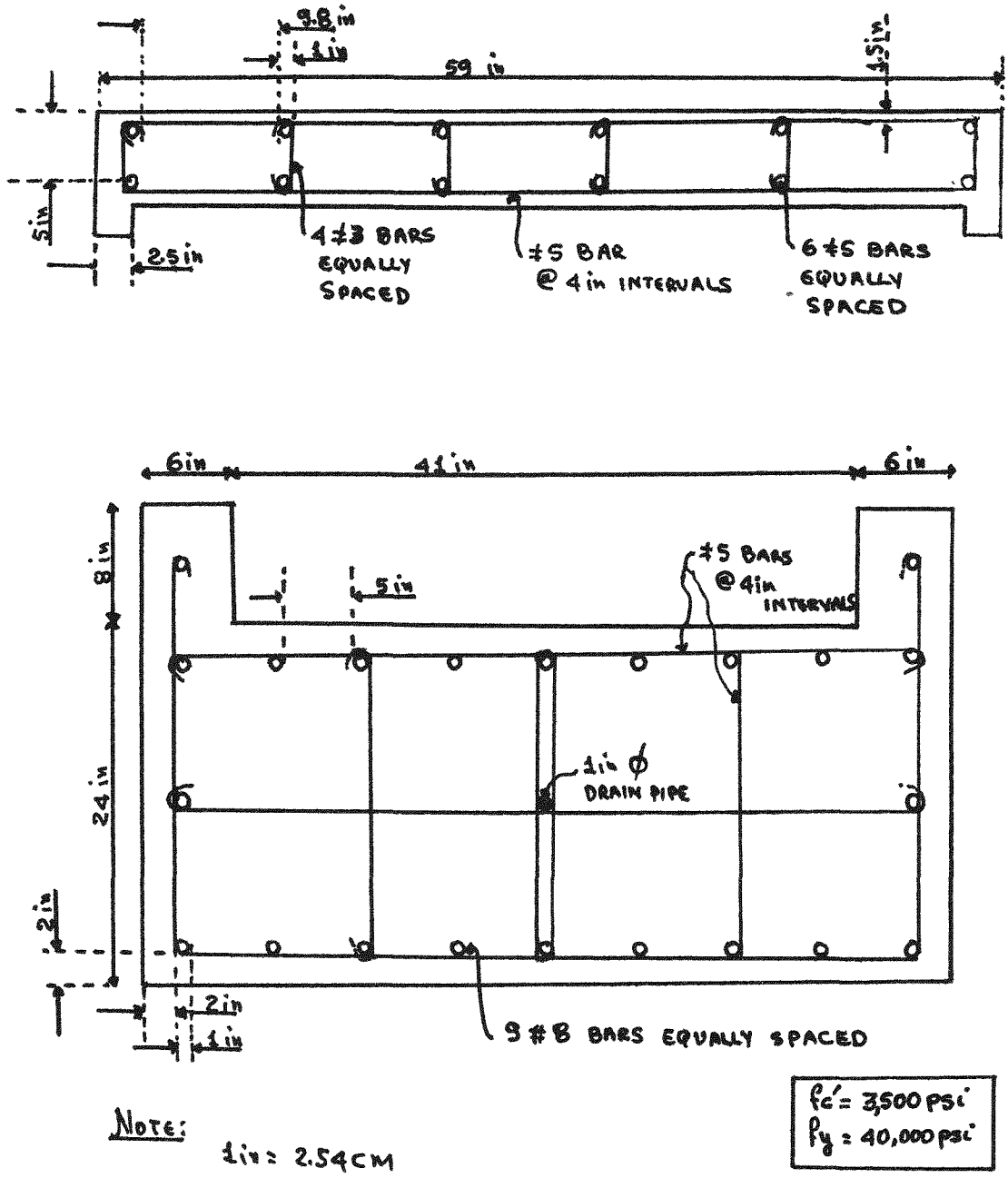

Figure 12. Design of Seismic Resistant Concrete Trough

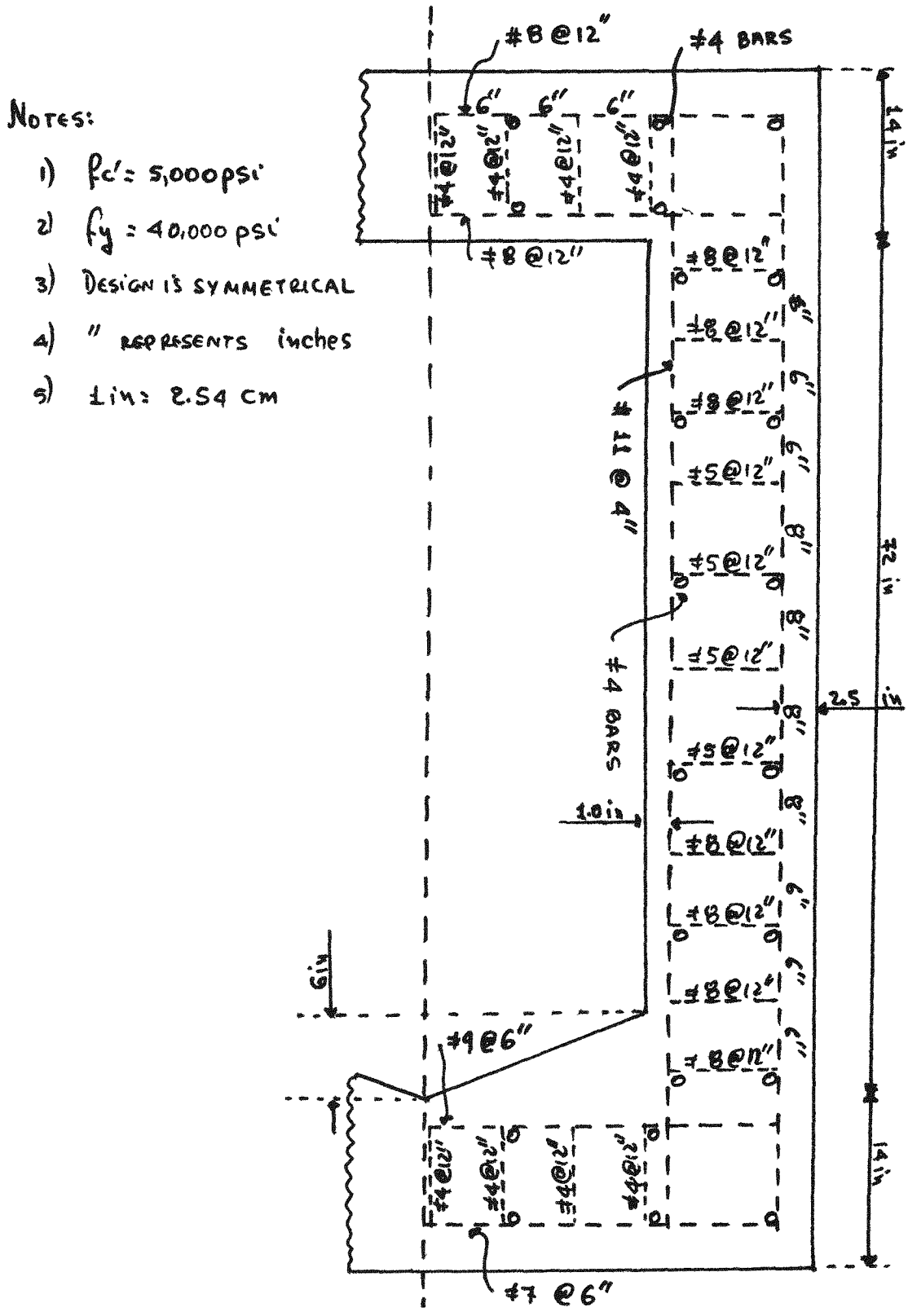

Figure 13. Design of Seismic Resistant Concrete Walk-In Manway

Plans for Next Quarter

(1) Continue disbonding tests.

(2) Determine the corrosion rates of metals in CPP soil.

(3) Find the cathodic protection level needed to halt corrosion in soil.

(4) Start accelerated corrosion tests.

(5) Start programs with the potentiostat to evaluate the relative corrosion resistance of different metals in various soil media.

V. ICPP WASTE MANAGEMENT DEVELOPMENT

1. Rover Flowsheet Development (S. A. Birrer)

Prior to the reporting period, several runs were made using the 10-centimetre-diameter (4-inch) calciner. The results showed that a blend of 1 to 2 volumes of zirconium waste with 1 volume of Rover waste could be successfully calcined. The 30-centimetre-diameter (12-inch) calciner was then used to demonstrate calcination of these blends on a larger scale. The 1:1 blend was demonstrated during the last reporting period; a final pilot-plant run using the 30-centimetre-diameter calciner was conducted during this period. Run 62, a 106-h run, was completed on April 22, 1977. This run used a feed blend of one vol simulated Rover first-cycle waste with two vols simulated zirconium first-cycle waste. The run operated smoothly throughout its entirety. However, as was the case in Run 59 (30-centimetre calciner run using a 1:1 feed blend), many small fragile agglomerates appeared in the product after 8 h cumulative operating time (COT). They neither increased in size or quantity throughout the rest of the run and they disappeared from the final bed after the feed had been shut-off and the bed was allowed to fluidize while cooling. These agglomerates should not adversely affect WCF operation. Both Runs 59 and 62 produced calcine with characteristics very similar to zirconium calcine as shown in Table 18.

TABLE 18

Comparison of Rover and Zirconium Calcine Properties

Waste Type	Attrition Resistance Index	Product Bulk Density, (g/cc)	Product-to-Fines Weight Ratio
1 vol Rover:1 vol ZFW	8.6	1.26	3.67
1 vol Rover:2 vol ZFW	10.4	1.32	3.03
ZFW	12.0	1.24	3.50

Based on the pilot-plant testing, either flowsheet (1:1 or 1:2) is acceptable for demonstration in the WCF.

Plans for Next Quarter

A topical report will be issued summarizing all of the laboratory and pilot-plant work on Rover waste calcination.

2. Tank WM-183 Flowsheet Development (J. T. Nichols)

A total of 12 calciner runs (eleven in the 10-centimetre-diameter (4-inch) calciner runs and one in the 30-centimetre-diameter (12-inch) run were made in an attempt to calcine WM-183 waste (a mixture of aluminum waste, electrolytic waste, and evaporator bottoms). Iron was added to the waste to control sodium and prevent particle agglomeration. Iron addition was only partially successful; agglomeration of the entire bed did not occur, but small agglomerates (up to 1/2-inch diameter making up 2 to 4 wt% of the product) were made continually and could not be eliminated; the flowsheet is not acceptable for WCF use.

A new approach was begun by blending WM-183 waste with zirconium waste. The feed for the first run was a blend of 2 volumes zirconium fluoride waste with 1 volume WM-183 waste (concentrated to 60% of its original volume). After 53-h of operation, the Ca/F mole ratio was changed from 0.55 to 0.7 in an attempt to eliminate the particle nodules which had begun to form.

The addition of excess calcium caused the particles to become smoother, but the particles were very irregular in shape by the end of the run (88 h). During the last 16 h of the run, the bed temperatures would occasionally spread by as much as 25 K. By increasing the fluidizing air rate from 0.27 m/s (0.9 ft/s) to 0.35 m/s (1.15 ft/s) the temperatures could be kept within 10 K of each other. There was very little formation of agglomerates during the run and no agglomerates were found in the calciner after shutdown.

Plans for Next Quarter

Three more runs will be made using the 10-centimetre-diameter calciner. The most promising combination of blend and additives will be tested in the 30-centimetre-diameter pilot-plant calciner.

3. Sodium-Bearing Waste Flowsheet Development (B. J. Newby)

The flowsheet proposed for calcination of ICPP sodium-bearing waste called for blending 3 volumes of ICPP first-cycle zirconium waste with 1 volume of sodium-bearing waste and adding sufficient calcium nitrate ($Ca(NO_3)_2$) to give a calcium to fluoride (Ca/F) mole ratio of 0.7. Flowsheets tried in the WCF using 3-1/2 or greater volumes of zirconium (Zr) waste blended with 1 volume sodium-bearing waste to which was added the appropriate amount of $Ca(NO_3)_2$ resulted in some fluidized-bed particle roughness and possible release of excessive chloride to the off-gas scrubbing system. Additional work is needed to: (1) modify the flowsheet consisting of a blend of Zr waste and sodium-bearing waste with $Ca(NO_3)_2$ added to prevent

fluidized-bed particle agglomeration, nodule formation, and excessive chloride volatility, or (2) create a new flowsheet that will prevent fluidized-bed particle agglomeration, nodule formation, and chloride volatility.

A series of scoping flowsheets are being tested by making 14-h runs using a 10-centimetre-diameter (4-inch) fluidized-bed calciner. Fluidized-bed calciner runs or differential thermal analyses have indicated that each of these flowsheets show promise for preventing fluidized-bed agglomeration. Scoping flowsheets tested were:

(1) Run SBW4-1:1 vol first-cycle Zr waste-1 vol sodium-bearing waste; Ca/F mole ratio=1; Al/F mole ratio=0.33.

(2) Run SBW4-2:2 vol first-cycle Zr waste-1 vol sodium-bearing waste; Ca/F mole ratio=1; Al/F mole ration=0.32.

(3) Run SBW4-3: sodium-bearing waste plus 0.7 moles of Cr_2O_3 per mole of sodium present.

Fluidized-bed agglomeration did not occur in any of the runs. Run SBW4-1 produced calcine with nodules. Run SBW4-2 produced smooth calcine, but wet fines which is an indication that agglomeration might occur if the run were continued. Run SBW4-3 produced rough calcine, the feed contained excessive solids, and the fines weren't soluble in the off-gas acid scrub.

Plans for Next Quarter

Four additional flowsheets will be scoped during 14-h tests. The flowsheets will use CrO_3, phosphoric acid, or sugar as additives. One flowsheet will use 1 vol Zr waste-1 vol sodium-bearing waste containing a Fe/F mole ratio of 0.1 and a Ca/F mole ratio of 0.1. Studies will be made to determine how the most promising of the scoping runs affect fluoride and chloride volatility, calciner operability, and calcine properties.

4. Feed Control Valve Testing (S. A. Birrer)

Major problems experienced with the WCF feed control valves are: (1) plugging and (2) bellows failure due to valve cycling. A ball-type control valve having materials of construction resistant to radiation, waste solutions, and decontamination solutions was purchased and installed for testing in the CPP-620 feed make-up module.

Testing, which was started in the previous quarter, was completed. A pneumatic actuator was connected to the valve and a cycling test was run. The valve was allowed to cycle from fully open to fully closed and back again once every 4 minutes for a period of 4 weeks. An average leak rate of 200 cc of solution/day occurred through the stem packing during operation with simulated zirconium waste. This small leak rate would be acceptable; when a bellows fails on the current WCF feed valves, leak rates of 450 L/d have been measured.

Following cyclic testing, a pressure leak test was performed; no leakage occurred through the body seats or seals. The final test was that of valve controllability. Three separate runs were made at nine different valve positions to determine flow repeatability over the full range of expected feed flow rates. Feed rate control was excellent.

As a final test to determine the consequence of gross stem packing failure, the valve was operated with all of the stem packing removed. During valve rotation, the leak rate was large, but when the valve was stopped (in any position) the leakage decreased to approximately the 200 cc/day rate.

The kynar seats and body seals held up very well throughout the testing, and the valve was shown to operate very reliably. It is concluded that this type of ball valve would be a satisfactory feed control valve for either the WCF or NWCF.

Plans for Next Quarter

A topical report will be issued summarizing the details of the ball valve testing. Other previous feed valve testing will also be reported.

5. Transport System Moisture Monitoring (G. L. Cogburn)

Plugging in the transport air return line at the WCF has been a problem since switching to Bin Set 3. Heat losses, because of the increased line length, can result in a gas temperature near the dew point. The moisture enters the system with the secondary air from the primary cyclone. Since secondary air flow depends on primary air flow, the amount of secondary air entering the solids transport system can be controlled. Installation of a dew point hygrometer probe just downstream of the bin cyclone and a thermocouple in the line entering the calciner cell will provide the capability for determining whether or not condensation is occurring in the line. Secondary air flow could then be controlled to reduce the moisture content in the solids transport system, thereby preventing condensation and resultant plugging in the transport air return line.

A Panametrics M22R probe with extended dew point range has been ordered for this application.

Plans for Next Quarter

The panametrics probe will be tested in the pilot-plant to determine its accuracy, its reliability, and the effect of solids loading on its performance. If the tests are successful, it will be recommended for installation in the WCF system.

6. Calciner Nozzle Cap Material Testing (S. A. Birrer)

Testing has been completed to determine which of eight materials (Haynes 25, Haynes 188, Hastelloy-X, Types 304L and 440C stainless steel, and three ceramic coatings over 304L base metal) would make the most

suitable nozzle caps, i.e., which material would deteriorate the least under conditions of high-temperature oxidation, erosion, and corrosion. The high-temperature oxidation and erosion tests showed the ceramics to be unsuitable due to cracking and 304L stainless steel to be unsuitable due to severe erosion. Corrosion tests using feed and various decontamination solutions showed 440C to be unsuitable, since it completely dissolved and Hastelloy-X to be resistant to all of the above conditions a and have been recommended for use as nozzle cap material in the WCF and NWCF.

Haynes 25 and 188 materials have been ordered for cap fabrication and installation in the WCF.

Plans for Next Quarter

A topical report will be issued describing the details of the testing.

7. Waste Feed Chemistry Studies (B. J. Newby)

Laboratory and 10-centimetre-diameter (4-inch) calciner studies have shown that magnesium nitrate ($Mg(NO_3)_2$) can be used to effectively suppress fluoride and chloride volatility during calcination of a blend of 3 vol first-cycle zirconium waste with 1 vol ICPP sodium-bearing (formerly called second-cycle) waste with minimum production of gelatinous solids in calciner feed. Studies using the 10-centimetre-diameter (4-inch) calciner were made to determine the minimum magnesium to fluoride (Mg/F) mole ratio in the blend needed to produce calcine without nodules and effectively suppress fluoride and chloride volatility. A 64-h, 10-centimetre diameter calciner run using feed with a Mg/F mole ratio of 0.7 produced smooth calcine, allowed <0.5% of the fluoride to volatilize from the calciner, kept 74% of the chloride in the fluidized-bed (the same results were realized when calcium nitrate was used instead of $Mg(NO_3)_2$); chloride concentration in the acid scrub was kept below 330 ppm. A 64-h 10-centimetre-diameter calciner run using feed with a Mg/F mole ratio of 0.5 produced smooth calcine, allowed <0.5% of the fluoride to volatilize from the calciner, retained 38% of the chloride in the bed, and kept the chloride concentration in the acid scrub below 750 ppm.

Plans for Next Quarter

Determine if a Mg/F mole ratio of 0.6 will effectively suppress chloride volatility and if increasing the aluminum concentration prior to adding $Mg(NO_3)_2$ will retain more chloride in the bed.

8. Alternate Calciner Startup Bed Material (D. H. Munger)

Due to the high erosion potential and wide size distribution of the presently used Dolomite startup-bed material, a search was undertaken to find a suitable alternate. Important properties of a good startup-bed material are: narrow size range, high melting point, 2-3 N nitric acid solubility, high attrition resistance, calciner process compatibility, low erosion potential, and reasonable cost.

Two materials have been compared with Dolomite. The first material, Magnorite, is a fused MgO manufactured by the Norton Co., Refractories Division. The second material, Fluorapatite, ($Ca_5(PO_4)_3F$) is a phosphate rock mined by the phosphate industry in Florida. Numerous other candidates are also being considered and/or procured. These include: Sodium Silico-Aluminate (cold-rolled spheres using a clay binder manufactured by Grace), amorphous alumina, calcium carbonate, manganese oxide, and zinc oxide.

The test results show the Fluorapatite to be superior to both Dolomite and Magnorite in the areas of attrition resistance and erosion potential. The attrition tests, conducted in an elutriation column, showed the Fluorapatite to be greater than 200% more resistant to particle degradation than Dolomite. The erosion tests, using a jet grinder with 304L stainless steel impingement plates, demonstrated the erosion potential of Fluorapatite to be 0.029 and 0.005 as great as Dolomite and magnorite, respectively. These tests are particularly encouraging, since many serious problems resulting in lost production time have been traced to the abrasive qualities of Dolomite.

Plans for Next Quarter

Testing additional materials will continue. Fluorapatite will be scrutinized for overall compatibility with the calcination process.

9. Calcine Erosion During Transport (D. H. Munger)

Tests have been undertaken to determine the relative erosion potentials of the various calcined products from the 10-, 15-, and 30-centimetre-diameter calciner runs. The study is being conducted using a jet grinder apparatus having a 304L stainless steel impingement plate set at an angle of 30°. Both the product and fines of simulated Rover, AGNS, WM-183, zirconium, and sodium-bearing wastes are being tested for their relative contributions to pneumatic transport pipe erosion rates.

Preliminary results have shown that the sodium-bearing waste calcine is 5 to 7 times more erosive than the zirconium waste. One possible reason for this result might be that the attrition resistance of the sodium-bearing waste calcine is substantially higher than zirconium waste calcine and therefore, harder.

Plans for Next Quarter

Experimental tests will be completed and a letter report will be issued discussing the results of the study.

VI. EFFLUENT MONITORING METHODS EVALUATION AND DEVELOPMENT

1. Evaluate In-Place Test Methods for Determining HEPA Filter Efficiencies (R. C. Girton, M. A. Wong)

The purpose of this project is to evaluate the dioctyl phthalate (DOP) test method used for testing the efficiency of HEPA filters used in corrosive off-gas environments, particularly off-gas systems from waste solidification facilities. A laboratory experiment will be assembled to simulate the Waste Calciner Facility off-gas environment consisting of the following conditions: (1) temperature of about 90°C, (2) relative humidity of 90-95%, and (3) an NO_x concentration of 10,000 ppm. These parameters will be tested for interactions with DOP. Comparison studies of other filter test methods will also be conducted. The objectives in FY-1977 are to design the experiment, purchase materials and capital equipment, construct the test apparatus, and start testing.

Two 8-inch by 8-inch HEPA filters will be tested in tandem. DOP concentrations will be measured before filtering and again after each filter. Each parameter will be studied as to the effect on filtering efficiency. Both polydispersed and monodispersed DOP generators will be used, and concentrations will be compared by light-scattering photometers and a laser spectrometer. The NO_x concentration will be measured by a chemiluminescence monitor and the relative humidity measured by a hygrometer.

Plans for Next Quarter

The experimental test apparatus will be constructed, instrumentation and equipment checked out, and testing begun.

2. Methods Evaluation for Monitoring of Radionuclides with Low-Energy Emissions (R. C. Girton, A. K. Herbst, M. A. Wong)

The purpose of this project is to investigate and evaluate stack monitoring techniques for low-energy emitting radionuclides released in the off-gas from fuel reprocessing facilities, particularly fission products from PWR and BWR fuels. The scope of the work will include an evaluation of current analytical and sampling techniques and the necessary modifications and development of methods to meet required sensitivity levels for the specific nuclide. A literature search was initiated to determine the capabilities of existing methods and instrumentation, but minor emphasis is planned on this work in FY-1977.

Plans for Next Quarter

A literature search of current technology will be completed and test plans for methods modification or development will begin.

RESULTS

OTHER PROJECTS SUPPORTING ENERGY DEVELOPMENT

I. LIQUID FLUIDIZED-BED HEAT EXCHANGER FOR GEOTHERMAL APPLICATIONS

(C. A. Allen, O. Fukuda, E. S. Grimmett, R. E. McAtee)

A 20-centimetre-diameter (8-inch) heat exchanger is operating at the GCTF near Holtville, California. The GCTF is operated for ERDA by Lawrence Berkeley Laboratory, and is made available to experimenters to test components for the geothermal power cycle. The objective of this test is to determine the scale-control properties of a liquid-fluidized-bed heat-exchanger with geothermal fluid of greater scaling potential than Raft River. To enhance scaling, flashed and unflashed water are mixed just ahead of the heat exchanger inlet. Mixing produces an overall temperature drop of up to 35°C. This temperature drop should promote precipitation of silicon compounds. Flashing the brine releases dissolved CO_2 and promotes calcite-deposition. The brine inlet is composed of about 40% flashed brine; it enters the heat exchanger at about 126°C. A flow diagram for the brine, cooling water, and electrical service is shown in Figure 1.

During initial testing, a gas separator was found necessary, a larger motor was required for the mixing pump, and the flow distribution system required alteration. The gas separator and pump were acquired. Vessel modifications include expanding the plenum size to decrease brine velocity and addition of a bubble-cap distributor plate. With these modifications, an extended test was started on May 16. After two weeks of operation, the pump seals failed; the experiment was continued until June 21 on unflashed brine. On June 21, following 38 days of operation, the heat exchanger was visually inspected; the outside tube surfaces appeared clean. The inside tube surfaces were badly fouled, accounting for the reduction in heat transfer coefficient shown in Table 1.

Following visual inspection, the insides of the tubes were cleaned, thus providing a basis for computation of inside and outside fouling factors. The equations used to compute h_o combine both fouling resistances into the outside heat transfer coefficient. After the insides of the tubes are cleaned, the heat transfer coefficient should nearly recover to its initial value.

Providing uniform flow in horizontal vessels creates a problem due to the variable cross-sectional area of the shell. To aid in the design of a distribution system, an experimental unit was designed which allows visual and photographic observation of flow patterns, and is instrumented to measure pressure drop and heat transfer. During the last quarter, the vessel was instrumented and initial testing begun. The first series of tests were aimed at determining the pressure drop across the distributor and measuring heat transfer at different points in the exchanger. The horizontal, cylindrical vessel is 91 centimetres (3 feet) in diameter and about 30 centimetres (1 foot) long. It contains 662 dummy tubes, 6 heat transfer tubes, and two distributor plates. Both ends of the vessel are covered by transparent lucite. The heat transfer tubes are

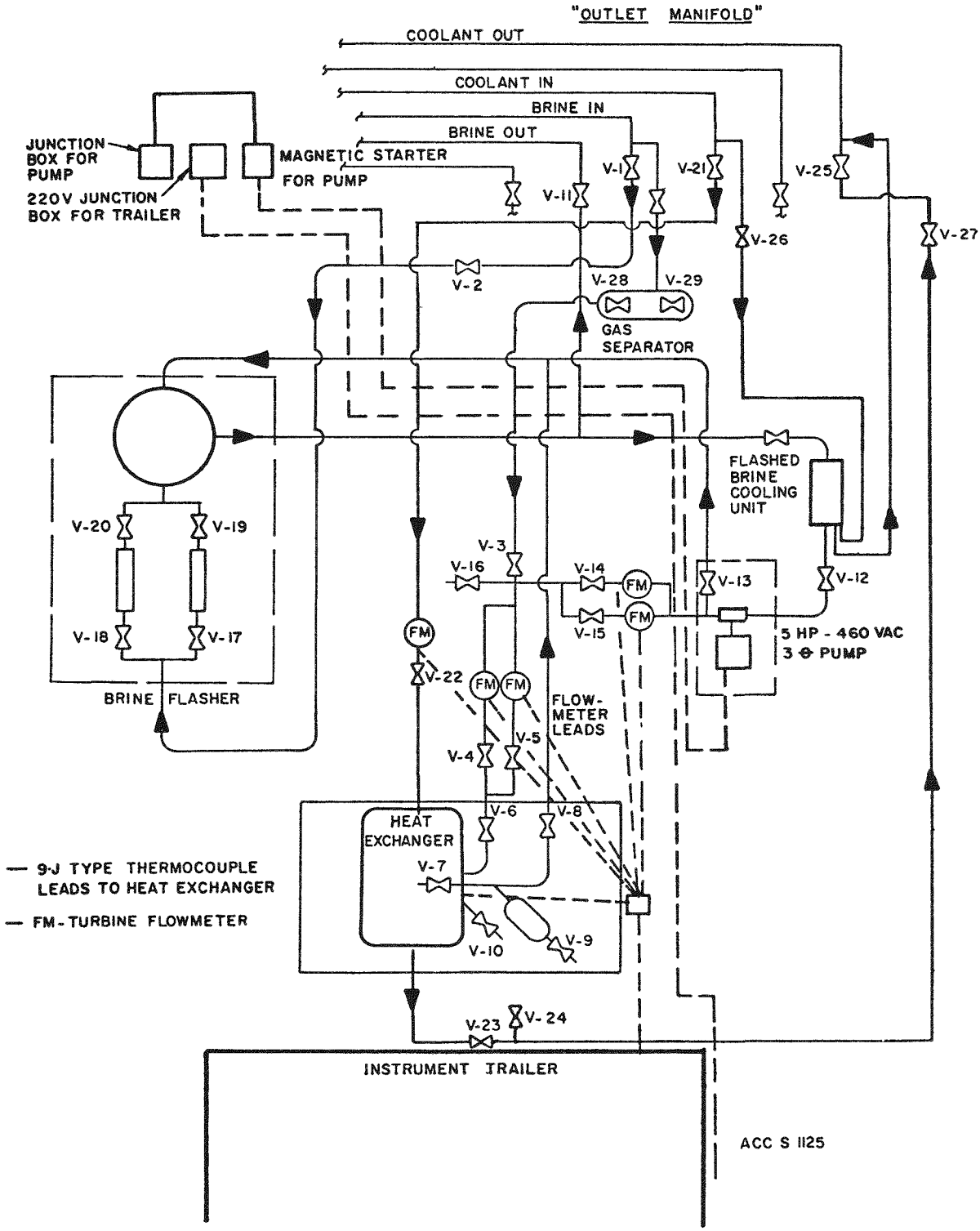

Figure 1. Flow Diagram for the Liquid Fluidized-Bed Heat Exchanger Experiment at the GCTF

TABLE 1

BED-TO-TUBE HEAT TRANSFER COEFFICIENTS

		Start-up	9 Days	18 Days	25 Days	35 Days
h_o	$W/m^2 \cdot K$	6358	3525	3587	3781	3435
	$Btu/h \cdot ft^2 \cdot °C$	1120	621	632	666	605
Deviation (%)		0	48	47	44	49

installed such that the tube can be rotated on its axis to determine heat flux around the tubes. The temperature difference is measured by thermocouples embedded in the inner and outer tube surfaces. The heat sources are resistance heaters located in the centers of the heat transfer tubes. All tubes, 1.9 centimetres (3/4 inch) O.D. by 30 centimetres (12.5 inches) long, were mounted on a triangular pitch with a pitch-to-diameter ratio of 1.5. A sectional view of the apparatus is shown in Figure 2. All experimental apparatus, including instrumentation, were assembled. Calibration was delayed because of difficulty in adjusting to the low pressure range of 2.4 kPa (0.5 psi). Pressure and leak tests of the system are complete with flow rates of up to 13 L/s (200 gpm) of water. Two demonstration runs with fluidized sand were made for exhibition to the public, Raft River Coop and ERDA officials.

The size and cost of a liquid fluidized-bed preheater for the Raft River thermal loop were recalculated for a stainless steel tube bundle. The costs of verical, horizontal, and conventional tube and shell heat exchangers were compared. Table 2 summarizes the size and cost of these units.

Calculating the size and cost of a fluidized-bed heat exchanger with a tube bundle of admiralty brass was made for comparison to the conventional unit. A material as soft as brass can not be used in a fluidized-bed exchanger. Table 2 indicates that fluidized-bed heat exchangers remain competitive with conventional heat exchangers. Vertical exchangers have a slight cost advantage over horizontal exchangers. However, these calculations are all based on cross-flow heat-transfer coefficients. The advantage could disappear when parallel flow coefficients become available.

A 60 kW(e) pilot-plant preheater is being designed for installation at Raft River. This pilot-plant preheater will contain three vertical stages and three horizontal stages. When it becomes operational, a direct comparison will be possible between the two types of liquid fluidized-bed heat exchangers.

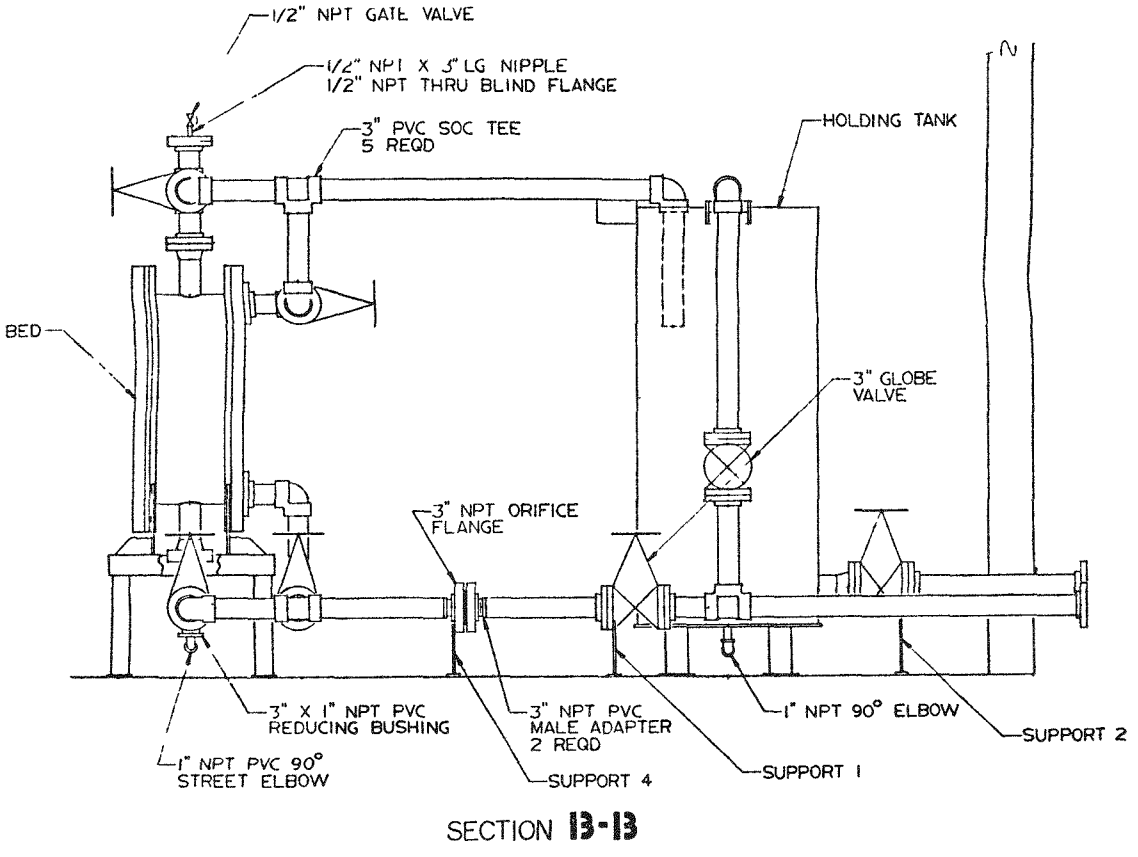

Figure 2. Side View of the Flow Distribution Apparatus

TABLE 2

Size and Cost of Liquid Fluidized-Bed and Conventional Tube and Shell Heat Exchangers

Type	No. of Passes	No. of Stages	Heat Transfer Area		Tube Material	Diameter		Length Per Stage		Total Cost ($)
			m^2	ft^2		m	ft	m	ft	
Horizontal FB	2	6	777	8360	Type 316	2.7	9	~1.8	~6	203000
Horizontal FB	1	6	778	8479	Type 316	1.5	5	~3.6	~12	191000
Vertical FB	2	6	769	8274	Type 316	1.8	6	~1.8	~6	187000
Vertical FB	2	6	621	6682	Admiralty Brass	1.8	6	1.5	5	103000
Horizontal Conv.	2	1	~1579	~17000	Admiralty Brass					~200000

II. IN-PLANT SOURCE TERM MEASUREMENTS

(J. H. Keller, B. G. Motes, D. W. Akers, T. E. Cox, S. W. Duce, J. W. Tkachyk)

The current program is concerned primarily with Pressurized Water Reactors (PWR) with emphasis on:

(1) The determination of the specific sources of radionuclides

(2) Determination of the pathways for movement through the plant

(3) The quantification of the radionuclides present

(4) The determination of the DF's of process equipment

The measurement program has continued through this period at the Zion Nuclear Generating Station. Draft data reports were issued covering the time period July 1976 to December 1976 for Zion Station and from November 1976 to February 1977 for the Fort Calhoun Station. The Fort Calhoun report presents data in addition to a previous report. Comments were received on both reports from the NRC personnel involved with the program. Preparation of final reports and issuing of EG&G documents await comments from the operating staff at the stations. A third draft report on procedures has been reviewed by the NRC and will be also issued as an EG&G report.

In general, the data from the Fort Calhoun Station is in agreement with the predictive models currently being used by the NRC.

The selection of the third and fourth plants for the measurement program is underway and measurements should begin early in the next quarter at the third plant and later at the fourth plant.

III. BURNUP METHODS FOR FAST BREEDER REACTOR FUELS

(W. J. Maeck, R. L. Tromp, J. E. Delmore, A. L. Erikson, J. W. Meteer, W. A. Emel)

The purpose of this program is to measure absolute fast reactor fission yields and to develop methods for the determination of burnup on Fast Breeder Reactor (FBR) fuels. During this period, analysis of the two dissolved ^{241}Am samples irradiated in EBR-II was started.

Recent improvements in the mass spectometric analysis of La and Ce has prompted the remeasurement of these elements for the capsules of ^{237}Np, ^{239}Pu, ^{240}Pu, ^{241}Pu, and ^{242}Pu. The results were more precise than previously obtained, and we believe, more accurate. Remeasurement of La and Ce for the previously analyzed samples of ^{233}U, ^{235}U, and ^{238}U are planned.

A rigorous error analysis of the results from the analysis of four irradiated samples of ^{239}Pu has been completed. This study indicates that the total number of fissions are known to $\sim\pm$0.8%, and hence, essentially all of the fission yields are known to $\sim$1%.

The first draft of a report giving all of the measured analytical data, error analysis, spectral information, and fast reactor fission yields for ^{239}Pu and ^{241}Pu was completed. Publication is projected for July or August, 1977. An update of the status of this program was submitted to the IAEA Nuclear Data Section for inclusion in the third edition of "Progress in Fission Product Nuclear Data", INDC(NDS)-86.

A review paper, "Fission Product Nuclear Data Requirements for Investigation of Irradiated Nuclear Fuel Material: Burnup, Neutron Dosimetry, Safeguards" is being prepared for the IAEA Second Advisors Group Meeting on Fission Product Nuclear Data, to be held at Petten, Netherlands, 5-9, September 1977. The purpose of this meeting is to collect the input thoughts and fission product nuclear data needs from various nuclear data users from laboratories throughout the world, to review and present the needs, and finally, to recommend the direction of future research based on the current status of the available nuclear data.

To date, approximately 30 contributions have been received. The review of these contributions and preparation of the report will be completed during the next quarter.

IV. ABSOLUTE THERMAL FISSION YIELD MEASUREMENTS

(J. E. Delmore, F. A. Duce, R. L. Tromp, W. J. Maeck, W. A. Emel)

Based on recent data[1], relative thermal fission yields measured on thermally irradiated samples of ^{235}U and ^{239}Pu for Kr, Rb, Cs, Xe, Ba, and Nd show large differences for several isotopes when compared to previous measurements made in this laboratory.

The initial analyses for all fission products for six ^{235}U capsules were completed and the results are currently being reviewed. To date, the only problems that have been observed relate to the La and Ce values on five of the capsules. These analyses were performed prior to the development of a new mass spectrometric technique that allows for improved differentiation of fission product La and Ce from the natural contamination. To improve the precision and accuracy of these data, the five samples will be reanalyzed using the improved technique. To more accurately correct for the amount of ^{236}U transmuted to ^{237}Np, four of the samples which experienced high burnup (>30%) will be analyzed for ^{237}Np. Analysis of the ^{239}Pu capsules is scheduled to begin in September 1977.

---

[1]W. J. Maeck, W. A. Emel, J. E. Delmore, F. A. Duce, L. L. Dickerson, J. H. Keller, R. L. Tromp, USERDA Report, ICP-1092, "Discrepancies and Comments Regarding ^{235}U and ^{239}Pu Thermal Fission Yields and the Use of ^{148}Nd as a Burnup Monitor", December 1976.

In the past, it was reported[2] that the use of ^{148}Nd as a burnup monitor for LWR fuels could produce biased burnup data because of a high cross section on 11d ^{147}Nd, especially if the irradiation was done in a high flux reactor. To further quantify this problem for the users of Nd fission yield data, we have obtained a series of 36.2 centimetre (14-1/2 inch) dia punchings from an irradiated ATR fuel plate. The burnup on this plate varied from ∿7% to ∿40%. These samples will be dissolved and analyzed for U, Cs, and Nd and the burnup calculated by several different means. The goal is to show the preferred method and monitors for the accurate measurement of burnup in fuel of this type, and hopefully, to extract cross-section data for some of the isotopes, especially, 11d ^{147}Nd, as well as ^{137}Cs, ^{143}Nd, and ^{145}Nd. These samples are ideally suited for this study, because they were all obtained from one plate which will eliminate the effect of irradiation history and allow direct comparison as a function of burnup.

A status report of this program was submitted to the IAEA Nuclear Data Section for inclusion in the third edition of "Progress in Fission Product Nuclear Data", INDC(NDS)-86.

V. LIGHT WATER BREEDER REACTOR (LWBR) - ANALYTICAL SUPPORT

(D. E. Adams, D. H. Meikrantz, G. W. Webb, W. A. Emel)

The Radiochemistry Branch at ICPP has agreed with Bettis Atomic Power Laboratory to analyze 42 irradiated fuel rod sections for uranium depletion. Bettis Atomic Power Laboratory also requested that three additional irradiated duplex fuel pellets be analyzed on an urgent basis. Each duplex pellet consists of either a UO_2, $UO_2 + ZrO_2$ or $UO_2 + CaO_2 + ZrO_2$ annulus plus a central ThO_2 pellet. Additional funding covering development cost and fuel segment analysis would be provided, and present commitments would be postponed for the work. ICPP has received 28 irradiated fuel rod segments for analysis and 9 unirradiated duplex fuel pellets for analytical methods development.

Analysis of the first 15 high priority fuel rod segments is in progress. To date, the fuel from 9 segments has been dissolved in nitric-hydrofluoric acid using a pressurized autoclave. Samples weighing 36 grams have been completely dissolved by this method. Dissolution times of 100 to 200 h were required for the heavy fuel samples.

VI. RESEARCH ON ANALYTICAL METHODS

1. A Rapid Determination of ^{241}Am in Soil Samples Around the Radioactive Waste Management Complex (I. L. Doggett and B. R. Hunter)

Eight highly alpha-contaminated soil samples from the INEL Radioactive Waste Management Complex (RWMC) were received for analysis. As ^{241}Am was suspected to be one of the major contributors to the alpha activity in

[2] ibid.

the samples, this laboratory was requested to quantitatively determine this nuclide concentration.

Previously ^{241}Am has been measured in the presence of other alpha emitting nuclides by chemical separation followed by alpha counting the ^{241}Am fraction with an α pulse height spectrometer system.[3] However, the ^{241}Am results are subject to possible error from ^{238}Pu interference. Plutonium-238 with an alpha decay energy of 5.50 MeV will be mistaken for ^{241}Am with a 5.49 MeV energy if Pu is not completely removed from the Am chemically separated fraction. Because of this and because the separation procedure is fairly lengthy and tedious, a better way was sought to determine ^{241}Am in the RWMC samples.

Taking advantage of the 60 KeV gamma-ray photo peak characteristics of ^{241}Am, this radionuclide was successfully measured in the soil samples using the laboratory's low energy Si(Li) detector system. To insure sample homogeneity, the soil samples were ground to a fine powder in a SPEX mixer mill using the throwaway grinding chamber developed by this laboratory.[4] Next a series of blank soil samples, of equivalent density to the unknown soils being analyzed, were spiked with known quantities of ^{241}Am and mixed in the mill in the same fashion as the unknown soils. The standards and unknown soils were normalized to one gram to cancel self adsorptive effects, placed in 1-dram glass vials and counted at the same source-to-detector distance. This technique has the advantages of no spike for yield determination and no tedious and lengthy chemical separations.

The samples were also found to contain ^{239}Pu and ^{240}Pu with small amounts of ^{238}Pu, ^{134}Cs, and ^{137}Cs. The plutonium x-rays were recognized in the sample spectra, but as they are of much lower energy than the 60 KeV ^{241}Am peak, no interference was encountered. The ^{134}Cs and ^{137}Cs gamma-ray peaks have too high an energy and too low an intensity to affect the ^{241}Am spectrum from the low energy Si(Li) detector.

2. Determination of Am-241 in CPP Stack Filters (I. L. Doggett)

The ICPP stack filter monthly composite is routinely analyzed for plutonium. This composite is made by using a portion of the daily stack filter sample, and leaching and boiling it down each day in a large beaker spiked with ^{236}Pu. At the end of the month, the plutonium is carried as a precipitate with $Fe(OH)_3$, dissolved in HNO_3, reprecipitated with LaF_3, dissolved in HNO_3, the acidity adjusted to less than 1 M H^+ and then a TTA extraction is used to isolate the plutonium. It has been requested that ^{241}Am be determined on this same composite. This has been successfully done by taking the HNO_3 dissolution of the LaF_3 (concentrated HNO_3) and using half of it for the plutonium determination and the remaining

[3] C. W. Sill, et. al., Analytical Chemistry, 46, 1725 (1974).

[4] Analytical Chemistry Branch Annual Report for FY-1976 and Transition Quarter, December 1976, ICP-1103, p 47.

half extracted into a bidentate solvent DDCP (dibutyl, N, N-diethylcarbamylphosphonate)[5]. Am-243 is used as a spike and added at the start of the composite so a yield can be determined. The americium is measured using the Ge(Li) detector and calculating the 0.059 mev peak for ^{241}Am and the 0.075 mev peak for ^{243}Am.

In both of the above cases, the organic extractant is measured for the indicated actinide. For the plutonium, the organic is pipetted to a stainless steel planchet and alpha counted and a pulse height analysis performed. For the americium, the DDCP is counted directly as a liquid using a Ge(Li) detector.

3. Revision of the Chemical Analysis Work Sheet for Direct Computer Output (I. L. Doggett and L. E. Trejo)

In the past, routine calculations of alpha, beta, total Sr, and $^{89}Sr/^{90}Sr$ were made on the HP-9830 Programmable Calculator. The printed output obtained was attached to the "Chemical Analysis Work Sheet:, Form INEL-5801, as part of the analysis record.

With the acquisition of an HP-9871A Printer, the work sheet has been revised (see Figure 3 for an example) and the computer program updated so that all pertinent input data, as well as the calculation results, are printed directly on the chemical analysis work sheet. This serves several purposes and has advantages over the previous system. The input and output data are all on one sheet making checking by the supervisor easier and less prone to error. Transfer of data from computer output to work sheet is no longer required. All this means that pertinent data are on one page and can be easily rechecked at a later date with little difficulty and with assurance that no data have been lost.

Additional calculation programs of a less routine nature such as ^{3}H, ^{55}Fe, and ^{63}Ni, will be modified or written to allow use of the improved work sheet.

The calculator programs have also been changed so that "less than" answers are no longer reported. Although the standard deviation of the methods increases dramatically as the lower detection limits are approached, it was felt that the customer would obtain more useful information by receiving the calculated results along with a standard deviation instead of the "less than" value.

4. Potentiometric Determination of Mercury in Fuel Dissolvent Solutions (R. P. Lash)

A method was developed for the determination of Hg(II) in nitric acid fuel dissolvent solutions including those containing gadolinium. The procedure

[5]F. E. Butler and R. M. Hall, "Determination of Actinides in Biological Samples with Bidentate Organophosphorous Extractant", Analytical Chemistry, 42 (1970) p 1073.

IDAHO NATIONAL ENGINEERING LABORATORY
CHEMICAL ANALYSIS WORK SHEET

SAMPLE NAME _____ LOG NUMBER _____

WA NUMBER _____ ACTIVITY (DPM) _____

Column No.	1	2	3	4	5	6
Procedure	Sr 89/90		Gross β	Gross β	Gross β	Gross α
Sample Code						
A1, D1, A2, . . .,	1 mL		.1/10.1/.1	G/100/1	S/250/5	1 mL
Final Aliquot	1		.1,10.1,.1	G,100,.1	S,250,5	1
Gross Wt.	63.60					
	63.6			1.0663		
Tare Wt.	26.58					
	26.58			0.9112		
Net Wt.	37.02			0.1551		
Carrier	41.16					
Yield	0.8994					
Sr 89/90 Gross Cts.	3474	2523				
Absorbers 1, 2	3474	2523				
Sr 89/90 Gross Cts.	1314	673				
Absorbers 3, 4	1314	673				
Gross Counts	5022		5166	4588	1122	1362
	5022		5166	4588	1122	1362
Time	100		100	60	1000	1000
	100		100	60	1000	1000
Background	.5035		.5035	.5035	.5035	.00500
	0.5035		0.5035	0.5035	0.5035	0.00500
Performance Factor						
Geometry	5.8559		14	2.73	2.73	2.62
Shelf No.	3		5	2	2	Charlie
	3		5	2	2	
Results	1.19E-03	7.27E-03	7.63E+05	1.40E+06	8.78E+01	3.56E+00
Units	UCI/ML	UCI/ML	B/S/ML	B/S/G	B/S/SPLE	A/S/ML
Deviation	±6.24E-06	±9.39E-05	±3.26E+04	±7.67E+04	±1.31E+01	
Analyst - Date						
	SR 89	SR 90				

Approved _____

Figure 3. Sample Work Sheet

is an adaptation of Overman's procedure[6] which describes the potentiometric titration of Hg(II) with sodium iodide using an iodide selective indicator electrode to mark the equivalence point.

The reaction of Hg(II) with I^- in solutions more concentrated than 5 x 10^{-6} M in Hg(II) follows the stoichiometry 1:2[7]:

$$Hg^{2+} + 2I^- \longrightarrow HgI_2 \qquad (1)$$

As the Hg(II) concentration decreases below 5 x 10^{-6} M, the formation of HgI_4^{2-} becomes more predominant and a more complex equilibrium exists:

$$Hg^{2+} + 4I^- \rightleftharpoons HgI_4^{2-} \qquad (2)$$

$$HgI_4^{2-} + Hg^{2+} \rightleftharpoons 2HgI_2 \qquad (3)$$

Mercury is present in fuel dissolvent solutions at approximately 10^{-2} M and is further diluted to approximately 10^{-4} M for analysis; therefore, reaction (1) predominates for this analysis. When all of the Hg(II) has been precipitated as HgI_2, excess I^- is detected by the iodide selective electrode and measured as a change in the potential of the solution.

The potential change near the endpoint is often affected by a sudden coagulation of the colloidal HgI precipitate. As a result of this phenomenon, a small potential change is noted at the onset of the equivalence point. This potential change is followed immediately by a large potential change of greater slope at the true equivalence point.

5. Application of Ion Chromatography to Anion Analysis (R. P. Lash and J. R. Delmastro)

An analytical ion chromatograph was acquired to study the determination of anions in a variety of matrices. The chromatograph combines the separations capability of ion exchange with a sensitive and universal conductimetric detector. The system is equipped with a 3 x 500 mm anion separator column and a 6 x 250 mm anion suppressor column. The determination of sulfate in complex inorganic solutions containing large quantities of other anions is currently being investigated and preliminary results appear promising.

Encouraging results have also been obtained for the determination of organic phosphate anions which result from the decomposition of tributyl phosphate. Future studies will include boron fluoride complexes and multiple anion analysis of various water samples.

---

[6] R. F. Overman, "Potentiometric Titration of Mercury Using the Iodide-Selective Electrode as Indicator", Analytical Chemistry, 43, (April 1971) pp 616-617.

[7] ibid.

6. Determination of Ruthenium in Solid Samples (C. M. Young)

In support of studies on the solidification of nuclear wastes being conducted at the ICPP, it was necessary to determine very low concentrations of ruthenium in the calcined product. The most commonly used method is time consuming and involves fusing the sample with an appropriate flux, dissolving the melt, distilling the ruthenium, trapping it in a solvent, and determining the concentration by a colorimetric method. This study describes a rapid method for the determination of as little as 100 parts per billion of natural ruthenium in solid samples. The method employs a fusion step followed by extraction of the ruthenium as an ammonium pyrrolidinedithiocarbamate (APDC) complex. The ruthenium concentration is determined directly in the organic phase by atomic absorption spectroscopy with a flame or a Varian Model 63 Carbon Rod Atomizer as the absorption cell.

To analyze low concentrations of ruthenium in the calcine particles, the ruthenium must be in solution. The ruthenium in the aqueous waste solutions is present as nitroso ruthenium nitrate complexes. When these liquid wastes are solidified by calcination, the ruthenium is retained in the calcine as an oxide of ruthenium. A basic oxidizing flux is necessary to break down the calcine particles and convert the ruthenium oxide to a water soluble species. Sodium peroxide was the most efficient flux for the complete decomposition of the calcine. The sample and flux are mixed and heated at 675°C for 15 minutes. The ruthenium is leached into solution with water. The leachate is very basic and results in a preliminary separation step by precipitating many of the diverse ions, including iron, nickel, and zirconium.

To separate the ruthenium from the remaining diverse ions, several different complexing agents and organic phases were tested. The complexing agents used were sodium diethyldithiocarbamate (NaDDC), diethylammonium diethydithiocarbamate (DDDC), and APDC. The various complexes were each extracted into 10 mL of butanol, butanone, ethyl acetate, methyl isobutyl ketone (MIBK), and amyl acetate. The extractions were performed at pH 3 with 100 μg of ruthenium. The organic phase was aspirated into an air/acetylene flame and the atomic absorption measured. APDC and amyl acetate were chosen as the optimum combination because of the increased extraction of ruthenium with APDC and the immiscibility of amyl acetate with the aqueous phase.

The effect of pH on the extraction of ruthenium was then studied. The results are shown in Figure 4. The solutions were buffered either with potassium hydrogen phthalate or with phosphate buffer, depending on pH. The extractions were performed with 100-μg of ruthenium and extracted into 10 mL of amyl acetate. The organic phase was aspirated into an air/acetylene flame and the atomic absorption measured. The increasing absorbance at higher pH was investigated further by using molar concentrations of sodium hydroxide with measurements taken as previously described. The results are shown in Figure 5. Figure 5 shows that the extraction of ruthenium levels off at a hydroxide concentration of $\sim$1.5 M.

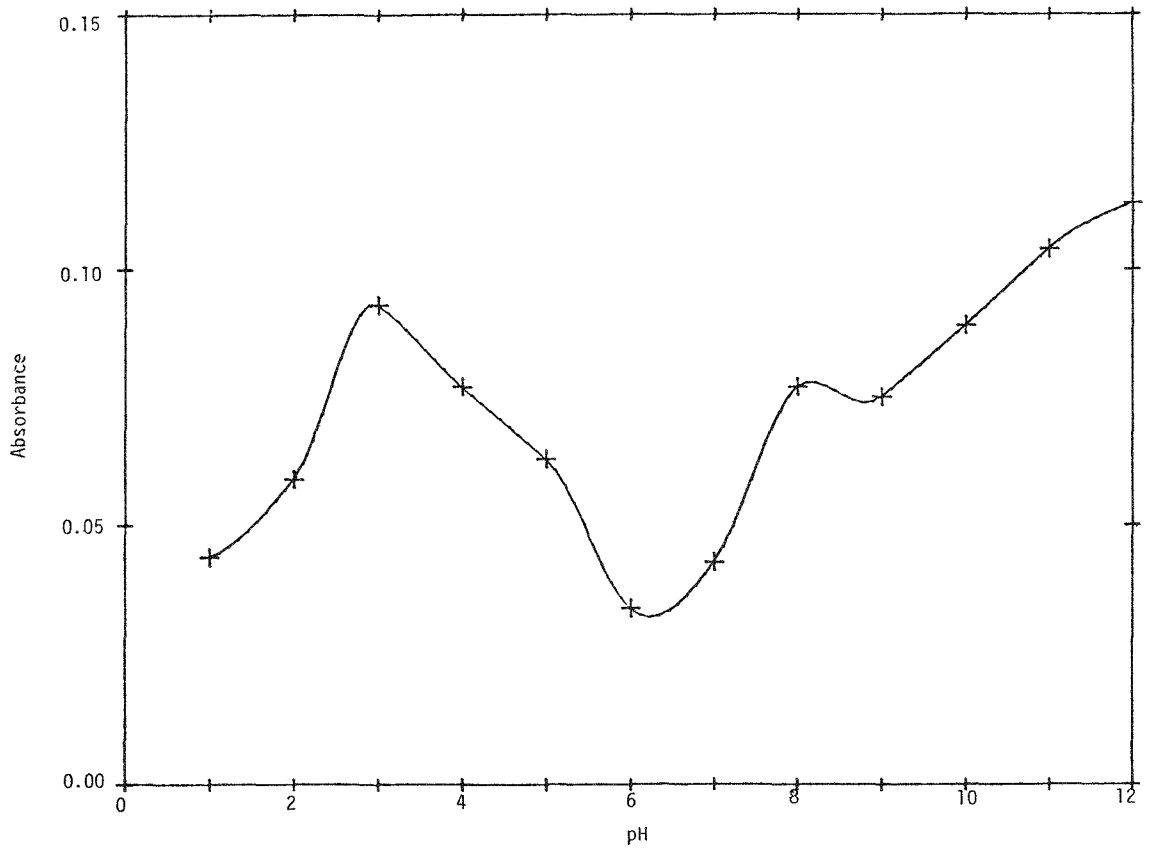

Figure 4. pH Effect on Extraction of Ruthenium

To extract the ruthenium from these solutions, it must be present in a form which is soluble under these conditions. Ruthenium (III) and Ru(IV) form hydrous oxide and hydroxide precipitates in basic solutions whereas Ru(VI) and Ru(VII) both form soluble species under these conditions. Ruthenium (VI) is used for the extraction step because it can be obtained conveniently without danger of producing volatile RuO_4. The generation of hypoiodite in solution is the easiest method of producing the necessary oxidant. Iodine crystals react with the basic solution to produce hypoiodite which oxidizes Ru(IV) to Ru(VI). The pertinent reactions are:

$$I_2 + H_2O \longrightarrow HIO + H^+ + I^-$$

$$RuO_2 \cdot XH_2O + IO^- + 2OH^- \longrightarrow RuO_4^{-2} + I^- + (X+1)\ H_2O$$

The various steps in the procedure for analysis of solid samples ultimately result in conversion of ruthenium in the samples and standards to the same oxidation state. To investigate the oxidation state of ruthenium in each of these steps, 16 mg of ruthenium dioxide was fused in 5 g of sodium peroxide. The melt was leached with water and the uv-visible spectrum of a portion was obtained. It matched the spectra of RuO_4^{-2}. Then the leachate was added to 15 mL of concentrated hydrochloric acid. After cooling and dilution to 100 mL, the uv-visible spectrum

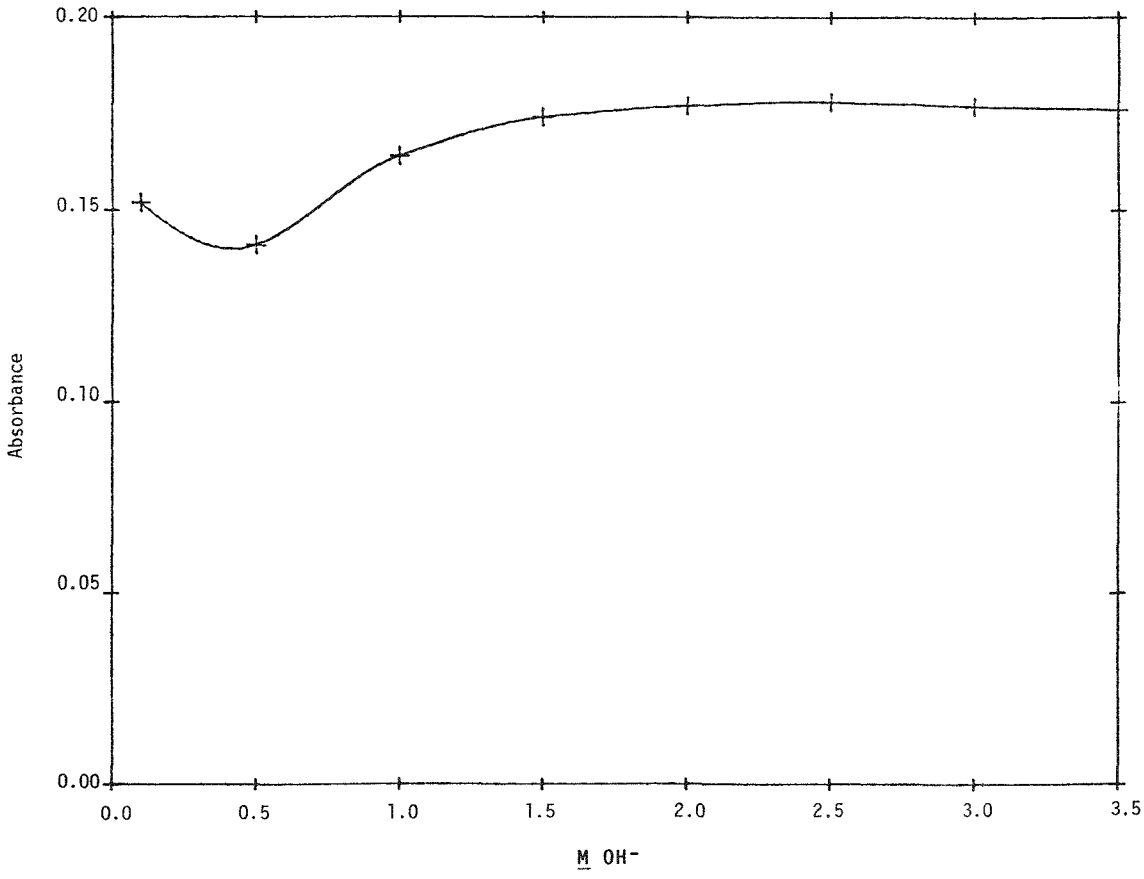

Figure 5. Effect of Hydroxide Ion Concentration on Extraction of Ruthenium

of this solution was obtained. It corresponded to the spectrum reported for Ru(IV) oxychloride complexes. The solution was then made 2 M in sodium hydroxide, several crystals of iodine were added, and the solution was stirred until the iodine crystals dissolved. The spectrum of this solution was that of RuO_4^{-2}. The solution was then complexed with APDC and extracted into amyl acetate. The spectra of the organic phase and that of Ru(IV) extracted at pH 3 with APDC/amyl acetate are shown in Figure 6, indicating that the ruthenium is reduced to Ru(IV) in the final extraction procedure.

The completeness of the separation of ruthenium from the diverse ions was investigated. Samples of the zirconium/aluminum and AGNS calcine were fused with sodium peroxide and leached with water. The leachate was acidified and spiked with ruthenium. The acidified leachates of the two calcines were analyzed by emission spectroscopy by the Spectrochemical Group and they were found to contain major amounts of aluminum and sodium and minor amounts of chromium, molybdenum, ruthenium, and zirconium (only in Zr/Al calcine). After extracting the ruthenium, the organic phase was evaporated and wet ashed with nitric acid. The residue was dissolved in 1 N nitric acid and analyzed by emission spectroscopy. It was found to

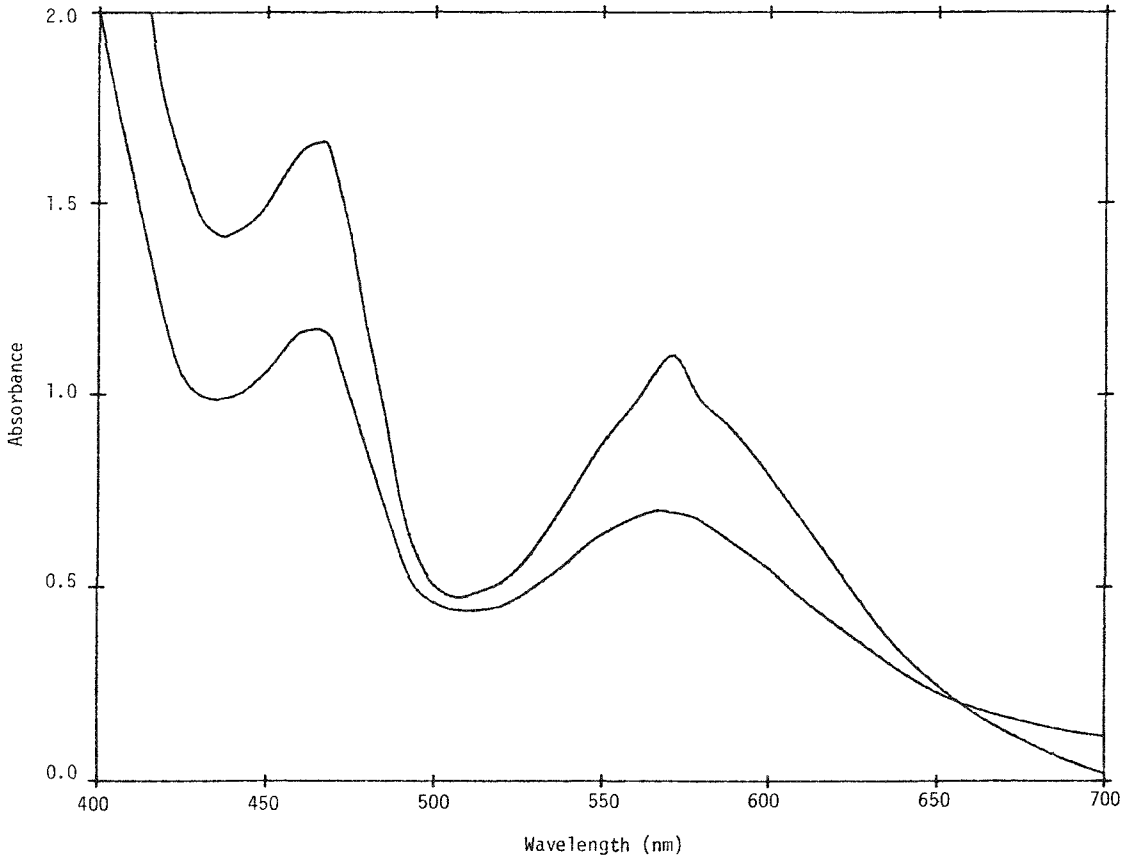

Figure 6. Absorbance Spectra for Extracted Species

contain major amounts of ruthenium and only traces of aluminum and sodium; The latter probably came from incomplete separation of phases before transferring the organic phase.

Solid ruthenium standards with composition similar to the samples being analyzed are not available; therefore standards were synthesized by grinding weighed portions of RuO_2 with weighed portions of the various ruthenium free calcine materials. The known values were then calculated and are shown in Table 3 along with the results of analyses of the standards by the method developed.

TABLE 3

Analysis of Standard Calcines for Ruthenium

Standard	Calculated wt%	Concentration Found wt%	Standard Deviation
Zr/Al-1	0.0086	0.0075	± 0.0008
Zr/Al-2	0.055	0.058	± 0.004
Zr/Al-3	0.27	0.25	± 0.02
AGNS	0.76	0.77	± 0.02

7. The Accurate Determination of 5-25 mg of Uranium by Redox Titrimetry (S. D. Reeder and J. R. Delmastro)

A precise and selective potentiometric titration method for determining 5-25 mg of uranium has been developed. The method is particularly useful in reducing the amount of fissionable uranium expended in an analysis and is especially attractive for the determination of ^{233}U in solutions used to prepare spikes for isotope dilution mass spectrometry. The waste solution is less than 25 mL per sample so that it is practical to extract and recover the expensive spike material.

The method is essentially a scaled-down version of Method U-Vol-1 of this laboratory which is based on the work of Davies and Grey.[8] Although only one-tenth the amount of uranium is required for an analysis, there is no appreciable reduction in accuracy or precision. Uranium is reduced to the quadrivalent state with ferrous ion in a phosphoric acid-sulfamic acid medium, the excess ferrous ion is selectively oxidized by nitric acid with a molybdenum catalyst, and the uranium is then oxidized with standard potassium dichromate with the aid of a vanadium catalyst. The titration with 0.01 N or 0.02 N $K_2Cr_2O_7$ has been automated by interfacing a 10 mL Mettler buret with a pre-programmed HP 9830 calculator. The calculator controls the delivery of titrant so that the end-point is approached as rapidly as possible and yet, delivers small increments of titrant (0.002 to 0.004 mL) near the end-point. A hard copy of the data (mL of titrant vs. Electrode Potential) is printed as the titration proceeds and the volume of titrant equivalent to the uranium in the sample is computed. A plot of the data and storage of the data is possible if desired.

Development work initially began by following Method U-Vol-1 with the volume of the reagent scaled down by a factor of ten and the dichromate by a factor of five. The results were inconsistant and less than the desired 0.05% precision and accuracy. The major problems were found to be the result of improper temperature control of critical reactions and the presence of oxidizable impurities in the phosphoric acid. The later problem was readily solved by adding potassium dichromate to the phosphoric acid to react with oxidizable substances. Any excess dichromate is destroyed by ferrous sulfate solution during the reduction of uranium.

A temperature of about 35°C is needed for the uranium reduction and the selective oxidation of ferrous ion by nitric acid. This temperature is generated naturally in method U-Vol-1 by the chemical reactions and is retained for sufficient time because of the large volume of the solution. On a reduced scale the proper temperature is difficult to achieve and maintain. As a solution to the problem, the sample and reagents are preheated in a water bath to a temperature of 30°C before proceeding with the analysis. The sample beaker is insulated to prevent loss of heat and the reactions create additional heat to obtain the proper temperature.

---

[8]W. Davies and W. Gray, UKAEA Report TGR-716(D), 1964, Talanta 11, 1203 (1964).

The volumes of the various reagents have been optimized to give the best results with the miniaturized method and therefore the overall scale-down factor is only roughly 1 to 10. The recommended normality of titrant is 0.01 N for ~5 to 12 mg of uranium and 0.02 N for up to 25 mg of uranium when using a 10 mL buret. A precision and accuracy of 0.05% or better is obtainable by adherence to the recommended procedure.

The method will be used to verify various uranium standards prepared by the Quality Control and Accountability group and can be used whenever Method U-Vol-1 is appropriate.

8. The Chemical Separation and Purification of Uranium for Mass Spectrometric Analysis (S. D. Reeder)

The determination of uranium concentration and isotopic composition in ICPP reprocessing streams for accountability purposes is accomplished by isotope dilution mass spectrometry (IDMS). When difficulties were recently experienced with this method in the analysis of certain samples originating with a zirconium fuel dissolution process, a "Task Force" was organized to investigate analytical problems of this kind which are related to uranium accountability. This group of chemists traced the problem of poor loading and running characteristics, and ion current instability to contaminants in the uranium fractions submitted for mass analysis. Since Method U-Sep-1 is used to separate uranium from plant samples for IDMS, attention was given to improving this method so that the zirconium-type samples could be mass analyzed. Two "clean-up" procedures following Method U-Sep-1 were developed. These methods, based on the anion exchange properties of uranium (and potential contaminants) are effective in eliminating the mass analysis problems associated with the zirconium dissolver product samples and other zirconium bearing samples that are solubilized by pyrosulfate fusion and hydrofluoric acid dissolution.

One procedure uses a short column of Dowex - 1 x 10, 100-200 mesh, anion exchange resin to absorb uranium from a 10 M HCL solution. Certain metals which do not form strong chloride anion complexes (as does uranium) are eluted from the column with 8 M HCl. Some of these elements are the alkali and alkaline earth metals, thorium, the rare earths, aluminum, and zirconium. The uranium is subsequently eluted from the column with a small volume of water (~1.5 mL) and the evaporated water fraction is submitted to the mass lab for analysis.

The other procedure uses a liquid anion exchanger, triisooctylamine (TiOA), to accomplish the same ion exchange purification as the resin column. Uranium is extracted into a solution of triisooctylamine in xylene from a 4 M HCl solution. The elements mentioned above are not extracted. The separated organic phase is diluted with isopropyl alcohol and uranium is precipitated from this medium with hydrogen peroxide. After washing with acetone the uranium peroxide is rapidly dried in an oven and submitted to the mass lab for analysis.

With either procedure the uranium is first stripped from the hexone phase resulting from Method U-Sep-1 with an ammoniacal acetone (or isopropanol)

water solution and the centrifuged uranium hydroxide is dissolved in the appropriate concentration of hydrochloric acid (10 M or 4 M) prior to ion exchange. The plutonium scrub used in Method U-Sep-1 is eliminated with a favorable increase in uranium yield. If plutonium is present, 0.1 mL of hydroiodic acid (~50% HI) is added to the hydrochloric acid solutions to reduce plutonium to the trivalent state so that it will not absorb on the resin column or extract into TiOA-xylene. Hydroquinone, ascorbic acid, hydroxylamine, and hydrazine were tested for the reduction of plutonium but were found to be inferior to hydroiodic acid for these procedures.

The liquid ion exchange procedure is considerably faster and simpler than the resin-column procedure. It also has the advantage of a peroxide precipitation which gives excellent decontamination. Two samples can be processed in about 15 min starting with the hexone phase from Method U-Sep-1. If plutonium is present, an additional 5 min is required for the reduction with hydroiodic acid.

Trammell and Wade[9] modified the anion resin procedure by having a direct exchange of uranium from the hexone phase to the resin followed by a column-type elution of impurities with 8 M HCl. However, both procedures based on the use of ion exchange resin give satisfactory end results and use the same procedural time.

9. Rapid Spectrophotometric Determination of Uranium (S. D. Reeder)

The development of a simple, sensitive, and rapid method to determine uranium in certain ICPP fuel reprocessing solutions is desired for accountability purposes. Such a method would not replace the usual determinations by isotope dilution mass spectrometry (IDMS), but would provide a preliminary analysis of less accuracy in situations where a rapid determination of uranium would be helpful. Two methods based on the colorimetric determination as the yellow thiocyanate complex have been evaluated for this purpose. Both are relatively fast and capable of better than the suggested 3% accuracy. Because these methods are nonselective, a prior separation of uranium from fission products and other interferences must be performed. The extraction of uranium into hexone from an aluminum nitrate salting solution is especially suited for this purpose. Best results are obtained with 50 to 1000 μg U in a sample aliquot, but as little as 10 μg can be determined. This range effectively covers the concentration gap between method U-Fluor-1 and Method U-Color-1. At the 15 μg level an accuracy and precision of about 3% may be obtained. At 100 μg and above the results are better than 0.5%.

[9]Trammell, D. R. and Wade, M. A., "Investigation of Ion Exchange Purification of Uranium Samples After Method U-Sep-1 for Mass Spectrometric Analysis", Production Support Analytical Branch Progress Report for March 1977.

The first method is based on work reported by Nietzel and De Sesa[10]. After extraction of uranium into hexone under conditions similar to Method U-Sep-1, the yellow uranium thiocyanate complex is developed by mixing the extract with a solution of ammonium thiocyanate in a butyl cellosolve-water solvent. The color forms immediately and the solution may be poured directly into a 1-centimetre cell for spectrometric measurement of the sample absorbance. A wavelength between 425 and 360 mm is chosen so that the absorbances of the sample and standards are limited to about 1.0. There is no absorbance peak, i.e., the absorbance increases with decreasing wavelength. The reagents used in this study yellowed rather rapidly and had to be freshly mixed every 6-8 h to avoid a very high blank.

The second method which originated in this study involves the extraction of the uranyl thiocyanate - triisooctylamine anion complex into xylene, hexone, or a mixture of xylene and hexone. The absorbance of the yellow uranium complex which forms is measured as in the first method. Triisooctylamine (TiOA) is a liquid anion exchanger and is used in Method U-Fluor-2 to extract the chloride complex of uranium into xylene from a highly acid medium. In this application the thiocyanate anion complex of uranium is rapidly and completely extracted into a TiOA-xylene (5% V/V) solution from a 0.25 M H_2SO_4 solution. The yellow complex gives 30% more absorbance than the first method, and initially, the blank is very small. If hexone is used as the solvent instead of xylene, the absorbance is about the same as the first method. Although the method is applicable to either organic or aqueous samples, the procedure is more lengthy than the butyl cellosolve method. A solution of potassium thiocyanate and sulfuric acid is added to the sample and then 5 mL of the TiOA-xylene solution (3 mL of this reagent is used for a 2 mL hexone sample). The sample is shaken for 30 s, diluted with water, and shaken again for 30 s. After centrifuging, the organic layer is transferred to a 1-centimetre cell for measurement.

With either method the absorbance of the sample, standards, and blank increase with time. Since the blank absorbance does not increase at the same rate as the standards and samples, it is best to omit the blank and use standards having absorbances which bracket the absorbance of the samples.

The TiOA xylene-thiocyanate method was used to determine the effectiveness of Method U-Sep-1 in separating uranium from samples containing a high level of zirconium and fluoride. Samples of this type have not run well by IDMS and contamination of the separated uranium with extraneous ions or low yield is suspected. The results indicated that the uranium extraction was better than 90% so that yield was not the real problem. However, the uranium thiocyanate complex formed from the samples increased in absorbance much faster than the pure uranium standards and were slightly off color. This indicated that contaminants were carried with the uranium through Method U-Sep-1.

---

[10] O. A. Nietzel and M. A. De Sesa, "Spectrophotometric Determination of Uranium with Thiocyanate in Butyl Cellosolve-Methyl Isobutyl Ketone - Water Medium", Analytical Chemistry, Vol. 29, p 756, May 1957.

10. Unirradiated Rover Fuel Assay Program (L. E. Trejo)

The unirradiated graphite-uranium Rover fuel stored at ICPP is to be repackaged into cardboard tubes, assayed, and processed for burning and recovery of the uranium. It is necessary to nondestructively assay the Rover fuel after repackaging and prior to processing. This will be accomplished using an Isotopic Source Assay System (ISAS) which was purchased from Gulf Radiation Technology. The ISAS is a nondestructive active assay device which utilizes a stream of neutrons supplied by an isotopic source, usually ^{252}Cf, to interrogate and measure fissile material. When a neutron activated fission event occurs in the sample, several gamma rays and a few neutrons are emitted simultaneously. The ISAS detector head contains two pairs of plastic scintillation detectors. Each of the four detectors is optically coupled to a photomultiplier tube. In assaying the Rover fuel, the system will be operated at 3-out-of-4 coincidence - that is, the gamma radiation and neutrons emitted by the sample during neutron interrogation, must be simultaneously detected by 3-out-of-4 of the plastic scintillation detectors within 60 ns before a count is recorded. This relatively high degree of multiplicity (coincidence) reduces the number of counts recorded from the high background radiation due to the essentially sporadic radiation received from the source. Because fission events are characterized by a high degree of multiplicity, the fission events are preferentially counted, and the signal-to-background ratio is substantially improved.

The ISAS can be set up to measure ^{232}Th, ^{239}Pu, ^{240}Pu, ^{238}U, and ^{235}U in various matrices and in either homogeneous or heterogeneous samples. Also, percent enrichment can be determined; although, the calibration for this application is somewhat tedious.[11] While assaying the Rover fuel, the concern will be only with measuring the ^{235}U content at a constant enrichment factor of about 93%.

In preparation for the Rover assay, the ISAS has been assembled in the Unirradiated Fuel Storage Facility (UFSF), where the Rover fuel is now stored. Personnel from the Computer Applications Group checked the electronics of the ISAS and found some deficiencies. A new Quad discriminator and two new photomultiplier tubes were needed to bring the ISAS into peak performance. Using a borrowed discriminator, which was too slow for the system, the operation of the rest of the equipment was checked, and a preliminary calibration curve was plotted. The initial Fuel Storage Standard Operating Procedure (SOP) prevented leaving the equipment on while the building was unattended. Count rate readings taken during the instrument check-out showed continued instability, i.e., 100-s background counts varied significantly over a period of several hours. This led to the conclusion that there must be a fairly long warm-up period required before stable readings could be obtained. A new SOP eventually was issued which allowed leaving the equipment on while unattended, and the ISAS was recycled on 30-min counts over a 2-day period. A printer was attached for a permanent record to be available for study. The system stabilized in approximately nine hours giving consistant readings of background radiation with a one sigma standard deviation of 0.25% as shown in Figure 7.

[11] Isotopic Source Assay System Operational Manual, GULF-RT-C10958, Gulf Radiation Technical Division (1972).

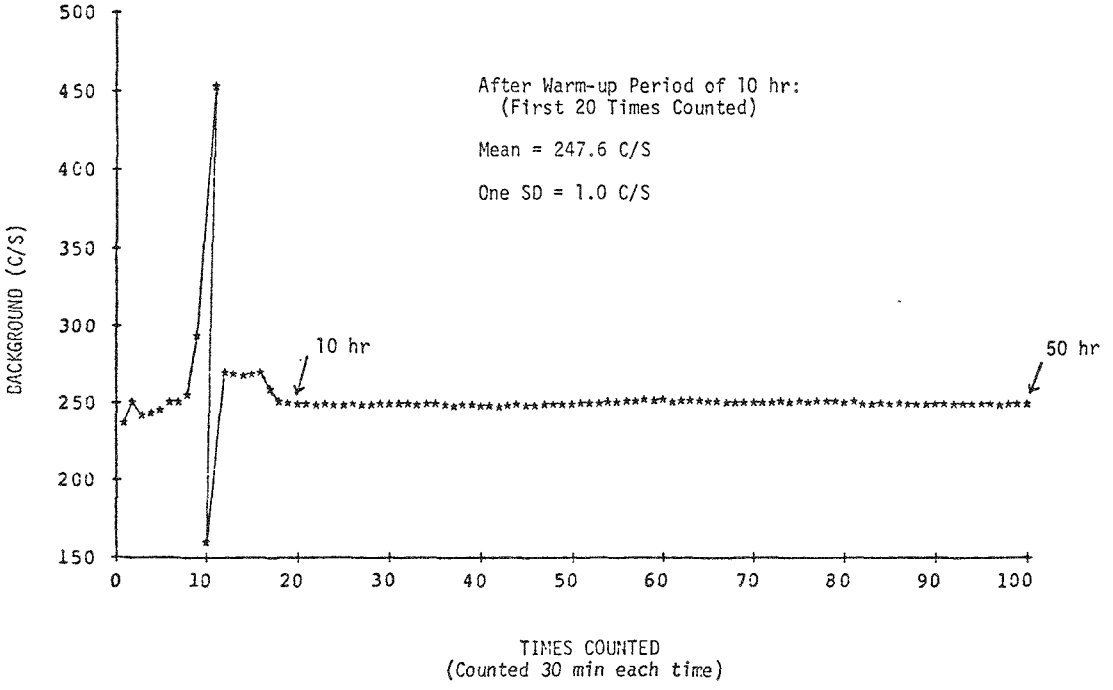

Figure 7. ISAS Warm-Up and Stability

The Rover Fuel Repackaging Project is divided into Phases I, II, and III. Phases I and II are repackaging and assaying Rover rods. Phase III is repackaging and assaying of Rover ash and broken fuel segments. A series of ISAS calibration standards used at other sites[12] have been shipped and stored in the Irradiated Fuel Storage Facility (IFSF) at CPP-603. These standards, which will be used to calibrate the CPP ISAS, each consist of seven Rover rods packaged in 63.5-mm diam by 1.37-m long cardboard tubes sealed at each end with a wooden plug. To calibrate the ISAS for Phases I and II, five of these standards covering a range of 250 to 960 g of ^{235}U will be used. The cardboard tubes containing the standards were externally contaminated either before arrival at ICPP or during storage at the IFSF. The fuel had to be repackaged into clean cardboard tubes before use for calibration. These are now stored in area 107 of CPP-651 in a storage rack specifically built for this purpose. A preliminary calibration curve has been established as shown in Figure 8.

An HP-9825A Programmable Calculator and an HP-9871A Printer will eventually be dedicated to the ISAS. With the calculator system interfaced to the ISAS, the sample will be automatically scanned, the data collected and analyzed, and the results printed in grams of ^{235}U. The 9871A Printer will have provisions for optional data input such as operator and fuel element indentification numbers so that the printed output will contain permanent record information useful for nuclear material. An HP-97 Programmable Desktop Calculator with paper tape printout or equivalent will be used for interim calibration calculations.

[12] W. D. Lewis, Nondestructive Assay of Rover Fuel Rods by Gamma Ray Spectroscopy (1974).

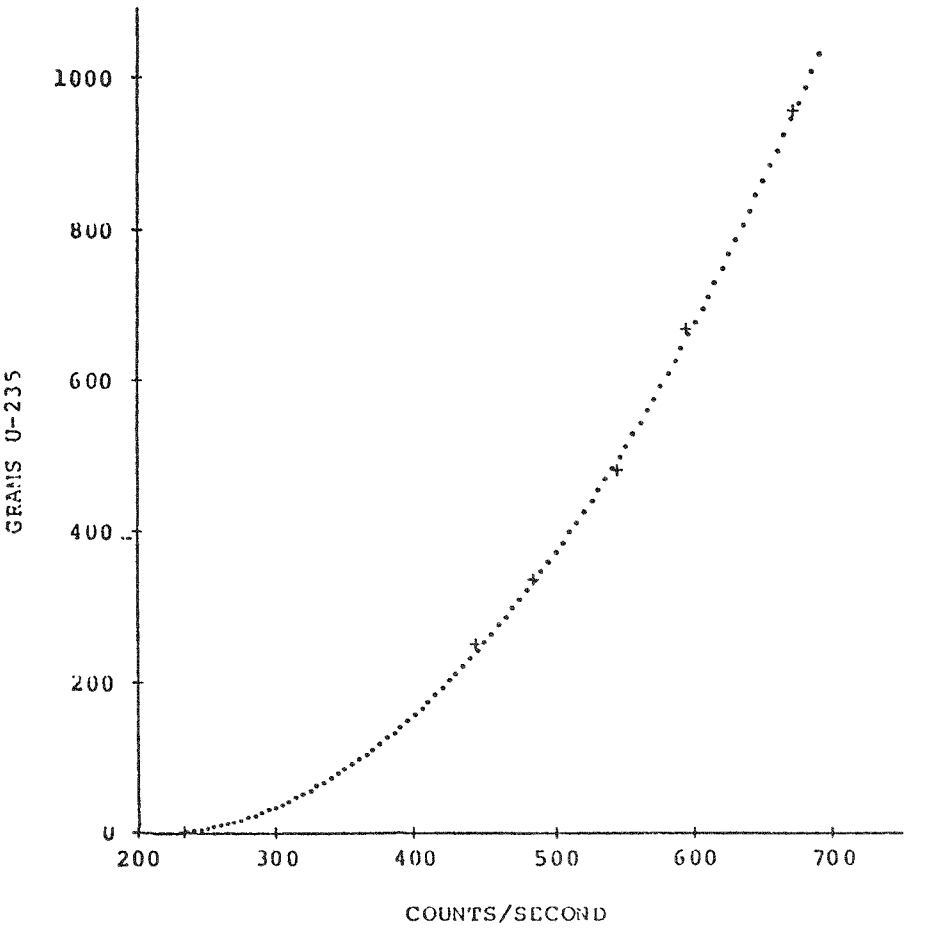

Figure 8. ISAS Calibration Curve

Phase I of the Rover Repackaging Project is now scheduled to begin during October of 1977. This schedule should allow ample time for the equipment to arrive and the ISAS to be calibrated.

VII. ENVIRONMENTAL IODINE SPECIES BEHAVIOR

(J. H. Keller, B. G. Motes, F. A. Hohorst, S. W. Duce, J. W. Tkachyk)

An objective of this program is to verify and/or suggest modifications to the presently used NRC atmospheric dispersion models. An empirical X/Q will be obtained by measuring xenon concentrations at the release points of a nuclear power plant, and simultaneously measuring the xenon in the environment at various distances from the plant. To make the xenon measurements, two cryogenic air samplers have been purchased. During the report period, the samplers were tested in the laboratory and in the field. Recovery of the krypton and xenon (as measured by gas chromatography is nominally 80%.

As reported last quarter, an environmental chamber was installed for the evaluation of the wet deposition enhancement of iodine species on grass. After initial operating parameters were established, three tests were conducted using $CH_3{}^{131}I$. Final data reduction from these tests is in progress.

Work employing a specific ion electrode as a means of studying basic, aqueous iodine chemistry has continued. The parameters being investigated include initial molar concentrations of iodine, pH as a function of iodine formation rates, and subsequent equilibrium with other iodine species. To date, data indicate that at an iodide concentration above 5×10^{-7} M, the precision of the specific ion electrode is satisfactory for long duration tests. However, at lower concentrations, the electrode is unsatisfactory. Due to lack of funding and rearrangement of personnel, this phase of the program will be temporarily discontinued.

The NRC has selected the Quad Cities Nuclear Power Plant as the site for the Environmental Iodine Species Behavior Program field work. The NRC also has decided to make the field measurements a joint venture between Allied Chemical Corporation-Idaho Chemical Programs and the Electric Power Research Institute (EPRI). An initial visit to the site was made.

REPORTS AND PUBLICATIONS ISSUED DURING THE QUARTER

1. Idaho Chemical Programs Reports

1. J. D. Christian and D. W. Rhodes, Ruthenium Containment During Fluid-Bed Calcination of High-Level Waste from Commercial Nuclear Reprocessing Plant, ICP-1091 (February 1977).

2. W. J. Maeck, W. A. Emel, J. E. Delmore, F. A. Duce, L. L. Dickerson, J. H. Keller, R. L. Tromp; Discrepancies and Comments Regarding U and ^{239}Pu Thermal Fission Yields and the Use of ^{148}Nd as a Burnup Monitor; ICP-1092 (December 1976).

3. Cyril M. Slansky (ed.), LWR Fuel Reprocessing and Recycle Progress Report for April 1 - June 30. 1976, ICP-1101.

4. R. C. Shank (ed.), Analytical Chemistry Branch Annual Report for FY 1976 and Transition Quarter, ICP-1103 (February 1977).

5. P. C. Ahrens, Pilot-Plant Feasibility Studies of a Fluid-Bed Cooling Tower, ICP-1105 (March 1977).

6. Cyril M. Slansky (ed.), Waste Management Development Technology Progress Report for July - September 1976, ICP-1106.

7. M. W. Wilding, Survey on Corrosion of Metals and Alloys in Solutions Containing Nitric Acid, ICP-1107 (December 1976).

8. Cyril M. Slansky (ed.), LWR Fuel Reprocessing and Recycle Progress Report for July 1 - September 30, 1976, ICP-1108.

9. M. W. Wilding, Iodine to Control Microbiological Growth in Fuel Storage Basin Water, ICP-1109 (April 1977).

10. Cyril M. Slansky (ed.), LWR Fuel Reprocessing and Recycle Progress Report for October 1 - December 31, 1976, ICP-1110.

11. Cyril M. Slansky (ed.), Technical Division Quarterly Progress Report October 1 - December 31, 1976, ICP-1111.

12. F. A. Hohorst, Containment of ^{220}Rn Via Adsorption on Molecular Sieves for HTGR-OGCS, ICP-1114 (April 1977).

13. Cyril M. Slansky (ed.), LWR Fuel Reprocessing and Recycle Progress Report for January 1 - March 31, 1977, ICP-1116.

14. Cyril M. Slansky (ed.), Technical Division Quarterly Progress Report for January 1 - March 31. 1977, ICP-1117.

2. Papers Presented at Technical Society Meetings

1. 25th Annual Conference on Mass Spectrometry and Allied Topics, Washington, D.C. (June 1977).

   a. W. J. Maeck, "Mass Spectrometric Analyses of Samples from the Oklo Phenomenon".

   b. J. E. Delmore, "A Thermal Ionization Mass Spectrometer Data System".

   c. J. E. Delmore, "The Mass Spectrometric Analysis of Fission Products by Thermal Ionization".

2. International Specialist Symposium on Neutron Standards and Applications, National Bureau of Standards, Gaithersburg, MD (March 1977).

   a. W. J. Maeck, "Fission Yields: Measurement Techniques and Data Status". To be published in proceedings.

3. National Association of Corrosion Engineers, Corrosion 77, San Francisco, CA (March 1977).

   a. Bernice E. Paige, "Evaluation of Welds and Stresses in High Nickel Alloys in Fluoride Solutions".

   b. Cyril M. Slansky, "A Review of Materials of Construction in Nuclear Fuel Reprocessing and in Radioactive Waste Treatment.

3. Other Publications

1. J. R. Berreth, A. P. Hoskins, and J. A. Rindfleisch; "Stabilization and Storage of Solidified High-Level Radioactive Wastes"; Nuc. Tech.; 32; No. 1; 16-24 (January 1977).

2. E. G. Samsel and J. R. Berreth, "Preparation and Characterization of Sintered Glass-Ceramics from Calcined Simulated High-Level Waste", Nuc. Tech., 32, No. 1, 68-75 (April 1977).

3. E. W. Readey and C. R. Cooley (eds.); "Ceramic and Glass Radioactive Waste Forms". Summary of a work shop held at ERDA Germantown, MD; January 4-5, 1977; Conf 770102.

DISTRIBUTION RECORD FOR ICP - 1123

Internal Distribution

1 - Chicago Patent Group - ERDA
9800 South Cass Avenue
Argonne, Illinois 60439

1 - CA Benson
Idaho Operations Office - ERDA
Idaho Falls, ID 83401

1 - HP Pearson, Supervisor
Technical Information

10 - INEL Technical Library

20 - Authors

79 - Special Internal

External Distribution

230 - UC-02 - General, Miscellaneous, & Progress Reports (Nuclear)
UC-10 - Chemical Separations Processes for Pu and U, TID-4500, R65

55 - Special External

Total Copies Printed - 397